2013

A Decision Support System For The Intelligence Satellite Analyst

Gi Yeon Park
North Carolina Agricultural and Technical State University

A Decision Support System for the Intelligence Satellite Analyst

Gi Yeon Park

North Carolina A&T State University

A dissertation submitted to the graduate faculty

in partial fulfillment of the requirements for the degree of

DOCTOR OF PHILOSOPHY

Department: Industrial and Systems Engineering

Major: Industrial and Systems Engineering

Major Professor: Dr. Celestine A. Ntuen

Greensboro, North Carolina

2013

School of Graduate Studies
North Carolina Agricultural and Technical State University
This is to certify that the Doctoral Dissertation of

Gi Yeon Park

has met the dissertation requirements of
North Carolina Agricultural and Technical State University

Greensboro, North Carolina
2013

Approved by:

Dr. Celestine A. Ntuen Major Professor	Dr. Younho Seong Committee Member
Dr. Daniel Mountjoy Committee Member	Dr. Zongliang Jiang Committee Member
Dr. Tonya Smith-Jackson Department Chair	Dr. Sanjiv Sarin Dean, The Graduate School

Biographical Sketch

Gi Yeon Park was born on April 29, 1977, in Seoul, South Korea. He received the Bachelor of Science degree in Electronic Engineering from Andong National University, South Korea, in 2003 and the Master of Science degree in Electrical Engineering from North Carolina Agricultural and Technical State University, Greensboro, in 2007. He is a candidate for the Doctor of Philosophy degree in Industrial and Systems Engineering at North Carolina Agricultural and Technical State University.

Dedication

I dedicate my dissertation work to my parents, Junseo Park and Inja Lee, my wife Junghwa Park, and my sons, Jiwoo Park and Junwoo Park.

Acknowledgements

First and foremost, I would like to express my deepest gratitude to the Lord who gave me much-needed strength, power, and opportunity to become who I am today. Second, I would like to thank my graduate advisor, Dr. Celestine A. Ntuen, for his unyielding patience and support. Dr. Ntuen guided me a long way to where I stand now. In addition, special credit goes to my committee members, Drs. Younho Seong, Daniel Mountjoy, and Zongliang Jiang, for their invaluable comments and feedback that shaped my dissertation into a better one. I also thank Dr. Eui H. Park who gave me strong supports for graduate studies.

I would also like to thank all my colleagues from Center for Human Machine Studies, Mr. Policarpo C. deMattos, Dr. Jules Chenou, and especially brother-like Mr. Gwangmyong Kim. Because of their support and encouragement I was able to get through the challenging and important dissertation defense. I will never forget their sincere companionship. I would like to thank Korean First Presbyterian Church congregation who supported my family and me with prayers for the success of this journey and the spiritual life.

I am extremely grateful to my family. My parents have been waiting this moment in a while. They are always with me in any circumstances. Their rock solid support fueled me not to give up to this moment. I have three very special individuals who waited this moment more than eagerly than I did. My lovely wife, Junghwa, two proud of sons, Jiwoo and Junwoo, have been my source of energy and my shelter during my graduate years. I am especially indebted to Junghwa for raising our two sons, despite my limited presence and supports as a father and a husband. Thanks for raising them. But, most of all, thank you for being there for me throughout this journey.

Table of Contents

List of Figures

List of Tables

List of Acronyms

ACT-R	Adaptive control of thought-rational
AH	Abstraction hierarchy
AI	Artificial Intelligence
ANOVA	Analysis of Variance
CCV	Color Coherence Vectors
CIA	Central Intelligence Agency
CKS	Connectionist Knowledge Seeding
CM	Cognitive Model
CN	Cognitive Network
CTA	Cognitive Task Analysis
DAG	Directed Acyclic Graph
DSS	Decision Support System
DV	Dependent Variable
eCCV	Enhanced Color Coherence Vectors
e-ICU	electronic-Intensive Care Unit
EMS	Emergency Medical Service
GEOINT	Geospatial Intelligence
GIS	Geographic Information System
HCI	Human Compute Interaction
HSV	Hue Saturation Value
IA	Intelligence Analyst

IMINT	Imagery Intelligence
IV	Independent Variable
KE	Knowledge Elicitation (KE)
KM	Knowledge Management (KM)
KL	Knowledge Level
NGA	National Geospatial-Intelligence Agency
NRO	National Reconnaissance Office
SA	Situation Awareness
SAISI	Supporting Analyst Interpretation of Satellite Image
SIVS	Satellite Information Visualization System
SOAR	State, Operator and Result
SOP	Standard Operating Procedure
RGB	Red Green Blue
VACOM	Visual Analytic Cognitive Model

Abstract

The study developed a decision support system known as Visual Analytic Cognitive Model (VACOM) to support the Intelligence Analyst (IA) in satellite information processing task within a Geospatial Intelligence (GEOINT) domain. As a visual analytics, VACOM contains the image processing algorithms, a cognitive network of the IA mental model, and a Bayesian belief model for satellite information processing. A cognitive analysis tool helps to identify eight knowledge levels in a satellite information processing. These are, spatial, prototypical, contextual, temporal, semantic, pragmatic, intentional, and inferential knowledge levels, respectively. A cognitive network was developed for each knowledge level with data input from the subjective questionnaires that probed the analysts' mental model. VACOM interface was designed to allow the analysts have a transparent view of the processes, including, visualization model, and signal processing model applied to the images, geospatial data representation, and the cognitive network of expert beliefs. VACOM interface allows the user to select a satellite image of interest, select each of the image analysis methods for visualization, and compare 'ground-truth' information against the recommendation of VACOM. The interface was designed to enhance perception, cognition, and even comprehension to the multi and complex image analyses by the analysts. A usability analysis on VACOM showed many advantages for the human analysts. These include, reduction in cognitive workload as a result of less information search, the IA can conduct an interactive experiment on each of his/her belief space and guesses, and selection of best image processing algorithms to apply to an image context.

CHAPTER 1

Introduction

1.1 Background

The work of the intelligence analyst involves spatial cognition (Freksa, 2004), sensemaking (Weick, 1995; Malhotra, 2001; Ntuen, 2009), evidence investigation (Mukkamala & Sung, 2003), and significant use of intuition for decision making. For instance, the National Reconnaissance Office (NRO) designs, develops, and operates America's fleet of intelligence satellites, including signals intelligence and imagery intelligence satellites. Other agencies utilize the data produced by these satellites. The role of the intelligence analyst is to produce actionable intelligence from these data.

Satellites have been used over the past several decades to obtain a wide variety of information about the earth's surface, ranging from military applications to tracking global weather patterns, surface vegetation, ocean currents and temperatures, polar ice fluctuations, pollution, and many other aspects.

The National Geospatial-Intelligence Agency (NGA) is responsible for imagery analysis for intelligence purposes. The National Security Agency, for instance, takes the signals gathered by NRO satellites and processes and analyzes them. NGA experts utilize the imagery (both photographic and radar) produced by NRO satellites. There is imagery analysts in various other government agencies, including the Central Intelligence Agency (CIA), using the intelligence produced from the NRO, usually in the form of geospatial intelligence. Geospatial intelligence (GEOINT) is the exploitation and analysis of imagery and geospatial information to describe, assess, and visually depict physical features and geographically referenced activities on the

Earth. GEOINT consists of imagery, imagery intelligence, and geospatial information. The GEOINT analyst is of interest in this research.

GEOINT combines several disciplines such as mapping, charting, imagery analysis, and imagery intelligence. The basic principle of GEOINT is to organize and combine all available data around its geographical location on the Earth and then exploit it in order to prepare products that can be easily used by planners, emergency responders and decision makers. Some aspects of GEOINT analyst tasks include, but are not limited to, image processing in collecting, organizing, analyzing all-source geospatial and other intelligence information, Geographic Information System (GIS), and the fundamental principles for interpreting satellite. The rationale is simple, and it is important for analysts to understand the dynamics of data for the purpose of situational awareness, a product of cognition that is not well understood when dealing with GEOINT analyst tasks.

1.2 The Problem

While there have been significant advances in the technology that generate satellite data, little progress has been made on ways to translate the data into time sensitive and context based operational decision making. There are several reasons for this lack of progress: (a) the scaling of multiple data dimensions into minimal components for developing metrics for real-time judgment is complex; (b) the assumption by engineers and designers that scientific visualization quickly translates into information understanding; and (c) the tendency to lump or aggregate fused information into a common database without isolating artifacts. The scaling problem can lead to serious costs associated with the rendering and displaying of information, especially errors of comparative judgment.

While scientific visualization allows analysts to view multiple dimensions of data representation, the visual displays are intolerant and insensitive to the meaningfulness of information in context. Sometimes the costs may result in what Wickens (1999) refers to as "cognitive tunneling effect." This is seeing things to which the brain gives different interpretation due to scale of representation. On the other hand, information visualization generates a cohesive coupling of information characteristics and human cognitive processes since visualization is known to be embedded in mind through tacit knowledge (Polanyi, 1966), and externally controlled through situation awareness (Smith & Hancock, 1995). With this, Heuer (1999) observes that, "The mind is poorly 'wired' to deal effectively with both inherent uncertainty (the natural fog surrounding complex, indeterminate intelligence issues) and induced uncertainty (the man-made fog fabricated by denial and deception operations)… Tools and techniques that stimulate the analyst's mind to apply higher levels of critical thinking can substantially improve analysis on complex issues on which information is incomplete, ambiguous, and often deliberately distorted" (p. 4).

Satellite information has complex image footprints which consist of interlaced complex information with multimodal contents. For example, some information objects can be visualized and understood; others need the application of technology to scale them to the desired level for human interpretation; still some are complex beyond human cognition. Thus, a geospatial information domain may have at least one of the following characteristics:

1. *Equivocality*: each analyst has a different interpretation of information in context. This could be due to levels of training, and expertise in the spatial information contexts.
2. *Ambiguity*: each analyst attempts to describe (some) non-familiar information objects in a subjective manner with some vagueness, fuzziness, and impreciseness.

3. *Incompleteness*: when information or data is incomplete, an analyst tries to behave as an "intuitive statistician" (Peterson & Beach, 1967). Each analyst attempts to give the best estimate of the situation.
4. *Uncertainty*: spatial information may contain deception from the adversary, or it may change with respect to time and location. This "morphing" (Caers, 2011) phenomenon can present uncertainties to the analyst. In this case, the analyst may assume a certain level of certainty while interpreting the information in context.
5. *Unknown*: the spatial information object may be unfamiliar or unknown to even the expert analyst. This may occur as the environment experiences transient turbulence or dynamic changes. An example is replacing a known object at a usually known location with an unknown one which may possess properties as the known one, but in reality, it is only a deception. As in the case of incompleteness situation, the analyst tends to guesstimate the situation information. Here, the expert can be a better estimator than the novice (Ho & Liu, 2011).

1.3 Major Problems in Modeling the Intelligence Analyst

Human cognition has been the study of psychology and many other disciplines for a long time and will continue to be a subject of fascination in human visualization and evolution. In the GEOINT and intelligence analyst (IA) study, spatial cognition is an important element in situation understanding. Many observations inform us of many possible gaps in understanding and modeling the IAs within a GEOINT domain.

- Knowledge representation and interpretation of dynamic phenomena (Miller, 2008; Mark et al., 1999; Guo, et al., 2007) is not an exact science. Usually, there are a lot of guesstimates.

- Overemphasis to study spatial physical information (e.g., a lopsided tilt towards scientific visualization which supports data management) rather than the cognitive processes involved (Ogiela & Ogiela, 2009, p. 64; Shan, Berthod, & Giraudon, 1999). This is because satellite data requires significant scientific analysis discover fundamental characteristics.
- Identifying the causes of cognitive limitations associated with limited human memory capacity (Ogiela & Ogiela, 2009, p. 66). The human memory is not expanding but information assumption is increasing.
- Sensemaking of a problem situation that is not clearly defined (unexpected or surprising information) (Miller, 2008; Ntuen, 2006). Intelligence analysts are tasked in puzzle solving-putting observed stimuli in context of useful information.
- Attempts to approximate and interpret data which "do not compare all the available options in every possible regard to select the best one" (Ogiela & Ogiela, 2009, p. 66). For example, intelligent geographic information systems (GISs) are known to compromise gaps "between world's reality and the way humans interact with this reality" (Freksa & Barkowsky, 1996, p. 3).
- Decoupling dynamic changes in spatial information space, especially, lack of time to process massive information under pressure (Thomas et al., 2005). The IA rarely copes with the flood of information from satellite images over a spatio-temporal setting. Determining useful information in multi-level of source and characteristics remain a formidable change. This can lead to memory distortion of spatial information (Edwards, 1997, p.458).

- The IA has a limited information fusion capability especially, data with multi-dimension (Laudy & Ganascia, 2009). For instance, there are evidences of inconsistencies in data integration between spatial reality and human cognition (Fonseca et al., 2000).

1.4 The Research Study, Goals and Objectives

The study developed methods to support IA in information processing task to the GEOINT domain. The study sought to develop a decision support system (DSS) with visual analytics designed to aid the IA. The study was intended to capitalize on the existing cognitive science models of decision making and information processing. This was accomplished by building computer codes to capture the IA knowledge networks involved in spatial cognition tasks within a GEOINT domain.

The major goal of the research was to focus on the use of computational modeling to integrate the knowledge levels required by the IAs for satellite information processing. The following objectives lead to the realization of this goal:

(1) Reviewed the literature on cognitive task analyses and identified required for DSS development for GEOINT analysts' operations.

(2) Developed supporting visual analytic models for object detection in satellite images.

(3) Developed micro-cognitive networks for individual knowledge levels identified by cognitive task analyses.

(4) Used a Bayesian belief network analytics to determine and integrate subjective belief estimates of IAs.

(5) Developed a visual analytic cognitive model (VACOM) interface and conducted a usability study.

1.5 Research Questions

In this research, the following hypotheses statements were investigated:

1. There are statistical differences between the visual analytic tools used in the satellite image processing.

   This hypothesis seeks to explain the differences between four image processing methods. They are the histogram methods (RGB and HSV) and the non-histogram methods (CCV and eCCV). Data for the hypothesis is obtained by processing the same satellite images using the different methods. The dependent variables are accuracy, precision, and recall data often use din image analyses.

2. There are statistical differences between human confirming beliefs with the visual analytic tools.

   This hypothesis seeks to explain the differences in human confirmation beliefs to the outputs and supports from the visual analytic tools. Walkthrough experiments in which "an expert" confirms the output of visual analytics will be conducted.

3. There are statistical differences between GEOINT decision analysts with and without visual analytics.

   In this hypothesis, satellite images are presented to the human analysts to select objects that best match closely with their experience and mental model. A list of objects is presented to trigger their mental models. The analysts then use the visual analytics to do the same thing. Records are kept on the decision accuracy of the analysts.

1.6 Intellectual Contribution

This study is expected to lead to a set of theoretical frameworks that explore the relationship between cognitive performance and information visualization in reconnaissance tasks. Therefore, the study brings the following intellectual contributions:

1. Discovers the knowledge management (KM) bottlenecks often associated with spatial cognitive tasks.
2. Captures the latent abilities of human knowledge characteristics and suggest efficient representation for computational analysis.
3. Develops a method for cognitive understanding of geographic information system and the coupling sensemaking process.
4. Develops a method for visualizing human metal information processing in spatial domains.
5. Reveals the expert's insights (tacit knowledge) in internal mental processing of spatial tasks.

1.7 Broad Impact

This study has some broad impacts as follows: (a) reveals how the intelligent analysts understand and interpret geospatial information; (b) provides an understanding of modeling human cognitive networks with respect to geospatial information; and (c) reveals how to improve spatial information assets management. For example, in intelligence collection, analysis, and production with respect to a domain application.

There are many ongoing researches in 2D domain of satellite images. However, 3D image views bring a new era of feature detection and recognition as shown in Figure 1. It is considerably complicated to computationally derive all dimensions of colors and depths, but it gives the human operator a better visualization and quick cognitive process during a task processing. For instance, Fukushima Daiichi nuclear power plant that had a nuclear disaster after the 9.0 magnitude earthquake and following tsunami of March 11 in Japan. The situation was highly risky and dangerous to reach in order to investigate the accident at that moment.

Figure 1. Advance technology: 3D view of Google Earth at Fukushima nuclear power plant in Japan.

Decision makers in command and control centers rely highly on satellite images or air images from helicopters and airplanes. With a decision support system, the decision makers could be aided to identify many spatial characteristics of the nuclear facility image.

1.8 Chapter Summary

This chapter presented the general idea of IAs and their tasks. The motivations for this study were stated to solve the research problems of satellite information characteristics in modeling IAs. This chapter also introduced the research study, its goals and objectives. Three research questions were introduced to validate this dissertation works. The merits of this study were introduced.

1.9 Organization of Dissertation

This dissertation is organized as follows. Chapter 2 provides the past studies of cognitive task analyses (CTAs). CTA methods are used to recognize at knowledge levels of task

processing used by the GEOINT analyst. Chapter 3 introduces the analytical methods to support enhanced image processing. The data fusion using Bayesian belief network is introduced. Chapter 4 presents the design of VACOM and Bayesian belief network implementations. Chapter 5 presents the implementation of the VACOM interface and the description of interface components. Chapter 6 presents the VACOM functionality, and experimental design to validate usability. Chapter 7 presents the research summary, discussion of results, research limitations, research conclusions, and suggestions for future researches.

CHAPTER 2

Cognitive Task Analysis for the GEOINT

2.1 Background

In any of the major cognitive tasks related to GEOINT, the analysts are likely to deal with various levels of uncertainties at different levels of information abstraction (Vicente & Rasmussen, 1992, p. 589). These are identified as follows:

(1) Familiar events are routine in that analysts experience them frequently. As a result of a considerable amount of experience and training, the analysts have acquired the skills required to deal with these events.

(2) Unfamiliar, but anticipated events occur infrequently and thus analysts will not have a great deal of experience to rely on.

(3) Unfamiliar and unanticipated events are unfamiliar to the analysts because they rarely occur.

Given the above requirements, it is necessary to first recognize the knowledge levels in which the satellite analysts operate. This will help decision support designers in developing visualization tools to enhance the cognitive processes associated with the derivatives of intelligence from satellite imagery. In fact, converting satellite images into human intelligence is a part of human actions which requires an unobtrusive situational awareness. As noted by philosophers Allen (1983) and Searle (1983), a human action is constructed as being consequent upon planned behaviors and for a purpose. Along this line of thought, the purpose of interpreting satellite images is for specific actionable and contextual intelligence. The processes of conducting this exercise are defined by many steps of correlated cognitive activities. On the other hand, a human activity is what a group of people engages in to achieve a certain purpose

(Bodker, 1993); this is certainly true because the interpretations of satellite images are often performed by a team of intelligence analysts.

The purpose of converting satellite image data into information visualization is to enhance the analyst's situational and informational understanding of the context so as to support relevant intelligence activities. While scientific visualization allows analysts to view multiple dimensions of data representation, the visual displays are intolerant and insensitive to meaningfulness of information in context. Both situation and information understanding, as we think of it, include, e.g., (a) building cognitive codes to provide situation cognition, (b) making sense of a situation based on interpretation of available information, and (c) validating the utility of information based on experiences and beliefs of the analysts. From the IA perspective, the concept of a reconnaissance operation requires real-time segmentation of satellite information into meaningful chunks of intelligence for different operational applications.

2.2 Theory of Knowledge Levels

If the observations of Vicente and Rasmussen (1992) are followed, then, cognitively, human processes information at different knowledge levels. Knowledge entails what we know. Barr and Feigenbaum (1981) describe knowledge as data structures and interpretive procedures, which, if appropriately coordinated and executed, can result in some intelligent behavior. Engelkamp, Seiler, and Zimmer (2005), associate knowledge to cognitive processes stored as memory events, actions and episodes that, when retrieved and manipulated, can be used for exemplar-type problem solving and decision making. From human terrain understanding, anthropologists Allen (1975) and Asch (1952) defined knowledge as a collection of world experiences regulated by cultural norms and regulations.

Poppler (1969) first introduced the concept of knowledge as three worlds. He described World 1 as consisting of the physical objects and events; World 2 as the world of mental objects; and World 3 representing the world of the products of the human mind (e.g., decision processes). Newell (1982) introduced the notion of knowledge level to categorize behaviors and the kinds of knowledge that produce such behaviors. Used in the context of designing intelligence agents, Newell described an agent as having a set of objectives, a set of possible actions, and a body of knowledge. He associated intelligence to how well an agent can operate at each of the knowledge levels. It includes meeting a set of objectives or goals, taking actions using approximate behaviors that are adequate to solve the problem at hand, including being able to build its own body of knowledge as a result of lessons learned. The knowledge level is defined as being a level above the symbol or programming level.

Both Poppler and Newell developed their knowledge levels from Polanyi's tacit knowing concepts (1966) who described tacit knowledge as what someone knows as a result of experience, beliefs, and values. Tacit knowledge can generate actionable knowledge and is therefore most valuable to the expert intelligence analyst. Furthermore, tacit knowledge is the focus point for the generation of new knowledge in novel situations. According to Nonaka (1991, p. 96), "the key to knowledge creation lies in the mobilization and conversion of tacit knowledge." When satellite images are interpreted using the analyst's tacit knowledge, useful intelligence can be derived for many levels of applications, for both the civilian and military communities.

Extending the knowledge level hypotheses from the artificial intelligence and philosophy to cognitive engineering, Endsley (1995) recognized situation awareness (SA) operating at three-tier levels of knowledge: 1) perception of the information elements in the environment, i.e., the

states, attributes, and dynamics of relevant elements in the operator environment; 2) comprehension of the current situation by information processing, based on a synthesis of disjoint level 1 elements, by putting them together to perform patterns that get a holistic picture of the environment and an assessment of the current state; and 3) projection of future states on the basis of actions of elements in the environment. In the context of the satellite image analyst, perception simply occurs when looking at the photograph images. At the comprehension level, the analyst is engaged in the sensemaking process of conceptualizing and linking previously known situations to the satellite image at hand-hypothesizing, conducting pattern associations, and making "expert" guesses for interpretation of the image data. The projection state involves making linkages based on sensitivity analysis such as "what if" situations. For instance, when an image is rotated in a certain angle, does the same interpretation hold under invariants of the image features?

Holyoak and Thagard (1996) have identified two types of knowledge: implicit and explicit. Implicit knowledge is generally unconscious and relatively effortless. Procedural knowledge is implicit while declarative knowledge is explicit. Declarative information is stored as facts. Explicit knowledge requires thinking and reasoning. This makes it possible for us to selectively focus on specific attributes of objects and on relations between objects, rather than being limited to reacting to global similarities between objects (Holyoak & Thagard, 1996, p. 21). Using explicit knowledge often requires noticeable consumption of mental effort. Cognitive scientists and philosophers (Macdonald, 1995) claim that, in some instances, individuals do not have explicit knowledge of rule-based behaviors. Instead, certain individuals have the distinctive marks of a rule-following activity, as opposed to mere regularity, or mere physiological processes, since knowledge is located at a deeper level of consciousness.

This claim is important in discerning how the intelligence analysts perform their tasks.

2.3 Cognitive Task Analysis (CTA)

In order to understand how people act upon the world around them, it is necessary to understand what goes on in their mental processes. This process may arrive from simple or complex task situations. It is also important to find out how humans think, what humans know, how humans organize a structure of information, and what humans search for to understand better. Cognitive task analysis (CTA) helps us to understand these important cognitive aspects.

A cognitive task analysis is a process used to describe the mental process of the experts which represents the abstractions of their knowledge. The abstractions are constructed by a hierarchical information structure which is a categorization of concepts according to relationships, roles in the organization/system, and ranks. Rasmussen (1986) introduced the 'abstraction hierarchy' (AH) which is the method to decompose a system as the generic/abstract tokens with forms and functions. The decomposing of system behaviors are based on their functional properties, relations, and physical laws of the universe.

Cognitive task analysis (CTA), as the name implies, is the analysis of types of cognitive tasks and cognitive resources required to perform a task. The GEOINT analyst's tasks fit these criteria. The following suggested CTA (Randel, Pugh, & Wyman, 1996) procedures are employed throughout the GEOINT analyst knowledge process:

- development of a cognitive task process model, which was accomplished by reviewing GEOINT analyst tasks;
- development of an information flow model using task diagrams and information processing flow diagrams;

- performance of a misconceptions analysis by reconciling convoluted terminologies and stratification of intelligence products according to the stakeholders; and,
- performance of a structural knowledge analysis by developing conceptual maps or cognitive network representations of the GEOINT analysis knowledge levels.

MacLeod et al. (2005) identify three steps to a good CTA:

1. Knowledge Elicitation (KE) techniques used to discover, elicit, and understand the forms of specific work tasks and their properties (Hoffman et al., 1995);
2. Formal techniques for the analysis, depiction, validation, and improved understanding and use of task knowledge (Schraagen, et al., 2000);
3. Constructs of mental models, often computer based, to assist the understanding of human task concepts (Pew & Mavor, 1998).

From the three steps above, Crystal and Ellington (2004) observed that a CTA represents "an attempt to capture task expertise" (p.4). By seeking to capture the high-level cognitive functions (Militello and Hutton, 1998) used by the experts.

Schraagen et al. (2000) noted that a CTA, is used to describe the knowledge, mental processes and goal structures underlying observable task performances. At the system development level, Stanton et al. (2005) suggested that tools and protocols based on CTA method are useful to design a system and analyze its performance. Militello and Hutton (1998) associated CTA to describe and represent the cognitive elements that underlie the goal generation as different from physical task analysis techniques. In general, a CTA describes the cognitive processes which are associated with cognitive skills, or mental demands required to perform a task efficiently in complex domains (Militello & Hutton, 1998; Stannon et al., 2005; Prasanna et al., 2009). CTA methods can decompose complex tasks or information to select,

inspect, simplify, abstract, and transform information for developing explanations and extracting meaning to construct the cognitive models for the decision support. Table 1 summarizes the advantage and disadvantage of CTA.

Table 1

Advantages and disadvantages in CTA approach (adopted from Clark et al, 2006; Klein, 2000)

Advantages	Disadvantages

▪ A CTA generates detailed, precise information on the nature of expert performance in a specific task of interest.
▪ When implemented correctly, CTA techniques are highly valid sources of information on the expert cognitive processes.
▪ A CTA provides systematic procedures (rather than hit-or-miss steps) for ascertaining expert cognitive processes.
	▪ Analysis of the data gathered during a CTA can be time-intensive.
	▪ CTA does not always capture other non-cognitive attributes necessary for achieving results such as,
	  ▪ physical capabilities, access to resources, and interpersonal relationships.
	▪ The results of a CTA can be misleading when expert performers have performance capacities beyond that of others
	  ▪ for example, a CTA can be done with high performing professional athletes but implementation of cognitive processes alone will not duplicate performance.

2.4 Application of CTA and Knowledge Level Theory to GEOINT Analysts

A cognitive model (CM) is supposed to represent and mimic the human mental process. For example, how human makes sense out of ambiguous or contradictory message. Most likely, humans use experiential knowledge to compare patterns (pattern matching, pattern recognition, etc.) and making guesses using expert knowledge (heuristics). This scenario defines a cognitive simulation. Such simulation can be obtained by interlacing different knowledge levels and CTA strategies into network structure. As observed by Steyvers and Tenenbaum (2005), such a

cognitive network structure requires the knowledge of relationships between objects of knowledge, including their interrelated characteristics.

Figure 2 describes a framework for integrating knowledge level (KL) theory and CTA process.

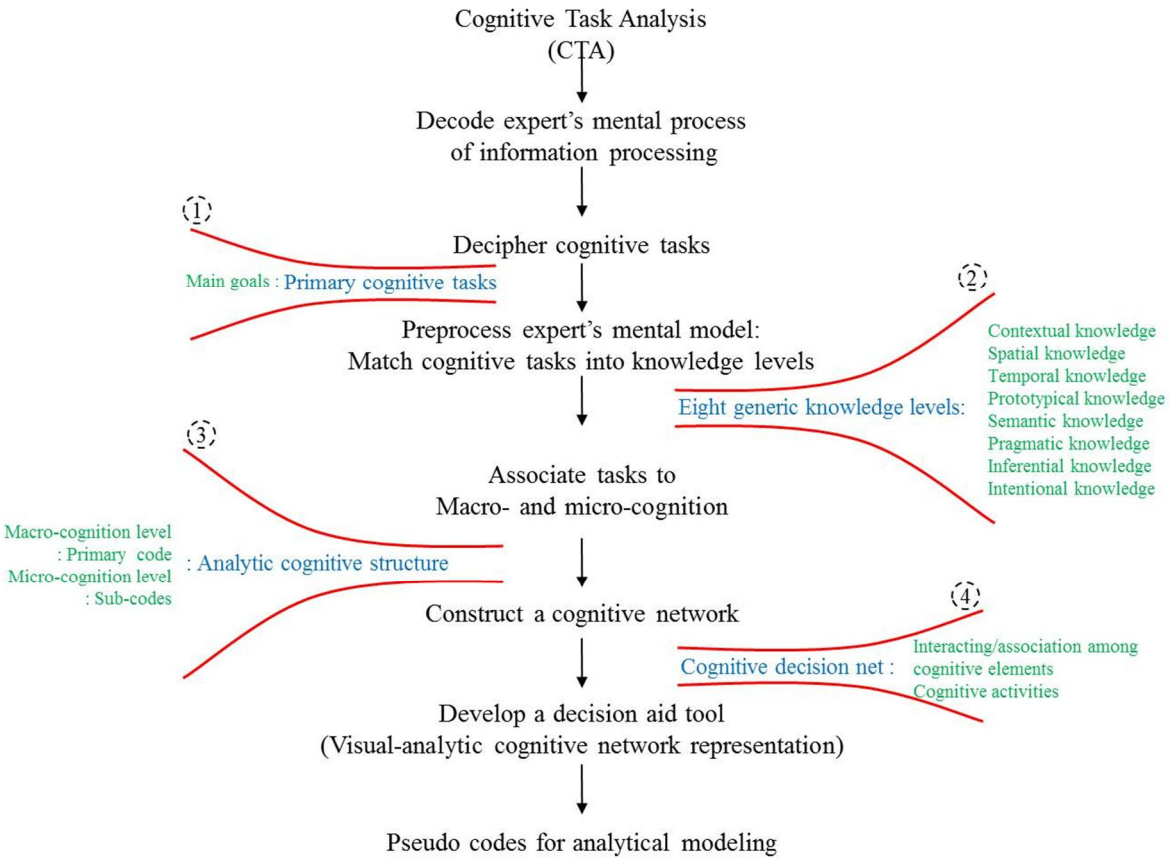

Figure 2. A comprehensive overview of analytic-cognitive process for supporting geospatial intelligence analyst.

The cognitive elements of Figure 2 are discussed below. The CTA is used to reveal human activities required for the primary cognitive tasks. Step 1 identifies the primary tasks of the analysts with respect to satellite information processing. This is available in the number of standard operating procedure (SOP). In step 2, identification is made of conceptual knowledge levels that shape the building blocks of micro- and macro-cognition. In step 3, the micro- and

macro-cognitive network structures are identified as sub-codes. A combination of sub-codes leads to a conceptual network. In the step 4, network representation methods are integrated. Chapter 4 of this dissertation shall give more details applications of Figure 2. In the next section, illustration is presented on the qualitative application of KL and CTA.

2.5 Cognitive Analytics Using Knowledge Level Theory

From the discussion of CTA, we have identified knowledge elements responsible for satellite information processing based on the cognitive task framework. The knowledge elements are spatial, prototypical, contextual, temporal, semantic, pragmatic, intentional, and inferential, respectively (Park & Ntuen, 2011). This is shown in Figure 3. A summarized description of each knowledge level follows.

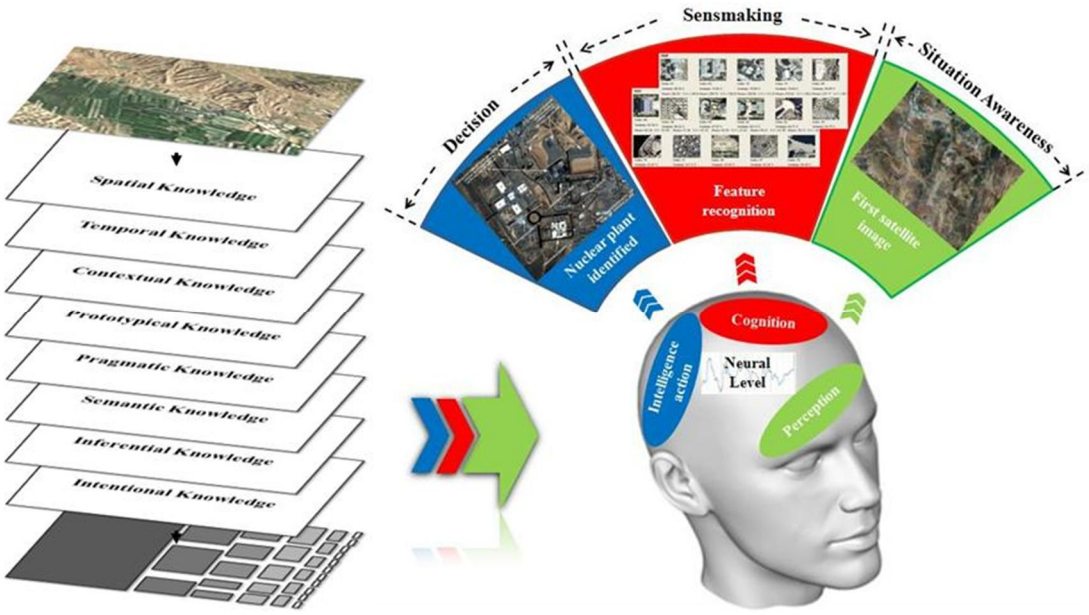

Figure 3. The conceptualized knowledge levels.

Cognitive task analysis (CTA), as the name implies, is the analysis of types of cognitive tasks and cognitive resources required to perform a task. Gott (1994) suggests that CTA only be used in situations where the task is complex, dynamic, unstable, ill structured, and difficult to learn

because the action occurs in the mind of the performer. The GEOINT analyst's tasks fit these criteria.

2.5.1 Spatial Knowledge. Spatial knowledge is about object location in space. Locations are natural ways of organizing data with important relationships or connections to other data. Burkhard (2004) observed that learning from architects, spatial knowledge has at least four utilization problems: (a) information depth due to a trade-off between an overview and details that need to be communicated, (b) limited time constraints, attention and memory capacity of the recipients, (c) different background caused by geospatial features of the surround, and (d) relevancy mitigated by the cognitive ability to discern important information by the decision maker. Figure 4 is an example of spatial knowledge from a satellite image. At this level, image processing is often used as the first of many processing steps to reveal significant typical features based on Level I situation awareness (SA) processing (Endsley, 1995).

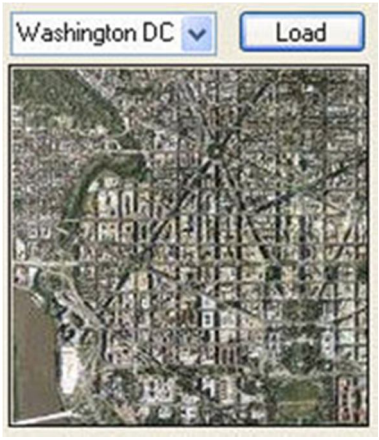

Figure 4. A sample spatial image.

2.5.2 Contextual Knowledge. Contextual knowledge has a composite situation cognition task because the analyst uses information within a defined context to create a sequence of situated actions or activities. Situatedness (Clancey, 1997; Suchman, 1987) holds that "where you are, when you do, what you do matters". By reviewing a satellite image, the analyst is

concerned with locating everything in a context so that the decisions are a function of both the situation and the way the situation is constructed and interpreted. The cognitive processes required to adapt to such changes must be dynamic because situations may change over time. This change is dependent on the constructive memory of the analyst which holds that memory is not a static imprint of a sensory experience, but is subject to continuous changes due to new information stimuli (Dietrich & Markman, 2000). As described by Malhorta (2001), by understanding a situation, we can form the conceptual link between information available and the expected result or anticipation of task outcomes. Figure 5 shows an example of contextual knowledge as indicated with a blue rectangle marking an area of interest.

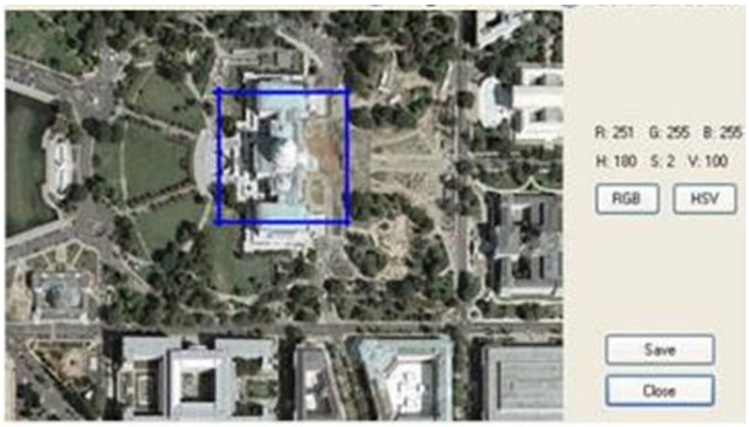

Figure 5. A contextual knowledge from elaborated area of interest.

2.5.3 Temporal Knowledge. A few seconds of satellite data sampling may yield millions of informational objects to be processed. For a real-time application, such as in the battlefield, time becomes a temporal constraint to the analyst. Decortis and Keyser (1988) noted that in order to make decisions in such a system, a model to support reasoning about temporal events must be formulated. Such models should help one a) reason about changes, b) predict the effects of actions and the changes, and c) continuously make reference to what has happened, what is happening (current events), and what might be happening (future events).

2.5.4 Prototypical Knowledge. Prototypical knowledge represents an exemplar of a conceptual class. The class characteristic is determined by the similarity of an object's attributes to the category's prototype. For example, a robin is a typical bird, whereas a chicken is not. Therefore, the prototype knowledge of the analyst, with respect to a particular satellite image, would represent a default value or a concept about the image based on some mental models associated with such objects. An example in identifying a hostile aircraft from a satellite image can clarify this point. Various concepts associated with this task include engine type, wing position, wing shape, tail, and bulges. A military cargo transport aircraft may likely have a conventional wing shape, whereas a civilian Boeing 747 is swept-back. Figure 6 illustrates an example image that may resemble a facility of intelligence interest.

Figure 6. An example image of a prototypical knowledge.

2.5.5 Semantic Knowledge. Semantic knowledge is the use of concepts and properties of objects to associate meaning and interpretation to contextual events in time and space. In cognitive psychology, images and concepts constitute the dominant building blocks of thought that make such associations possible. For example, when one is 'thinking about" a car, he or she must have formed a mental category of the type of car and the conceptual connection of the car to one's preference of model, size, color, etc. Conceptual structures and mental models, although interpreted as distinct and parallel, usually converge to form the knowledge used in the formation of semantic knowledge (Sowa, 1984). Theoretically, it is tied to a specific context and how the

use of lexicons, linguistic terms, and languages of one concept relates to, influences, or allows an individual or a group of people to gain a first level of interpretation of contextual information. In this respect, Berkeley (1710) notes that meaning exists in one's mind and it is often difficult to explain-an observation that leads to the paradigm that "we know more than we can tell" (Polyani, 1966, p. 4). Polanyi describes the semantic aspect of tacit knowing, how meaning tends to be displaced away from ourselves and toward the external. Meaning is also realized through the process of how we describe things, objects, events, and so forth. Meanings are embedded in language through semantic and syntactic descriptions of objects and their features (Macdonald, 1995). Figure 7 shows how semantic and syntactic knowledge emerge from two similar views of a satellite image.

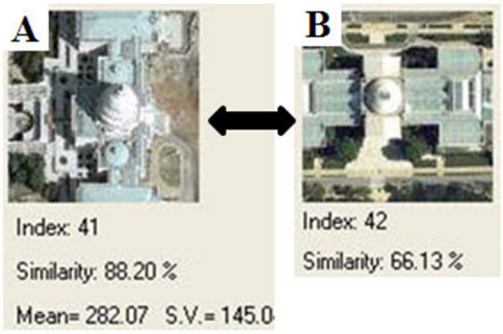

Figure 7. Semantic and syntactic comparison of images by their statistical mean features.

2.5.6 Pragmatic Knowledge. Pragmatic knowledge is the knowledge of practice and is a derivative of lessons learned from experience. The truthfulness and validity of the analyst's intelligence production is highly predicated on the expertise level of the analyst. This is considered a significant practical consequence relevant to the vital components of meaning and truth assessment. An immediate example is the testimony of General Powell to the United Nations on February 5, 2003, using satellite images to illustrate the possibility that Iraq may have been manufacturing weapons of mass destruction.

This led the U.S. and its allies to invade Iraq and depose Saddam Hussein, leading to the Iraqi Conflict or the Second Gulf War.

2.5.7 Inferential Knowledge. The need for the analyst to make quick inferences about an object of interest remains central to visual analytic designs. In general, most of the analyst's tasks are interpreting and assigning meaning to satellite images through a plausible diagnostic process. A diagnostic task is an example of an application of multiple reasoning that may include abductive-, deductive-, and inductive- techniques, respectively. In some cases, knowledge required for diagnostic reasoning is often incomplete, uncertain, and imperfect, leaving the analyst to estimate information through mental models. The primary way for making an inference in a satellite image diagnostic task is by abduction-a form of reasoning that seeks satisficing (Simon, 1960) and plausible explanations to phenomena. Abduction was developed (Peirce, 1931) to help explain scientific phenomena in four stages: (1) observation of an anomaly, (2) abduction of hypotheses for the purpose of explaining the anomaly, (3) inductive testing of the hypotheses in experiments, and (4) deductive confirmation that the selected hypothesis does predict the original anomaly. In this view, in addition to being a form of inference, abductive reasoning also constitutes a "logic of discovery" which describes how hypotheses are formulated and the subsequent cause-effect reasoning to confirm them (Ntuen, Park, & Kim, 2010).

2.5.8 Intentional Knowledge. Intentional knowledge is the object of goals or end states to be achieved for specific tasks. For example, it could be a strategic goal, an operational goal, or a tacit goal; all or some may occur concurrently. In teleological theories of intent (Davis, 1979), the act justifies the means. This is the basis for the general concepts of intentional systems which act with some sort of explanatory behaviors designed to mimic intelligent human behaviors such

as those exhibited by the GEOINT analysts. For example, an intelligent analyst may be asked to verify whether a satellite image, such as the one shown in Figure 8, is a nuclear facility or a government building.

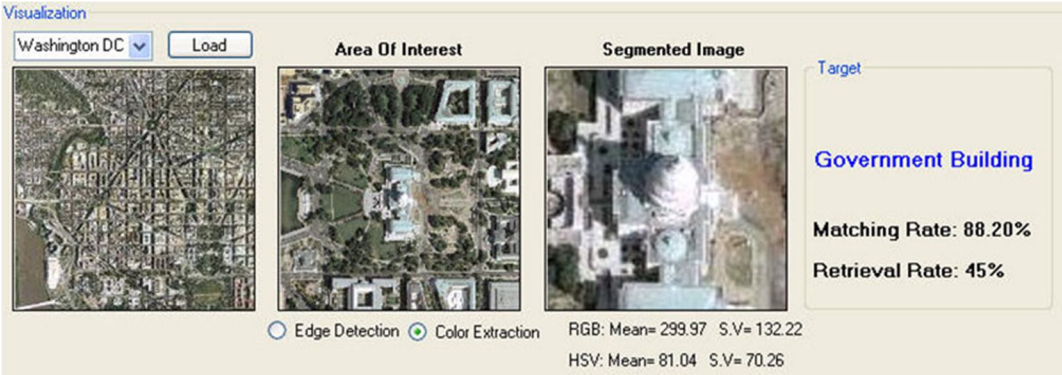

Figure 8. An example image to support an intentional objective.

2.6 Chapter Summary

This chapter presented the past studies on cognitive task analyses. Especially it uses the CTA methods to identify at least eight knowledge levels of task processing, a requirement of the GEOINT analyst. The eight-macro cognition levels are spatial, temporal, contextual, prototype, pragmatic, semantic, inferential, and intentional, respectively. Spatial ability, enabled by visualization, is the ability of an individual to view and make sense of object images. Temporal knowledge is identified with respect to how the analysts cope with time-based information changes. Contextual knowledge is situated and is a function of experience and is exposed to similar tasks. Prototype knowledge provides the standard for the analyst to instantiate his/her working memory and makes instant first-hand comparisons of what is known and unknown. Pragmatic knowledge is a function of expertise and skill derived in similar tasks. Semantic knowledge deals with the analyst's information sharing and communication with respect to situation description. Inferential knowledge is analyst dependent, each having a different way to diagnose situations and make conclusions. Intentional knowledge relates to the analyst and

system-level's (mission) goals as translated to intelligence requirement analysis for different applications. By using CTA, expert's mental process of information processing is decoded to decipher primary cognitive tasks (primary knowledge nodes), subtasks (sub-nodes) as knowledge elements (cognitive codes), which are summarized in Table 2.

Table 2

A summary of GEOINT analyst knowledge levels for a satellite map

Knowledge level	Task (Goal)	Knowledge element (cognitive code)	
		Prime-node (Macro-cognitive level)	Sub-node (Micro-cognitive level)
Contextual knowledge	State the hypothesis or intention of interest.	Situation cognition and understanding (information)	• Context: hypotheses • Situation (area of interest): location, space geometry
Spatial knowledge	Select an area of interest in the map for analysis.	Location and space geometry	• Developmental features (populated size): city, town, village, and metropolis • Geographical features: Forest, desert, coast, river, mountain (valley, rock, etc.) area • Military domain features: Cooperative (friendly), uncooperative area • Religious feature: Catholic, Islam, Hindu, Others
Temporal knowledge	Use known patterns to determine relations such as in the mobility of target object, emergence (appearance) or disappearance objects.	Patterns in time series; Recorded frame on image	• Static (stationary): non-periodic time with single image • Dynamic (active): periodic time by the time, day, month, and so on with multiple images

Table 2

(cont.)

Knowledge level	Task (Goal)	Knowledge element (cognitive code)	
		Prim-node (Macro-cognitive level)	Sub-node (Micro-cognitive level)
Prototypical knowledge	Use available similar prototypes as samples to compare with scenes from area of interest.	Database of prototypical objects and images	• Key feature (of a set of target object)-partial form of features (e.g. building, vehicle, missile launch, nuclear plant, etc.)
Semantic knowledge	Interpret concepts of contextual events in time and space.	Usually operational goal statement	• Lexicons • Linguistic terms • Descriptions
Pragmatic knowledge	Recognize practical implication of objects of interest.	Associate mental map with landmarks	• Analytical expertise of the analysts: Image interpretation, Pattern recognition.
Inferential knowledge	Makes inference about object of interest on the satellite image and confirm with the situated goal.	Diagnostic tasks; Compare operation goals to tactical requirement	• Abductive-technique • Deductive-technique • Inductive-technique
Intentional knowledge	Decide to accept or reject the hypothesis.	Intentional goals	• Strategic goal • Operational goal • Tactical goal

CHAPTER 3

Supporting Analytical Models

3.1 General Idea of Satellite Image Classification

With the advancement of science and technology, information processing methods, information storage capacities, and information retrieval techniques has increased and digital information has become a real demand in industrial, medical, and other applications (Wen & Tan, 2008). For the last few decades, digital image processing has been widely used in a variety of applications such as in information extraction from satellite images (Ooi & Lim, 2006; Singha & Hemachandran, 2011). For instance, the high resolution image acquired by aircraft from satellites are used in various applications as in assessment and environment monitoring such as classifying land uses, monitoring crop and forest harvests, tracking beach erosion, and determining regional geological structures (Boesch & Wang, 2008; Ooi & Lim, 2006; Shan, Berthod, & Giraudon, 1999).

Satellite images usually have a higher resolution than general purpose images because of the complexity. Furthermore many classical image analysis techniques have become inefficient. The classical classification methods do not provide satisfactory results, leading to relatively high rates of misinterpretation to various research fields of satellite imagery (Shan, Berthod, & Giraudon, 1999; Sapkal, Bokhare, & Tarapore, 2012).

Consequently, many papers have been published on this subject and numbers of algorithms are used to process satellite images in digital image processing. These algorithms manipulate the raw images and convert them into desired information. To extract features from satellite images, digital image processing follows the general image classification process as described in Figure 5. An input image is processed to smooth a source image and reduce noises.

The preprocessed image is decomposed (segmented) to distinguish meaningful partitions. The segmented image is to further understand the salient features. The satellite image classification follows this general image process.

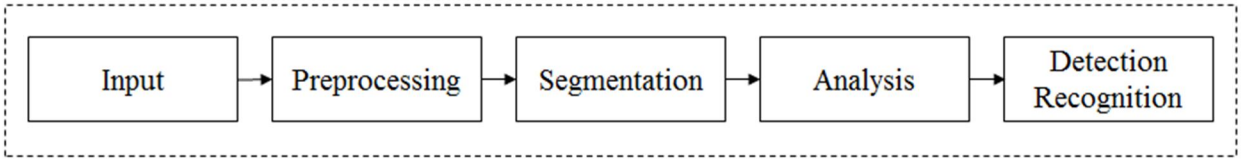

Figure 9. The architecture of general image processing.

The key factor to image classification is image segmentation. Image segmentation is a process of partitioning image pixels based on selected image features with homogenous features and with potential semantic contents (Kurugollu, Sankur, & Harmanci, 2001). Image segmentation is generally based on one of the intensity values of comparing images such as discontinuity and similarity (Rigau, Feixas, & Sbert, 2004). Segmentation is an important task to optimize the results of classification in pattern recognition and computer vision. In order to improve the results of image segmentation, researchers have employed different color techniques. For the robust image segmentation, a hybrid method that combines edge-based and region-based segmentation in satellite images segmentation has been previously proposed by other researchers (Ooi & Lim, 2006).

Kurugollu, Sankur, and Harmanci, (2001) applied a unique histogram method with multiband image for color image segmentations. This method has been widely used in various applications such as document image processing (O' Gorman, 1994), Magnetic Resonance (MR) image analysis (Tsai et al., 1995), quality inspection (Sezgin et al., 1997), video signal analysis for spatio-temporal segmentation (Altunbasak et al., 1998) and color palette design (Wan et al., 1990; Gentile et al., 1990; Balasubramanian et al., 1994). To improve the automatic extraction problem, Mena and Malpica (2005) empolyed a color texture algorithm for image segmentation.

This method is the interweaving of color information in the three bands with different order statistics and color coordinate systems. Rigau, Feixas, and Sbert (2004) proposed an information theoretic framework for image segmentation. This technique can retrieve information channel between pixel characteristics such as pixel's intensity and spatial position of the object's image. Recently, the combined techniques of image features for segmentation have received attention (Chang & Wang, 1996; Stefania, Ilaria, & Marco, 1999; Carson et al., 2002). According to Jolly and Gupta (1996), image features, which fuse color and texture features, can improve segmentation results for satellite image applications. Ooi and Lim (2006) proposed a new approach with color and texture features for segmentation using the fuzzy *c*-means clustering algorithm.

3.2 Color Scheme Methods for Image Analyses

According to Ooi and Lim (2006), "monochromatic" satellite imagery is not an effective source for image classification because it does not contain enough information for distinguishing objects. Different images having similar monochromatic values can lead to an inaccurate segmentation (Ooi & Lim, 2006). Unlike monochromatic, color satellite imagery provides additional information in the image (Schunders, 1997). Schunders (1997) claimed that color image increases the visual appeal of images because the human vision system is much more sensitive to small difference in color. The characteristic of color provides high sensitivity to the human eye, whereas the characteristic of non-color produces low sensitivity on human eye (Wickens et al., 2003). Non-color image is in effect indistinguishable in many cases.

The uses of color or multispectral satellite images have increased in many applications (Ooi & Lim, 2006). Therefore, the interests for color spaces have naturally increased, too. A color space is "a way of representing colors and their relationship to each other" (Van der Weken

et al., 2005). Different image processing systems use different color models for different reasons to solve particular problems, such as noise reduction, deblurring, and compression (Van der Weken et al., 2005). As an example, recently Ooi and Lim (2006) studied satellite image retrieval be means of new image segmentation, using new color based on fuzzy clustering. The following subsections introduce the most commonly used color spaces and their transformation employed in this research.

3.2.1 Common Color Spaces. YCbCr color space: The first common color space is YCbCr that is widely used for digital video digital photography systems (Poynton, 1996). Each single component of YCbCr is similar to RGB. The Y component represents the intensity of the light. The Cb and Cr components indicate the intensities of the blue and red components relative to the green component. A generic algorithm of color conversion from RGB to YCbCr is followed by the matrix equation as shown in Equation 1 (Poynton, 1996; Foley et al., 1990).

$$[Y \quad Cb \quad Cr] = [R \quad G \quad B] \begin{bmatrix} 0.299 & -0.168935 & 0.499816 \\ 0.587 & -0.331665 & -0.418531 \\ 0.114 & 0.50059 & -0.081282 \end{bmatrix} \tag{1}$$

CIELAB color space: The second common color space is CIELAB (Edward & Thomas, 1997). CIELAB color space is also known as CIEL*a*b* color space, where L^* denote lightness, a^* is a value from red to green, and b^* is a value from blue to yellow (Ooi & Lim, 2006), which was developed from the XYZ color space. CIELAB values are computed from each color component of XYZ that is followed by Equation 2. The subscript *n* of color suggests "normalized". These are the color values Xn, Yn, and Zn, in which the subscript *n* of color suggests "normalized" and are referred to the white point with the D65 standard (Edward & Thomas, 1997). CIELAB color space is computed for each component by means of Equation 3-6.

$$[X \quad Y \quad Z] = [R \quad G \quad B] \begin{bmatrix} 0.412453 & 0.357580 & 0.180423 \\ 0.212671 & 0.715160 & 0.072169 \\ 0.019334 & 0.119193 & 0.950227 \end{bmatrix} \tag{2}$$

$$L^* = \begin{cases} 166\left(\frac{Y}{Y_n}\right)^{1/3} - 16, & \text{if } \frac{Y}{Y_n} > 0.008856 \\ 903.3\left(\frac{Y}{Y_n}\right), & \text{if } \frac{Y}{Y_n} \leq 0.008856 \end{cases} \tag{3}$$

$$a^* = 500\left[f\left(\frac{X}{X_n}\right) - f\left(\frac{Y}{Y_n}\right)\right] \tag{4}$$

$$b^* = 200\left[f\left(\frac{Y}{Y_n}\right) - f\left(\frac{Z}{Z_n}\right)\right] \tag{5}$$

where,

$$f(x) = \begin{cases} x^{1/3}, & \text{if } x > 0.008856 \\ 7.787x + \left(\frac{16}{116}\right), & \text{if } x \leq 0.008856 \end{cases} \tag{6}$$

3.2.2 Color Histogram: RGB & HSV. Color histogram (Shapiro & Stockman, 2003; Pass & Zabih, 1999) is the most widely used image processing method for image comparison. Color histogram can be a useful representation for the purpose of image retrieval or object recognition (Shapiro & Stockman, 2003). It is basically a segmentation process and is used to preserve the maximum information of an image with the minimum number of colors (Rigau, Feixas, & Sbert, 2004). Pass, Zabih, and Miller (1996) introduced the usefulness of color histogram and discussed why and how it became a popular method. Color histograms are computationally trivial to compute, small changes in camera viewpoint tends not to effect color histograms; additionally, different objects often have distinctive color histograms. However, color histograms also have some limitations such as carrying no spatial information, poor recognition on similar histogram, and poor computation power with larger database.

Many studies in computer vision and image processing have investigated color histograms. For example, Swain and Ballard (1991) proposed the method of color histogram matching for object recognition. Hafner et al. (1995) also used color histogram to develop an efficient method for weighted-distance indexing. Using color histogram, Stricker and Swain (1994) analyzed the information capacity and sensitivity of object colors.

A histogram of a color image is used for image feature analysis. A histogram search characterizes an image by its color distribution. A color space is defined as a model for representing color in terms of intensity values. For color histogram methods, two color spaces, Red-Green-Blue (RGB) and Hue-Saturation-Value (HSV), are applied. The RGB color model is composed of the primary colors, Red, Green, and Blue. This system defines the color model that is used in most color Cathode Ray Tube (CTR) monitors and color raster graphics. They are considered the "additive primaries" since the colors are added together to produce the desired color and it is useful for directed attention management of the human operators (Hess, Dakin, and Field, 1998). The hue and saturation components are intimately related to the way the human eyes perceive color, resulting in image-processing algorithms with a physiological basis. As "hue" varies from 0 to 1, the corresponding colors vary from red, through yellow, green, cyan, blue, and magenta, and back to red, so that there are actually red values both at 0 and 1. As "saturation" varies from 0 to 1, the corresponding colors (hues) vary from unsaturated (shades of gray) to fully saturated (no white component). As "value", or brightness, varies from 0 to 1, the corresponding colors become increasingly brighter.

The color histogram for an image is constructed by counting the number of pixels of each color. The color histogram intersection was used for color image retrieval in the prototype visual analytic model design. The intersection value is normalized by dividing the number of pixels of

the model to get a match value. Other similarity measures can be defined; for example, the histograms can be normalized into frequencies by dividing each bin count by the total number of pixels and then use the Euclidean distance to compare two images $d(h, g)$.The intersection of image histograms (h) and a model histogram (g) is mathematically given by (Swain & Ballard, 1991):

$$d(h,g) = \frac{\sum_A \sum_B \sum_C \min\left(h(a,b,c), g(a,b,c)\right)}{min(|h|,|g|)} \tag{7}$$

where $|h|$ and $|g|$ gives the magnitude of each histogram, which is equal to the number of samples; a, b, and c of $h(a, b, c)$ represent the three color channels which is either RGB or HSV.

Colors that are not represented in the user's query image do not contribute to the intersection distance, therefore, it reduces the contribution of background colors. The sum is normalized by the histogram with fewest samples. Figure 10 shows two color images and histograms with 26-bins for HSV and 24-bins for RGB color scheme.

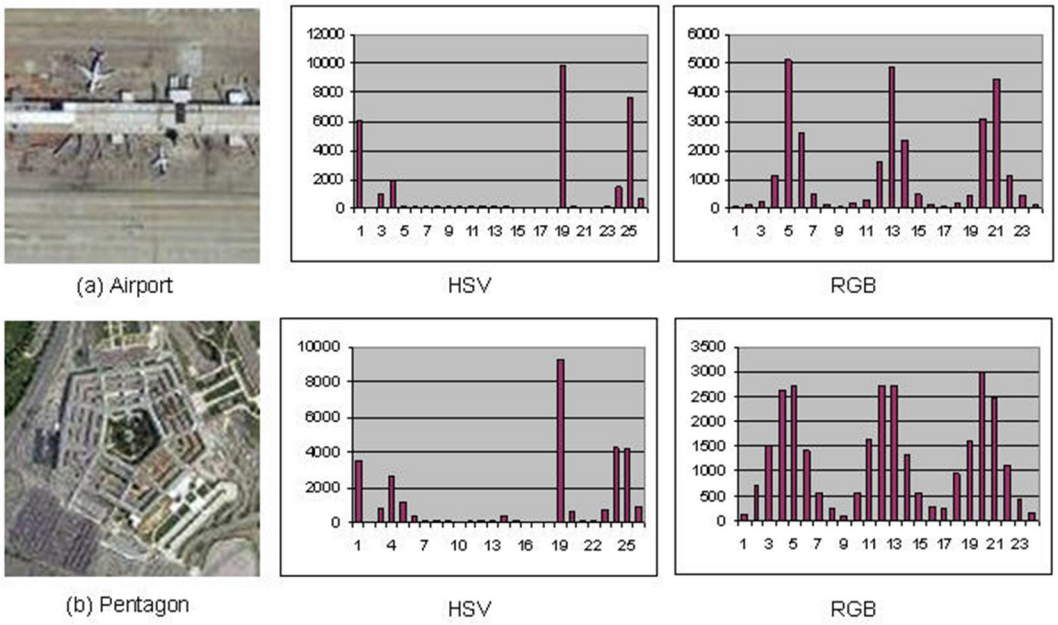

Figure 10. Color images and their histograms, 26 bins HSV (18-Hue, 4-Saturation, 4-Value) and 24 bins RGB (8-Red, 8-Green, 8-Blue).

The image is from a Google Earth satellite image. The experimental results in Figure 10 follow the procedure of the general image retrieval system as shown in Figure 11. Once a query image is captured from the Google map, the rest of the process is done automatically. However, the histogram data for all images in image databases are pre-calculated and saved in separate files in advance, so that only the image indexes and histogram data can be used to compare the query image with images in the databases.

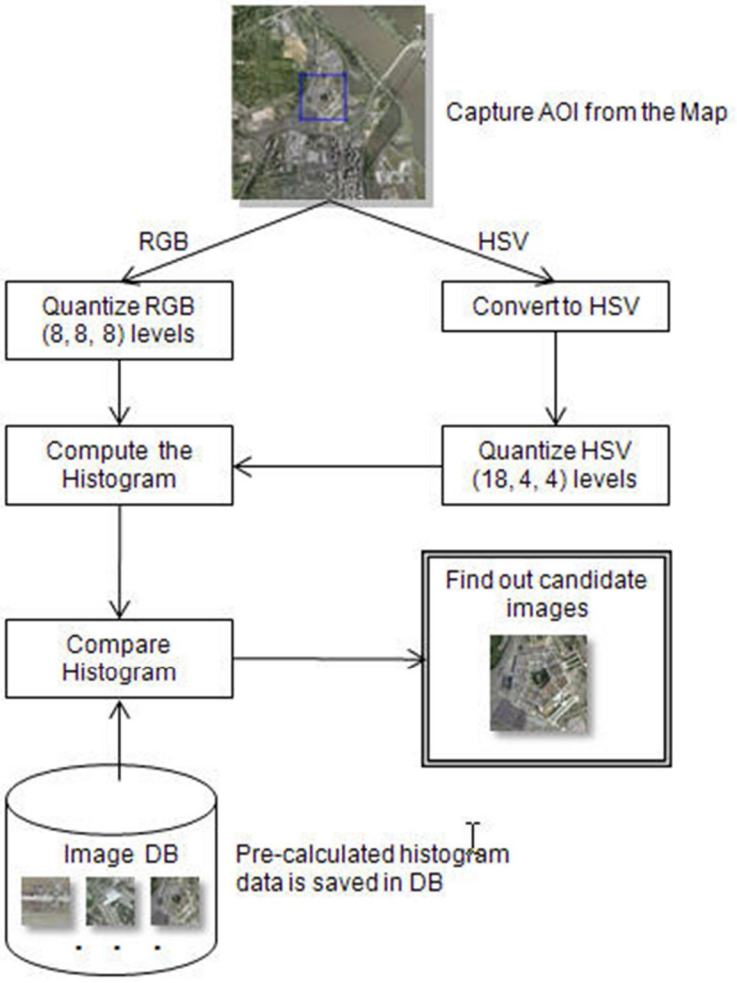

Figure 11. The fundamental algorithmic for implementing image processing as a part of visual analytics (adapted from Jeong, 2001).

Figure 12 describes the implementation of color histogram that provides statistical evaluations for retrieval effectiveness between a query image and the database.

Figure 12. Example of retrieval effectiveness in (a) RGB and (b) HSV color space.

3.2.3 Color Coherence Vectors (CCV). Pass, Zabih, and Miller (1996) defined "a color's coherence" as a member of large similarity-colored regions for classifying pixels as either coherent or incoherent. At this point, the numbers of vectors are generated to measure the coherence of pixels. The vectors are named in color coherence vectors (CCV). As stated by Wen and Tan (2008), CCV is commonly used for image retrieval method. CCV is easy to compute and appear to perform much better than color histograms even though it uses a histogram-refinement approach (Wen & Tan, 2008). Pass, Zabih, and Miller (1996) introduced "color coherence vectors (CCV)" method to compare images. This particular method is color-based, which is similar to color histograms. Unlike color histograms, we have a low rate of image

retrieval under similar histograms because CCV has more efficient rate of image retrieval. With a given color, the differences of both methods are that a color histogram counts the number of pixels and a CCV measures the spatial coherence of the pixels (Pass et al., 1996). Wen and Tan (2008) proposed a new CCV approach that uses the multi-CCV mixing location information as the indexing vector to enhance the similarity measure using the efficiency of indexing. However the original CCV (Pass et al., 1996) method is a candidate for use as a cognitive model to support analysis of satellite images for supporting expert-based decision aids.

The initial stage in computing a CCV is similar to the computation of a color histogram. First, an input image is blurred slightly by replacing pixel values with the average value in a small local neighborhood including the 4 adjacent pixels such as left, right, up, and down. The color space is then discretized the color space, such that there are only *n* distinct colors in the image. Next, classifying the pixels within a given color bucket (*n* distinct colors) determine either coherent or incoherent pixels. A coherent pixel is a part of a large group of pixels of the same color, while an incoherent pixel is not. The computing of connected components determines the pixel group. Two pixels are considered adjacent if one pixel is among the four closest neighbors (left, right, up, and down) of the other, then the same color of pixels are labeled with the same alphabets (e.g., A, B, C,…and R). Connected components can be computed in a single pass over the image. The pixels are then classified as either coherent or incoherent depending on the size in pixels and its connected component. A pixel is coherent if the size of its connected component exceeds a threshold τ; otherwise, the pixel is incoherent. Thus, for a given discretized color, some of the pixels with that color will be coherent and some will be incoherent.

Mathematically, a CCV algorithm (Pass et al., 1996) is described as follows. Let the *j*'th discretized color α_j and β_j represent the number of coherent and incoherent pixels respectively.

The total number of pixels with that color is equal to $\alpha_j + \beta_j$. A color histogram would summarize an image as $[\alpha_1 + \beta_1, \alpha_2 + \beta_2, \cdots, \alpha_n + \beta_n]$. The coherence pair for the *j*'th color computes a pair of (α_j, β_j). The color coherence vector for the image consists of $[(\alpha_1, \beta_1), (\alpha_2, \beta_2), \cdots, (\alpha_n, \beta_n)]$.

In this dissertation, some pixel thresholds are used (100, 150, and 200) to determine whether a pixel is coherence or incoherence. However, the threshold, τ may be used differently depending on the image database. For example, for *n=9* buckets, we have an evenly distributed RGB color space. Here, images in database are scaled to contain 10,000 pixels.

In order to compare CCVs of two images for searching and retrieval, let two of images *I* and I'have CCV's G_I and G_I'. From Pass et al. (1996):

$G_I = [(\alpha_1, \beta_1), (\alpha_2, \beta_2), \cdots, (\alpha_n, \beta_n)]$ and $G_I' = [(\alpha_1', \beta_1'), (\alpha_2', \beta_2'), \cdots, (\alpha_n', \beta_n')]$

Color histogram will compute the difference *I* and I' as

$$\Delta_H = \sum_{j=1}^{n} \left| (\alpha_j + \beta_j) - (\alpha_j' + \beta_j') \right| \quad (8)$$

The method for comparing is based on the quantity

$$\Delta_G = \sum_{j=1}^{n} \left| (\alpha_j - \alpha_j') \right| + \left| (\beta_j - \beta_j') \right| \quad (9)$$

A given color bucket *j* contain the same number of pixels in *I* as in I', i.e. $\alpha_j + \beta_j = \alpha_j' + \beta_j'$ but these pixels may be entirely coherent *I* and entirely incoherent in I'. In this case $\beta_j = \alpha_j' = 0$ and while $\Delta_H = 0, \Delta_G$ will be large. In general, $\Delta_H \leq \Delta_G$. Applying the triangle inequality $d(x + y) \leq d(x) + d(y)$, we have

$$\Delta_H = \sum_{j=1}^{n} \left| (\alpha_j - \alpha_j') + (\beta_j - \beta_j') \right| = \Delta_G \quad (10)$$

For searching and retrieving a query image, CCV method is used to find best relevant image from the database. The result of analysis represents best one in first order and then the rest of candidate images will be followed after the first one. Query image, which is the input image, is

entered into the image database for comparison purposes. The algorithm researches the database to find all the images that closely match the query image. The similarity measure Δ is a factor that finds a correct retrieval image from the database, as given by Equation 11. If a perfect images match is found, the similarity measure Δ points at '0'. If no images within the database match the query image, the similarity measure Δ becomes 'a high number'.

$$\Delta = \sum_{j=1}^{n} \left| \frac{\alpha_j - \alpha'_j}{\alpha_j + \alpha'_j + 1} \right| + \left| \frac{\beta_j - \beta'_j}{\beta_j + \beta'_j + 1} \right| \tag{11}$$

Figure 13 describes the overview of color coherence vector (CCV) process. A blur image is reduced to the number of pixels. After reducing the pixels, we use *n=9* distinct colors (buckets) to discretize the color space. As shown in Figure 13, the discretized color space computes the connected components to label color regions as highlighted in the same labels. The labeled image may become the last image of Figure 13.

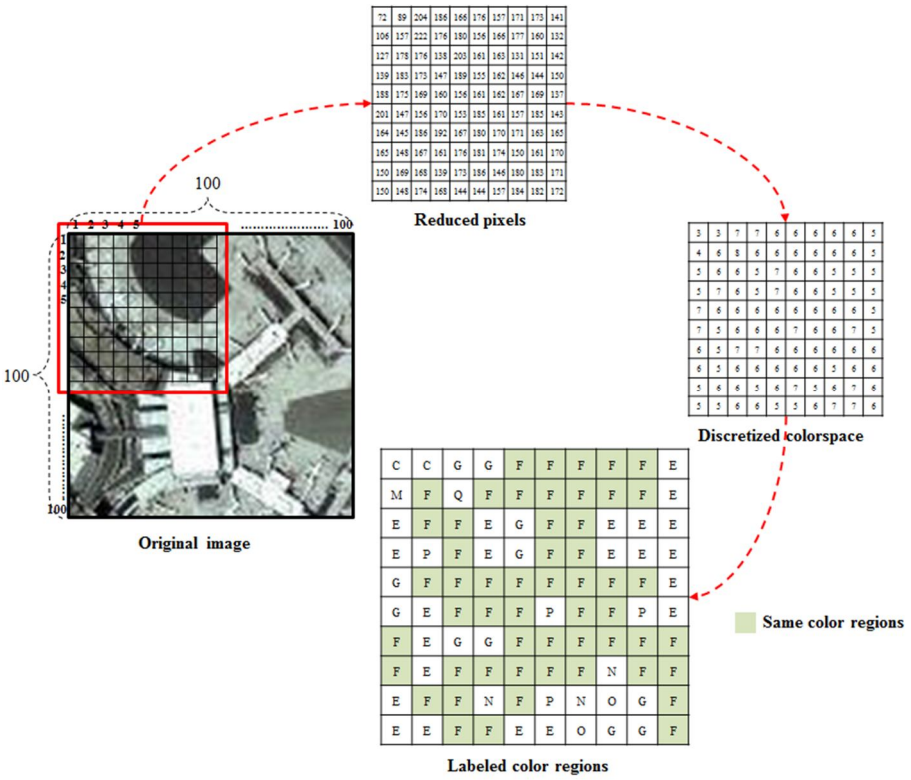

Figure 13. The overall scheme of CCV algorithm approach.

Based on the labeled image, we are able to create a table of connected components as described in Figure 14. Alphabets A to I represent coherent pixels and alphabets J to R represent incoherent pixels respectively in each coherent pixel (e.g, J is the same color as A, but J is not coherent). To determine each coherent pixel, we use the threshold (τ=200 pixels) on the example in Figure 14.

Label	A	B	C	D	E	F	G	H	I	J	K	L	M	N	O	P	Q	R
Color (Bucket)	1	2	3	4	5	6	7	8	9	1	2	3	4	5	6	7	8	9
Size	1238	2526	283	396	675	1393	2114	169	8	51	133	195	197	219	208	109	75	11

Figure 14. Connected components table.

Based on the determination of coherent and incoherent pixels, CCV tables are constructed as shown in Figure 15. For example, if a pixel size is less than the threshold (τ=200), the pixels add to β incoherent column of color. If pixel size is larger than the threshold, the pixels add to α coherent column of color (as shown in Figure 15). In other words, the highlighted pixels represent the incoherent colors, so those colors are placed in β incoherent column of color. The non-highlighted pixels represent the coherent colors, so those colors are placed in α coherent column of color.

Color (Bucket)	1	2	3	4	5	6	7	8	9
α	1238	2526	283	396	894	1601	2114	0	0
β	51	133	195	197	0	0	109	244	19

Figure 15. Color coherence vector (CCV) table.

Based on the 'CCV table' in Figure 15, a vector set of the $[(1238, 51), (2526, 133), (283,195), \cdots (0,19)]$ is created with the representation $G_I =$

$[(\alpha_1, \beta_1), (\alpha_2, \beta_2), \cdots, (\alpha_n, \beta_n)]$. By using CCVs, we compute a similarity measure between two images of vector sets (G_I and G_I') using Equation 11.

Table 3 describes sample results of comparing CCV's which is based on the calculation of similarity measures between query input image and a database. As shown in Table 3, the query image compares with 30 images in the database.

Table 3

Sample computations of similarity measure

Rank	1	2	3	4	5	…	30
Image # of Database	19	17	20	15	7	…	28
Similarity (Δ)	1.2940	2.4761	2.5481	3.2001	3.9172	…	14.1274

Figure 16 shows sample results, which is the procedure for image retrieval and similarity measure. In this procedure, a query image was entered and compared with each of the 30 images in the database and the algorithm searched and selected all images with a sufficient similarity, as shown in Figure 16 below.

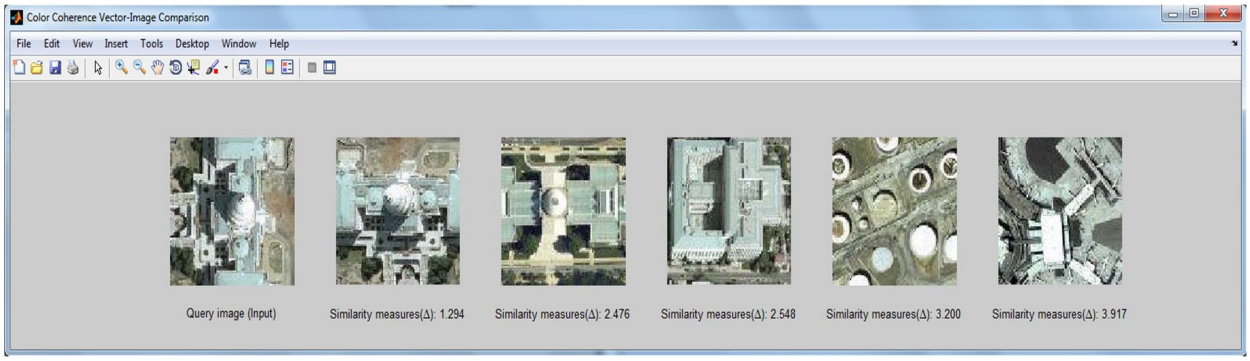

Figure 16. Example of search and retrieval image process.

Computed similarity measures are sorted from lowest to largest similarity. Candidate images within the top 5 are displayed in Figure 16. The similarity with the lowest Δ factor is the best selected image among the candidates as shown Figure 16 and Table 3.

If the similarity indicates a large Δ factor number, it means that the compared image is not close to the query image.

3.2.4 Proposed Enhancement Segmentation to CCV (eCCV). The proposed new method combines color space and feature segmentation. The process undergoes two stages of color space transformation that has a different approach from the existing color space transform approaches. Both color schemes 1 (RGB to YCbCr) and 2 (YCbCr to CIELAB) are common color space transformations in image classification research fields. Briefly explained, in the process of generating a new color space, the transformed YCbCr color space replaces the original RGB colors space to process the second color space transformation as described in Figure 17. The color models (RGB, YCbCr, CIELAB, and new color space) are represented as three-color components respectively. The color components (e.g., RGB- R, G, B, YCbCr- Y, Cb, Cr, CIELAB- L^*, a^*, b^*) are used in color space transformation for mapping from one color component of the original color space to another color component of the expected color space. Mathematically, the new color space is modeled by Equations 12 and 13. A^{-1} denotes an inverse matrix that come from YCbCr transform matrix by Equation 1. The process for generating a new color space is similar to CIELAB color space transformation (Color scheme 2) as described in Figure 17.

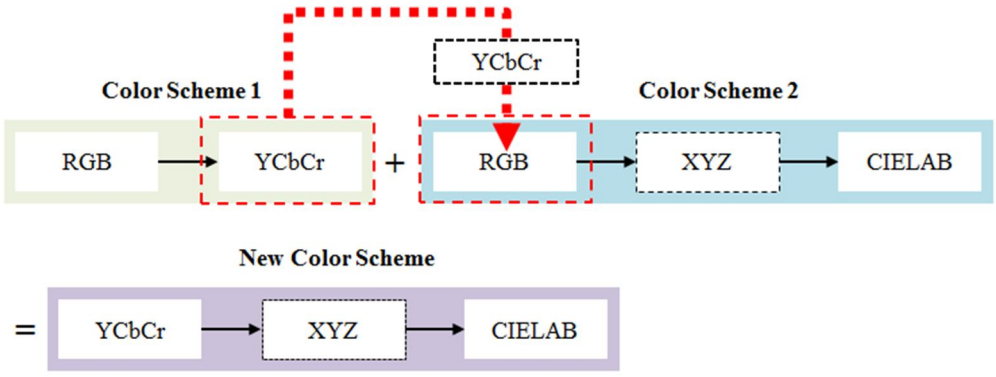

Figure 17. A diagram of color mapping for generating new color scheme.

The new color space also uses Equation 2 to Equation 6. However, Equation 2, $[R \quad G \quad B]$ is replaced by Equation 13 to generate the new color space.

$$A^{-1} = \begin{bmatrix} 1.0000 & 1.0000 & 1.0000 \\ 0.0000 & -0.3437 & 1.7699 \\ 1.4025 & -0.7144 & 0.0000 \end{bmatrix} \tag{12}$$

$$[R \quad G \quad B] = [Y \quad Cb \quad Cr] \times A^{-1} \tag{13}$$

From the new color space, a robust color mapping method is generated between the color models; the results serve as input to the new image processing. In image processing for cognitive model, the robust color mapping with new color scheme is used.

As reported in the literature (Ooi &Lim, 2006), there are many color mappings and color spaces that each one of them use for that purpose. Each study may use different color spaces due to the identical color characteristics. As Ooi and Lim (2006) stated, the selection of an apporiate color space is also important as much as the use of the effectiveness in segmentation algorithm. Ooi and Lim (2006) have conducted asystematic experiment to determine the relevant color space that best fits their application. They explored most of the commonly used eight color spaces such as RGB, XYZ, YIQ, YcbCr, HSV, HIS, $I_1I_2I_3$ and CIELAB. They proposed the qualitative measurement method based on human subjective evaluation to judge the fitness of a color space by using CIELAB.

In this dissertation, RGB, HSV and the new color space are applied to the image processing algorithm. Even though CIELAB provide the best color space (Ooi & Lim, 2006), it is not appropriate for use in satellite image analysis. Figure 18 shows the evaluation results of test images which inspire the idea for the enhanced color coherence vector (eCCV). Figure 18 represents different color spaces by Matlab implementation. The different color spaces have their own characteristics to apply in this study. As shown in Figure 18, even with the naked eye, the human can perceive the differences between color spaces of the images.

Figure 18. Example of color spaces within same image: RGB (left), YCbCr (center), and CIELAB (right).

YCbCr changes the orignal image to a lower color intensity image. CIELAB changes the orginal image to grouping pixels of similar color intensities that easily distinguish the area of interest from the environment. As explained, the benefit of both color mapping (YCbCr and CIELAB) is that these color mappings can enhance human visual recognitions. The proposed algorithm of image segmentation based on the new color mapping is given by Table 4.

Table 4

A proposed algorithm of segmentation using a robust color space

Algorithm: procedure
Read image I_{RGB}: a query image (input)
Convert a color space of original image (I_{RGB}) to I_{YcbCr}.
Convert a color space of I_{YcbCr} to I_{CIELAB}
Simplify colors of new color space by binary colors ('black' and 'white')
Set up a threshold (τ) to determine a binary image of each dimension.
If $a_{i,j}^{new}$ of the three dimensions> τ
'255' (white) ← $b_{i,j}$ of the three dimensions
Else if $a_{i,j}^{new}$ of the three dimensions < τ
'0'(black) ← $b_{i,j}$ of the three dimensions
End
: all three color dimensions become binary images; $I_b \rightarrow (I_{b^1}, I_{b^2}$, and $I_{b^3})$
Create a mask using binary images
M ← Compare each pixel of I_b: $b_{i,j}^1,\ b_{i,j}^2,\ and\ b_{i,j}^3$
If $b_{i,j}^1,\ b_{i,j}^2,\ and\ b_{i,j}^3$ have a pixel in the same location
$mask_{i,j}$ ← '255'
Else
$mask_{i,j}$ ← '0'

Table 4

(cont.)

18:	End
19:	Mapping a mask into original image
20:	$I_{RGB} \leftarrow mask_{i,j}$ (pixels consists of '0' and '255')
21:	If $mask_{i,j}$ have '0'as a pixel
22:	$I_{RGB} \leftarrow$ '0' pixel in the same position of $M\,(mask_{i,j})$
23:	: Identify a region (interest of area) with 'black' color
24:	Else if $mask_{i,j}$ have '255'as a pixel
25:	$I_{RGB} \leftarrow$ '255' pixel in the same position of $M\,(mask_{i,j})$
26:	: Identify a environment with 'white' color
27	End
28:	: Have segmented images
29:	End image segmentation

The proposed segmentation with a robust color space was applied to the eCCV algorithm. The segmentation is described as follows. The digital image, I (I_{RGB}), is commonly represented as n × m (2-dimensional array) matrix with element a_{ij}, $I = \{a_{i,j};\ i = 1,\cdots,n,\ \ j = 1,\cdots,m\}$. Each element of image (I_{RGB}), a_{ij} is called a pixel. $a_{i,j}^{new}$ denotes a pixel of new color space; the new color space has three color dimensions with threshold, τ defined as

$$\tau = \frac{\max\left(a_{i,j}^{new}\right)+min\left(a_{i,j}^{new}\right)}{2}, \text{ for } i = 1,\cdots,100, j = 1,\cdots,100 \quad (14)$$

The small number of image pixels can increase the computational time of comparing pixels. Therefore, as described in Equation 14, we use the pixels threshold (τ) to assign color space elements (e.g., black or white space). If a pixel of the $a_{i,j}^{new}$ is greater than the threshold (τ), then the pixel of the $a_{i,j}^{new}$ is transformed into the white pixel $b_{i,j}$ as defined Equation 15.

$$b_{i,j} = \begin{cases} 255 & if\ \ a_{i,j}^{new}\ \ \geq \tau \\ 0 & if\ \ a_{i,j}^{new}\ \ < \tau \end{cases}, \text{ for all three color dimensions} \quad (15)$$

From the Equation 15, $b_{i,j}$ represents a scaled pixel of a binary image I_b in the algorithm step 11. Based on the simplified color spaces (I_b), a mask, $M = \{mask_{i,j};\ i = 1, \cdots, n,\ \ j = 1, \cdots, m\}$, is created as described in algorithm steps 12 to18. A three dimensional binary image with elements (I_{b^1}, I_{b^2}, and I_{b^3}) are combined by Equation 16.

$$mask_{i,j} = \begin{cases} 255 & if\ \ b_{i,j}^1,\ b_{i,j}^2,\ b_{i,j}^3 = a\ pixel\ in\ the\ same\ position \\ 0 & otherwise \end{cases} \quad (16)$$

The mask M is a mapping that controls the direction for segmentation either to area of interest or an environment. If the $mask_{i,j}$ have 0, $mask_{i,j}$ overwrites 0 into a_{ij} of I_{RGB} in the same position. The areas of interest are set to a black color, and the remaining areas are kept as original color information. If $mask_{i,j}$ have 255, $mask_{i,j}$ overwrites 255 into a_{ij} of I_{RGB} in the same position, the environments (non-target areas) are set to white color and the remaining areas are kept as original color information.

Figure 19 depicts a segmentation process based on the proposed color mapping and segmentation algorithm. After the algorithm generates the color space, three color dimensions are retrieved. To reduce color intensities, the color dimensions are converted into binary images (black and white images) based on the threshold. Then, a decision mask for segmentation of the query image is created by converting to binary images from the previous step. Once a binary mask is created, the mask compares each single pixel with the original image pixels to construct mapping images. The mapping images are segmented into two categories such as a white mapping and a black mapping which distinguish the boundaries of the object. The white mapping describes the environments of objects including the non-target background, and turns it into a white color on these areas. The black mapping describes those objects with target foreground, and turns them into black color on these areas. The process generates a prototype image database to be used to compare with a query image.

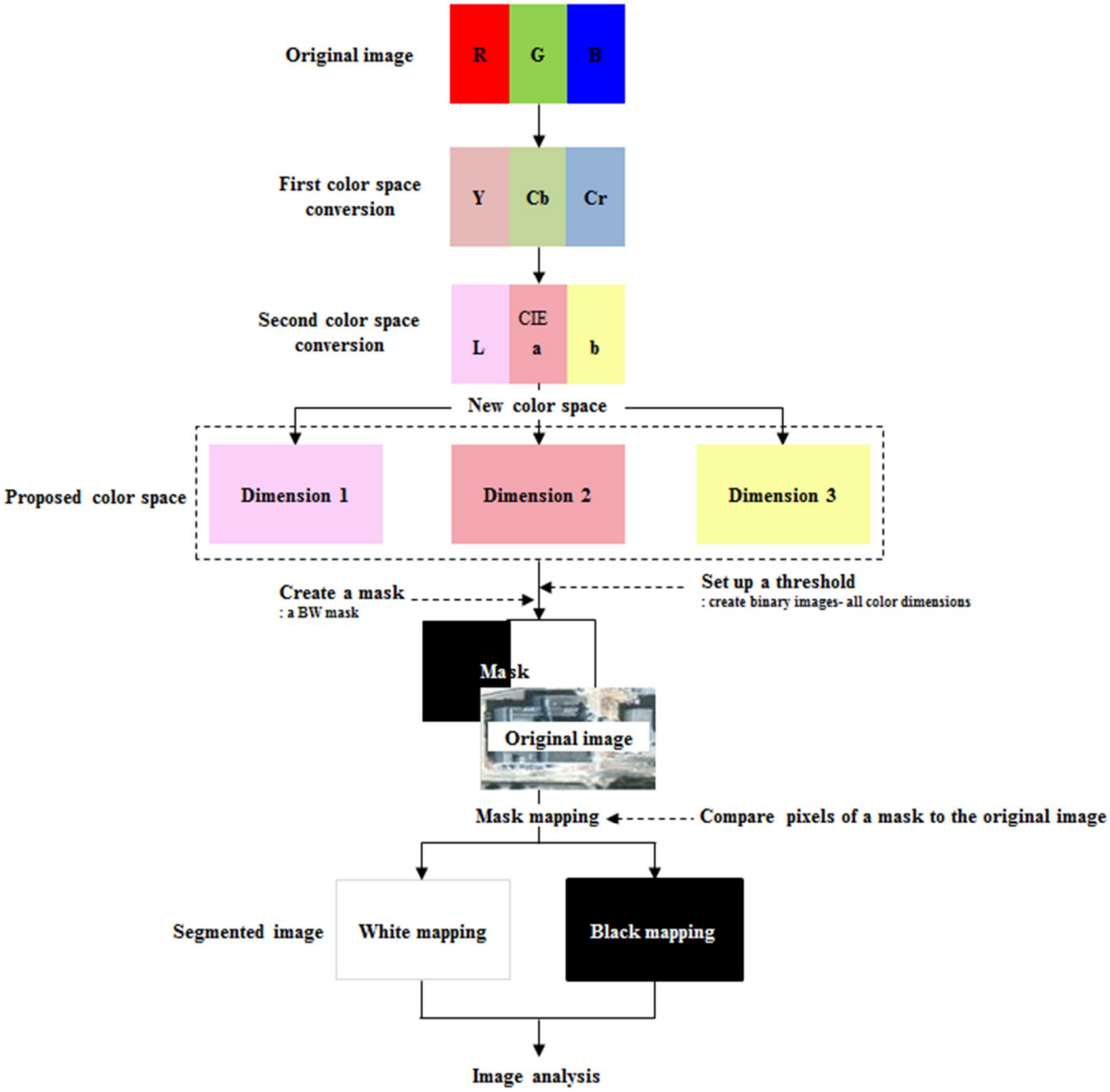

Figure 19. A segmentation based on the robust color mapping.

The Matlab implementation of the proposed color mapping is shown in Figure 20. As shown in Figure 20, during a color space transform, spatial regions are effectively distinguished as dimensions. Based on the Matlab implementation, the proposed color space method is expected to achieve less computational time, and salient regions of images can be effectively extracted. Moreover, the implementation is expected to result on a clear vision of segmented results.

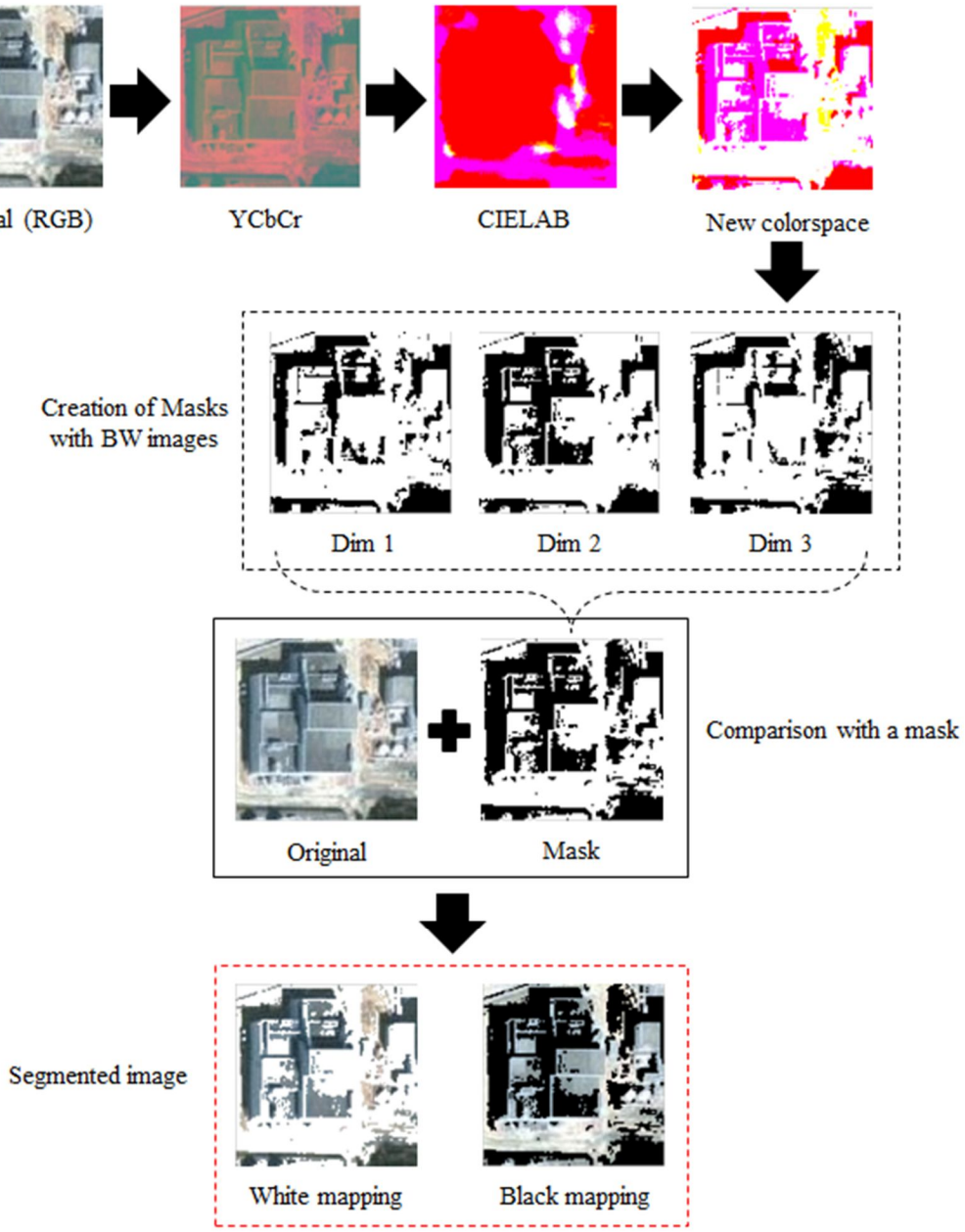

Figure 20. A Matlab implementation of segmentation based on the robust color mapping.

3.3 Comparing Image Analysis Methods for Use as Visual Analytics

The comparison metrics are used to measure the performance of image processing algorithms (RGB, HSV, CCV, and eCCV). The sample simulation experiments are discussed in the following sections. The meta-analysis is used in the comparisons of different color image characteristics to verify the benefits of eCCV.

3.3.1 Comparison Metrics. The performance of the algorithm is based on recall and precision as shown in Table 5 (Wynne, Chua, & Pung, 1995). Recall signifies the relevant images in the database that are retrieved in response to a query. Precision is the proportion of the retrieved images that are relevant to the query. Both recall and precision are defined as conditional probabilities in Equation 17 and 18.

Table 5

Summarized in terms of comparison metrics (adopted from Wynne, Chua, & Pung, 1995)

	Relevant	Not Relevant
Retrieved	A (Correctly retrieved)	B (Incorrectly retrieved)
Not Retrieved	C (Missed)	D (Correctly rejected)

$$recall = \frac{relevant\ retrieved}{all\ relevant} = \frac{A}{A+C} \tag{17}$$

$$precision = \frac{relevant\ retrieved}{all\ retrieved} = \frac{A}{A+B} \tag{18}$$

$$accuracy = \frac{A+D}{A+B+C+D} \tag{19}$$

With these conditions, image retrieval is said to be more effective if precision values are higher at the same recall values. The accuracy of identified image is determined by using Equation 19.

3.3.2 Sample Simulation Experiments. It is hypothesized that the proposed color space method (eCCV) is expected to produce more salient features for effective image extraction, and its performance is expected to be better than CCV, RGB, HSV methods on the selected metrics of performances such as precision, recall, accuracy, and similarity. We carried out some experiments to get the retrieval effectiveness for image verification using the different four

methods. The database used for simulation had 100 images obtained from Google Earth. The images are categorized into groups of similar features as airport, oil finery, government building, dams, and nuclear facility. The details of image database will be discussed in Chapter 6.

The experimental results are shown in Figure 21. Once a query image is captured from the Google map, it was compared with a database of prototype images. The retrieval process provided the statistical metrics and displayed the candidate images from the database to assist the human analysts during object identification tasks. The candidate images were displayed to the analyst based on the similarity ranks. The highest rank score indicated the closeness of the query image to the prototype.

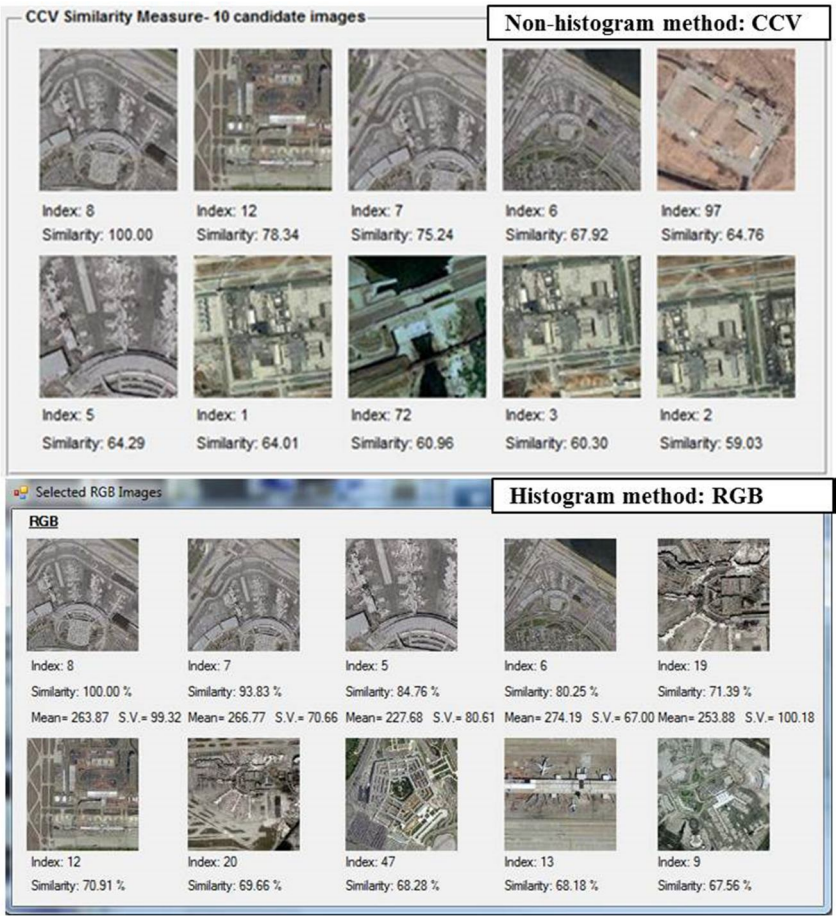

Figure 21. Example of retrieval effectiveness in non-histogram (CCV) and histogram (RGB) methods.

3.3.2.1 Results of comparing multi-methods. Table 6 and 7 show the statistics (accuracy and precision) of each image retrieval methods. The result of recall was excluded because a recall value is exactly half of a precision rate. The values in Table 6 and 7 showed the accuracy and precision rates for each method.

Table 6

Accuracy statistics for different color algorithms

Target	Accuracy			
	RGB	HSV	CCV	eCCV
Cat.1: Airport	81.1	79.9	82.1	79.2
Cat.2: Oil refinery	86.5	84.4	83.1	78.8
Cat.3: Gov. Building	81.0	84.7	80.8	78.6
Cat.4: Dams	80.7	78.0	77.8	77.9
Cat.5: Nuclear Facility	76.3	77.2	80.1	79.1

Table 7

Precision statistics for different color algorithms

Target	Precision			
	RGB	HSV	CCV	eCCV
Cat.1: Airport	57.0	49.5	60.5	46.0
Cat.2: Oil refinery	82.5	72.0	65.5	44.5
Cat.3: Gov. Building	55.0	73.5	54.0	43.0
Cat.4: Dams	53.5	40.0	39.0	39.5
Cat.5: Nuclear Facility	31.5	36.0	50.5	45.5

The experimental results showed that none of the methods were superior to other methods with respect to accuracy. eCCV was the only method that had the lowest of accuracy and precision values. It was unexpected that eCCV would produce the poorest results of the comparison

metrics. The precision metrics was proportional to the ratio of the accuracy to increase and decrease its results. The one-way ANOVA also confirmed that there were no significant difference in accuracy rates between the different image verification methods, $F(3,16) = 0.83$, $p = 0.5024$ ($\alpha = 0.05$). The precision metrics was highly correlated to the accuracy. Therefore, we only used accuracy value to conduct statistical test.

Figure 22 and 23 displays a comparison of accuracy and precision rates from the 100 images. As shown in Figure 22, the ranges of accuracy rates varied from minimum value of 76.3 to maximum value of 86.5. The results showed that histogram methods (RGB and HSV) have better accuracy outcomes and much higher range of precision rates from minimum value of 76.3 to maximum value of 86.5. The non-histogram methods had the range of precision rates between minimum value of 77.8 and maximum value of 83.1. For example, in 3 out of 5 image categories, the histogram methods had better outcomes.

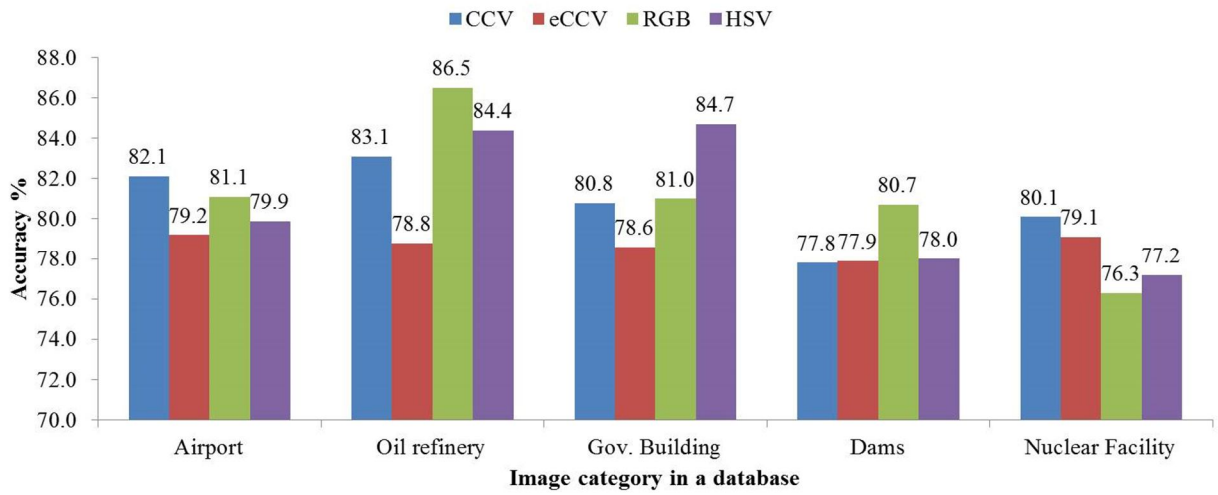

Figure 22. Accuracy rates for comparison of 100 images.

As shown in Figure 23, the ranges of precision rates were between minimum value of 31.5 and maximum value of 82.5. The results of precision also showed the same behavior with accuracy performance.

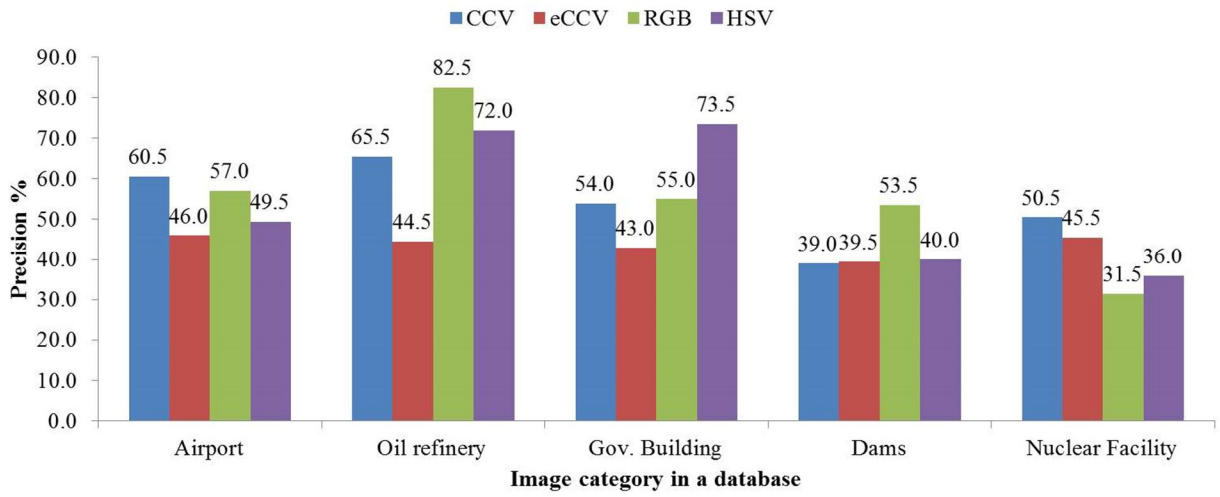

Figure 23. Precision rates for comparison of 100 images.

Table 8 summarizes the differences and the details in overall results of precision and accuracy. These comparisons could not determine the best method among the compared methods. Table 8 and Figure 24 represent the average values of accuracy and precision. The results showed that both histogram methods had better outcomes in both accuracy and precision.

Table 8

A summary of analytical evaluations by methods: All images comparison

Method		Accuracy		Precision		Best match (Rank)
		Mean	SD	Mean	SD	
Non-histogram	CCV	80.78	2.03	53.90	10.15	Best matched images are in higher ranks and high similarity rates
	eCCV	78.72	0.52	43.70	2.61	
Histogram	RGB	81.12	3.62	55.90	18.10	Best matched images are not always in higher ranks and high similarity rates
	HSV	80.84	3.53	54.20	17.64	

As shown in Table 8, both histogram methods had larger standard deviations. However, eCCV had the lowest standard deviations in accuracy (SD: 0.52) and precision (SD: 2.61), even though both means were not the highest. These results meant that eCCV generated more stable results.

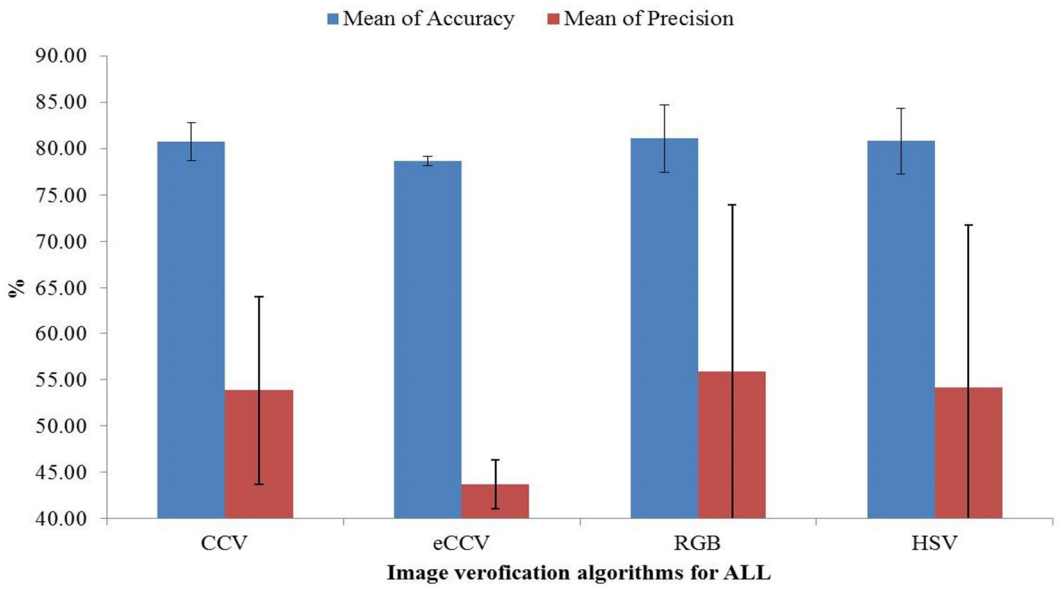

Figure 24. A summary of analytical evaluations by methods: All images comparison.

The no-histogram methods (CCV and eCCV) had the best matched images in higher ranks with higher similarity as described in Table 8. The histogram methods had better precision and recall rates in certain image groups, but the best matched images were not always placed in higher ranks and higher similarity.

3.3.2.2 Meta-analysis for comparing multi-methods. Based on both inference and descriptive statistics, the histogram methods (RGB and HSV) are more appropriate to the image of containing high density colors and detail (complex) pixels. The characteristic of histogram methods uses less distortion of color pixels in comparing genuine colors information. Unlike the histogram methods, the non-histogram methods (CCV and eCCV) use the vector information of the adjacent colors. This process causes colors to changes in the original image, so the non-histogram methods are not appropriate to dynamic color change within an image. The non-histogram methods had better outcomes in both accuracy and precision to non-dynamic color images. The 50 images were selected to conduct a meta-analysis to verify the superiority of non-histogram methods from the previous datum. As shown in Table 9 and Figure 25, eCCV had the

lowest standard deviations in accuracy (SD: 1.37) and precision (SD: 6.58) as the previous results to the non-dynamic images. As it was expected, the results showed that both non-histogram methods had better outcomes in accuracy (CCV: 81.97 and eCCV: 80.04) and precision (CCV: 59.84 and eCCV: 50.56) as described in Table 9.

Table 9

A summary of analytical evaluations by methods: non-dynamic color and object differences only

		Accuracy		Precision	
Method		Mean	SD	Mean	SD
Non-histogram	CCV	81.97	1.74	59.84	8.70
	eCCV	80.04	1.37	50.56	6.58
Histogram	RGB	79.96	4.05	50.7	20.12
	HSV	79.80	4.05	49.01	20.24

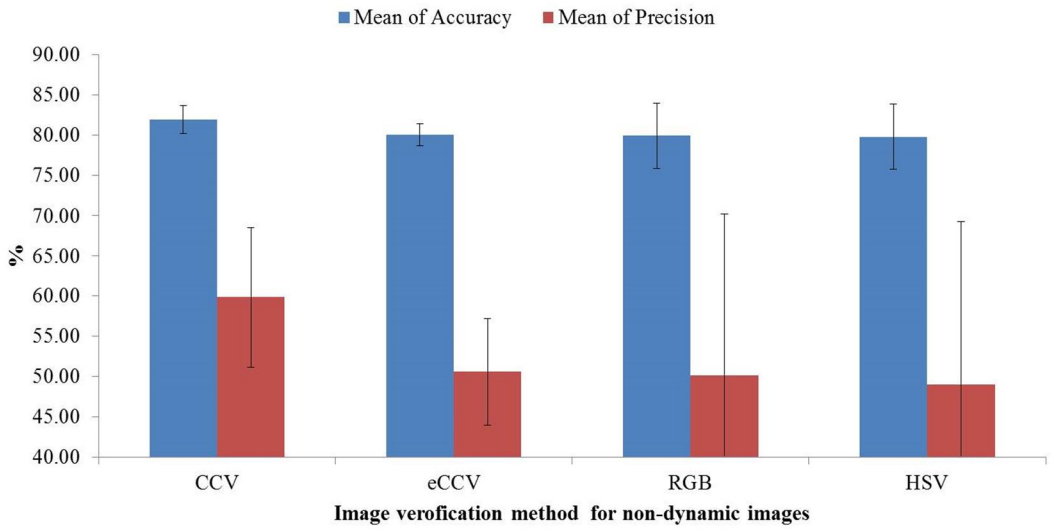

Figure 25. A summary of analytical evaluations by methods: non-dynamic color and object differences only.

A follow-up statistical test with one-way ANOVA confirmed that there was no significant difference in accuracy rates for non-dynamic images between the different image verification methods, $F(3,16) = 0.55$, $p = 0.6532$ ($\alpha = 0.05$). Again the results also confirmed there was no

significant difference in precision rates for non-dynamic images between the different image verification methods, $F(3,16) = 0.52$, $p = 0.6776$ ($\alpha = 0.05$).

Overall, eCCV is the only method which has lower variation in accuracy and precision to satellite images with dynamic changes in color, object size, and orientation. The statistical evidences were not strong enough to support the superiority of eCCV performances. Unlike color dependent methods (RGB, HSV, and CCV), eCCV intentionally looks for similarity based segmentation features, so it is likely to reduce standard deviation.

3.4 Date Fusion with Bayesian Belief Network

Satellite intelligence analysts are engaged in the process of information mining, seeking and confirming clues about the analytical cognitive processes to fit data and/or information into complex images analyses. When the analysts do the cognitive process, they conjuncture, hypothesize, and assume many possible states of image-based analyses; they create associations and linkages through notional cause-effect relations, thereby creating event trees. These relations are conditionally connected (influenced) by issues, causes, and effects. Data combination from such a network was developed by Pearle (1988) as a Bayesian network.

3.4.1. Rationale. The Bayesian belief network is constructed by analysts use belief functions. Belief functions are used to capture the expert notional beliefs using Bayesian conditional probabilities (Ntuen, Chenou, & Kim, 2010). The belief functions determine the degree of belief to the events or situations. The degrees of belief on a context do not necessarily add to 100%, making the assessment construct different from probability axioms. As an example, if an expert intelligence analyst says that he has 80% degree of belief that a certain image is identified from an airport image, then there is only 0% (not 20%) degree of belief that it is not an airport image. The 80% and the 0%, which do not add to 100%, together constitute a belief

function. Formally, the range of a belief function can be set to between 0 and 1. In these cases, belief networks are constructed and used to capture cause-effect relations as portrayed by edges of the network. The Bayesian network portrays a clear correspondence between the topology of the network and the dependence relationship of beliefs (Pearl, 1988).

A Bayesian belief network represents an augmented directed acyclic graph (DAG) that is not allowed to loop in network relationships (Pearl, 1988). Figure 26 show a Bayesian belief network of the knowledge levels. If an arc exists from node C to node D, the probability of node D assuming a given state D depends on the actual state of node C (C is a direct cause of D). The absence of an arc between two nodes implies that there is no such direct dependence. If in a Bayesian belief network, for all states of the root nodes, the prior probabilities are known, and in addition, for all non-root nodes the conditional probabilities, given the parent states, the joint probability distribution is completely known.

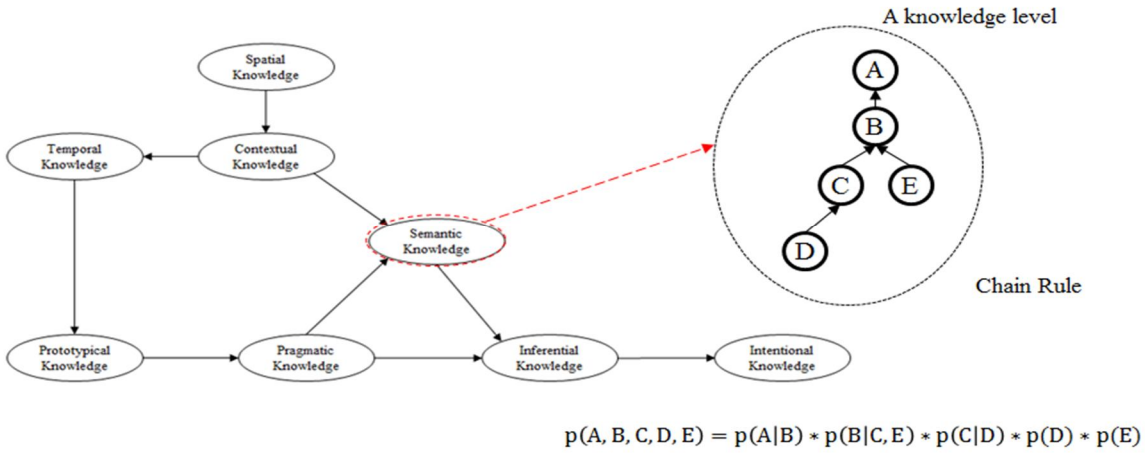

Figure 26. Example of a Bayesian belief network derived from knowledge level tree of Chapter 2.

The cognitive network is constructed from a collection of knowledge level network described below. Figure 27 depicts a cognitive map that illustrates how the analyst cognitively

engages in the analytic process of geospatial information processing. There are two parts to understand this network. At the left side (A) of Figure 27, the image features are passed through four primary nodes: spatial, contextual, temporal, and prototypical nodes. The contextual node provides the area of interest; temporal node provides time and location in which satellite image was obtained; spatial and prototypical nodes compare mental model of the object that is conceptually available in the analyst memory.

The right side (B) of Figure 27 deals with the formal logical process of mapping practical experience (pragmatic node) in combination with the analyst's lexicon and trade language (semantic node), reasoning (inferential) node, and intentional node. The temporal knowledge code has footprints on intentional knowledge while seeking time for meeting goals, semantic knowledge, and for pragmatic knowledge, respectively. In the decision support system to be developed, the analytic process (Y) executes 'A' and 'B' procedure concurrently.

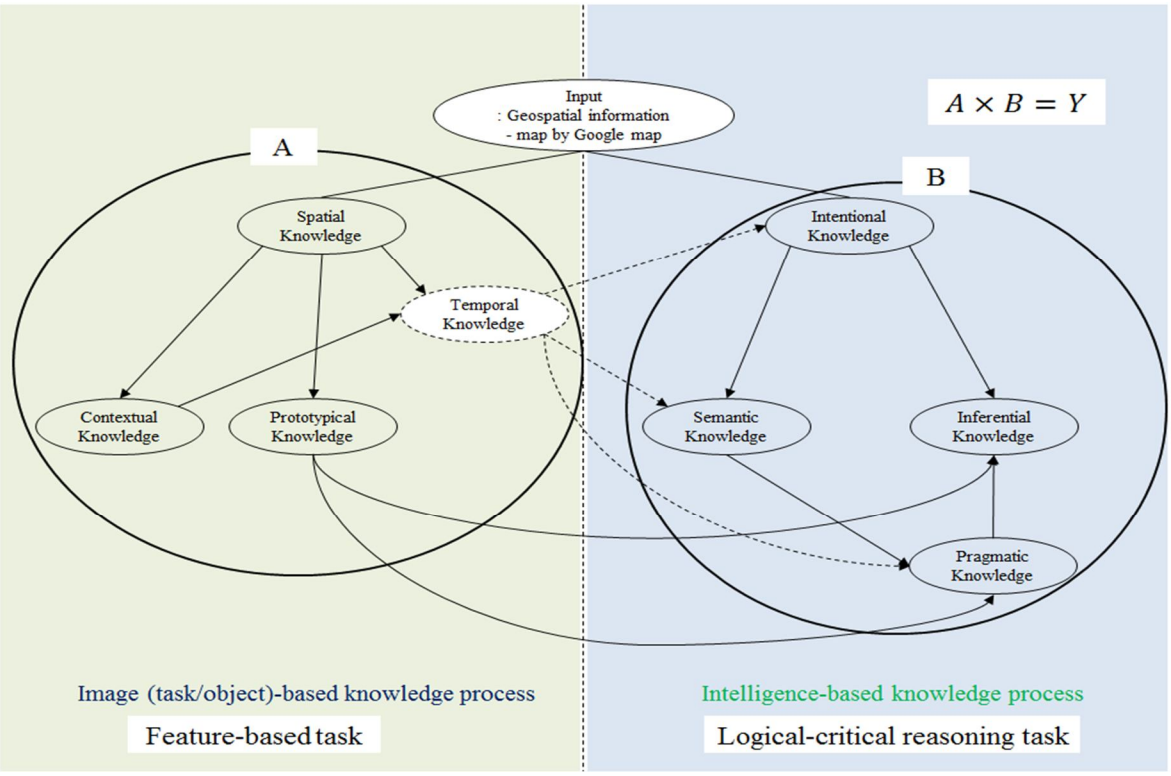

Figure 27. Cognitive map of analytic cognitive process for geospatial information.

3.4.2 Data Fusion Approach. The decision support system uses an information fusion model to support the analysts' beliefs on geospatial information analysis. Based on the expert's cognitive map above, Figure 27, a belief of the analyst network is constructed to represent the hypothesis-level experiment. The belief network represents the functional relationships between the knowledge levels (see Figure 26). Each knowledge level is based on the analyst's belief concepts. A belief state is derived by cognitive selections of subjective questionnaires in each knowledge level. Hence a belief state β is 3 tuple: $\beta = (S, p, r)$: where S is the number of processing nodes in the networks, p is the belief probability or possibility such that $p \to S \times r;\ r$ is the relationship between nodes.

The dependency structure of a Bayesian network has two major components. Only two-way associations and conditional independencies are depicted in directed graphs. The absence of an arc indicates conditional independence between two variables. The joint probability distribution is calculated using the conditional probability distribution associated with each node in the network. The conditional probability distribution of a node is the probability that the node takes on each of its possible values given every combination of values of its parent nodes. The joint and conditional probabilities are related according to the chain rule. In a Bayesian network estimating procedure, these probabilities are enough to infer by forward (deduction) or backward (abduction) probabilities of other nodes.

For example, the analysts would like to know probabilities such as $p(A|B, C, D, E)$ in order to assess the level of belief about the satellite image A. In Figure 28 the conditional probabilities are not given. However, in order to determine the confirmatory probabilities for the cause of knowledge levels, it is customary to estimate the conditional probabilities. That is why the concept of residuum is introduced.

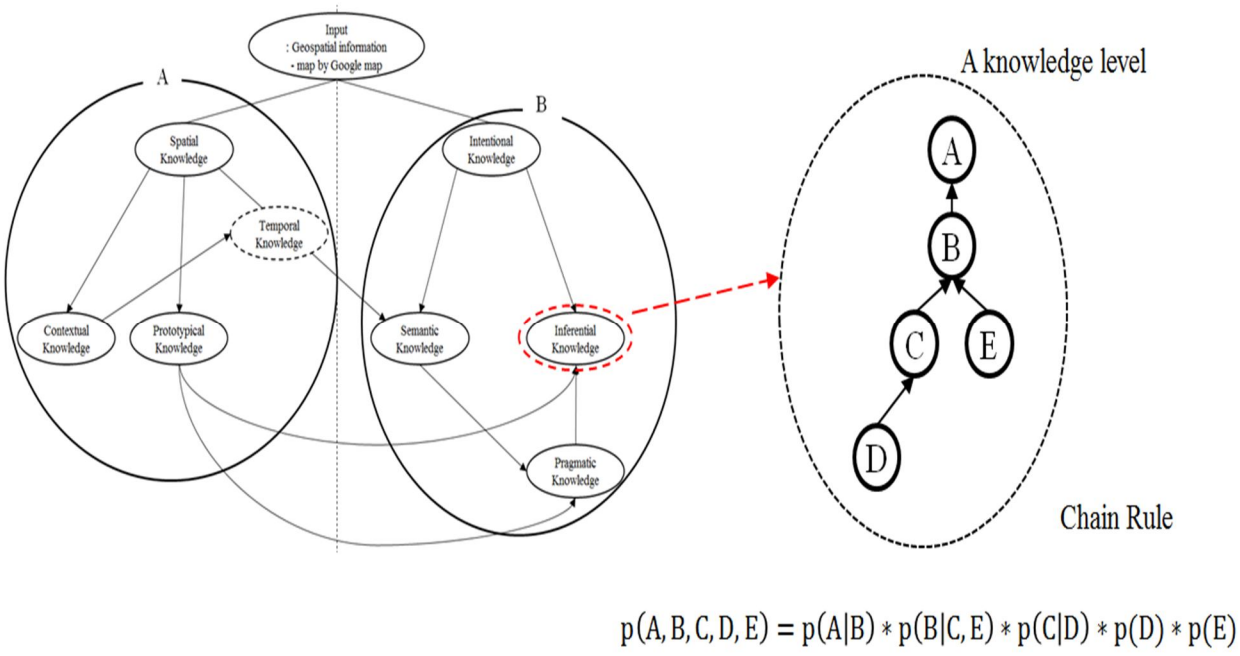

Figure 28. An example of cognitive computation.

Residuum concept is much related to T-norm and T-conorm from fuzzy set theory, respectively (Pedrycz, 1993). T-norm and T-conorm are generalization of logical conjunction and disjunction to fuzzy logic to model uncertainties. Both concepts inherit basic properties of intersection and union such as monotony, commutability and other associability. Examples of prominent non parametric t- norms are (Pedrycz, 1993):

- Minimum t-norm $t_{min}(x, y) = \min(x, y)$also called Gödel t- norm
- Product t-norm $t_{prod}(x, y) = x \cdot y$
- Drastic t-norm $t_D(x, y) = \begin{cases} \min(x, y) \; if \; \max(x, y) = 1 \\ 0 \;\; otherwise \end{cases}$
- Lukasiewicz t-norm $t_{Luk}(x, y) = \max(0, x + \; y - 1)$
- Hamacher product $t_{H_0}(x, y) = \begin{cases} 0 \;\; if \;\; x = y = o \\ \frac{x \cdot y}{x + y + x \cdot y} \;\; otherwise \end{cases}$
- Nilpotent minimum $t_{nM}(x, y) = \begin{cases} \min(x, y) \; if \; \min(x + y, 1) = 1 \\ 0 \;\; otherwise \end{cases}$

In a Bayesian network, knowledge of the system is given by the joint probability defined by $p(x_1, x_2, \dots, x_n)$; where $x_1, x_2, \dots, x_n$ are variables representing nodes of the network. This probability is rarely available. However, in practice when one has the marginal probabilities of all nodes without the parent nodes, and conditional probabilities of all other nodes, any types of queries in terms of probabilities can be inferred. Throughout the rest of this study, X and Y are two binary random variables. It is known in probability theory that $p(x, y) = p(x) \cdot p(y)$ if x and y are independent; we argue that this is a product-independency and can be generalized to other types of independency for a given T-norm.

The heuristic for obtaining joint probability values for non-independent variables proposed here are based on the observation that in the case of product independency, it has in general $p(x|y) = p(x, y)/p(y)$. In this study, the user is able to select a dependency rate (α) for manipulating the dependency between variables. α is dependency rate which is used to determine information dependency ($0 \leq \alpha \leq 1$). The created dependency general joint and marginal probabilities that allows calculating the residuum of between variables. If α has 0 % dependency, the variables are independent of each other.

For example, consider the random variables with $x = x_1$ and y= x_2 with values $p(x_1) = 0.77$ and $p(x_2) = 0.80$; this is the belief of one analyst on two nodes of a belief network. When the analyst states that his belief on x_1 is 0.77, in Boolean reasoning, this means that he believes on the complement of x_1 to be 0.23. This assertion automatically changes our belief values to probability values, and can invoke Bayesian updating methods easily. Figure 29 describes the process of obtaining a residuum between x_1 and x_2 variables for this example. Given $p(x_1) = 0.77$ for spatial knowledge, and $p(x_2) = 0.80$ for contextual knowledge, the following action is to calculate $p(x_2|x_1)$.

Using the product T-norm, the dependency rate (α) is set as 20 % dependency to the variables.

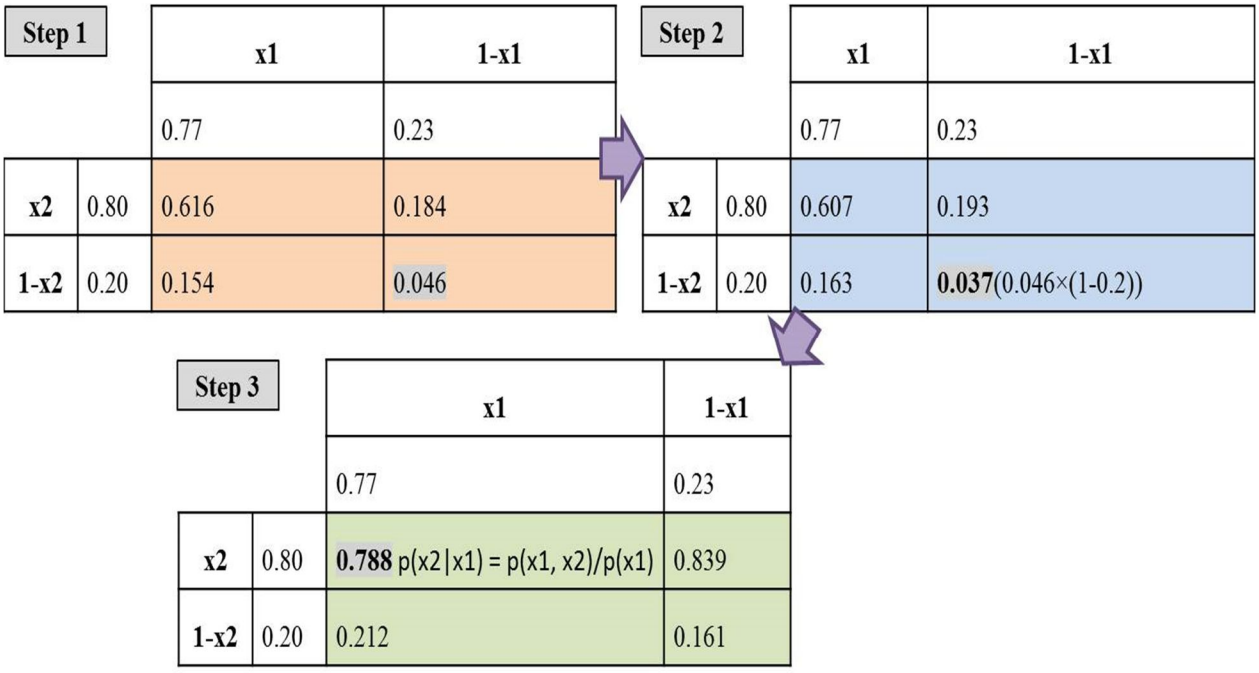

Figure 29. Example of heuristic method for obtaining residuum.

In step 1, the joint probabilities is calculated between x_1, x_2, $1 - x_1$, and $1 - x_2$. Then determine a minimum probability, which is defined by $\min[\, p(x_1) \cdot p(x_2), p(x_1) \cdot \big(1 - p(x_2)\big), \big(1 - p(x_1)\big) \cdot p(x_2),\ (1 - p(x_1)) \cdot (1 - p(x_2))] = 0.046$. The dependency rate (α) is applied to get 0.037 in step 2 which is followed by $\min \cdot (1 - \alpha)$. The minimum (0.046) derived from step1, so $0.046 \cdot (1 - 0.2)$ is equal to 0.037. After reducing the minimum value from 0.046 to 0.037, the rest of the probability values are obtained: $0.163 = 0.2 - 0.037$; $0.607 = 0.77 - 0.163$; $0.193 = 0.23 - 0.037$. After finishing step 2, step 3 creates the conditional probabilities with the variables in the table of step 2: $0.788 = 0.607/0.77 = p(x_1, x_2)/p(x_1)$; $0.839 = 0.193/0.23$; $0.212 = 0.163/0.77$; $0.161 = 0.037/0.23$. Therefore $p(x_2|x_1)$ is 0.788 between spatial and contextual knowledge for the Bayesian belief network computation. The concepts of Bayesian belief network and residuum will be applied as instruments for the decision support analytics in Chapter 4 and 5.

3.5 Chapter Summary

This chapter presented the analytical models used in the planned decision support system. Based on literature, color spaces, histogram algorithms (RGB, HSV) and non-histogram (CCV) algorithm were identified. eCCV was added to argument the consideration of feature segmentation with a robust color space. Sample simulations were conducted with comparison metrics (accuracy, precision, recall and statistics). The results of simulations showed that the histogram methods are more appropriate to the image of containing high density colors and detail (complex) pixels. The non-histogram methods have better outcomes in both accuracy and precision to non-dynamic color images. Another analytic model to be used is Bayesian belief. Bayesian belief network is used to capture beliefs on analyst beliefs of the images identified by the previous color algorithm. In addition, belief networks are used to capture the experts' belief on knowledge level information. That is to capture the initial ground truth information. The processes of transforming a belief function from no probability assumption to conditional probability are introduced using residuum concept.

CHAPTER 4

Design of a Visual Analytic Cognitive Model (VACOM)

A cognitive model should help the geospatial intelligence (GEOINT) analysts to visualize spatial satellite information at many layers of strategic, operational, and tactical abstractions. The model should also capitalize on the different strategies used by the human analysts during information processing. Using an analytic-cognitive task framework, these strategies are captured, according to the analysts understanding of satellite image displays.

The decision support model developed is visual analytic cognitive model (VACOM). The VACOM was designed to aid the human analyst process satellite images. By using color processing and feature segmentation algorithms, VACOM identified possible images from the selected areas of interest. Using personal belief, the analyst gives the likelihood of the identified image meeting the desired criteria. A Bayesian belief method was used to combine beliefs before a final image object selection.

4.1 Framework and Representation Theory

VACOM design was based on a network knowledge seeding. The knowledge seeding used cognitive-based questionnaires to collect analytic information on the analysts' interpretation of a satellite image. Knowledge seeding was a decomposition of graphic information about a node's properties in the network nodes summarized in Table 2 of CTA. The framework had hierarchical relationships as shown in Figure 30. This framework was classified into linkages, macro-knowledge level, and micro-knowledge level, respectively.

The macro-knowledge level is the higher level that serves as the knowledge manager. As an executive cognition manger, it instructs the micro-knowledge level units and sub-units in what to do to coalesce information chunks for decision making.

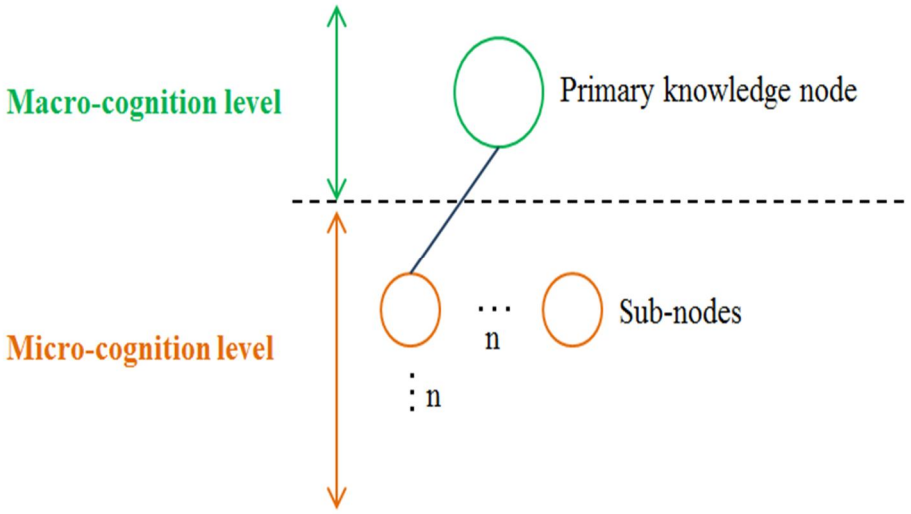

Figure 30. The hierarchical relations of knowledge seeding for a knowledge level.

In this level, knowledge operates contextually by hypotheses testing and functional inferences. At the micro-cognitive level, knowledge seeding takes place using two primary modes: symbolic and connectionist.

Symbolic knowledge seeding is discrete. That is information in the network is processed at time-steps by using information in the current position to proactively determine the future information states (MacLennan, 1994). Each symbolic knowledge represents source codes such as location, time, roles, and neighbors in the network. Figure 31 gives an example of a satellite information source code.

The connectionist knowledge seeding captures the dynamic features of state changes in a continuous manner (Shastri, 1988). State changes with respect to time and relationships between information objects are connected together via the micro-cognitive processes of connectionist knowledge seeding (CKS). Under the CKS paradigm, some or all of micro-cognitive knowledge elements in the current state are simultaneously carried to a new state of the system. During the CKS process, new knowledge seeds can be created and/or old knowledge seeds can be deleted. CKS is noted by MacLennan (1992) to have “image spaces with path-connected spaces.”

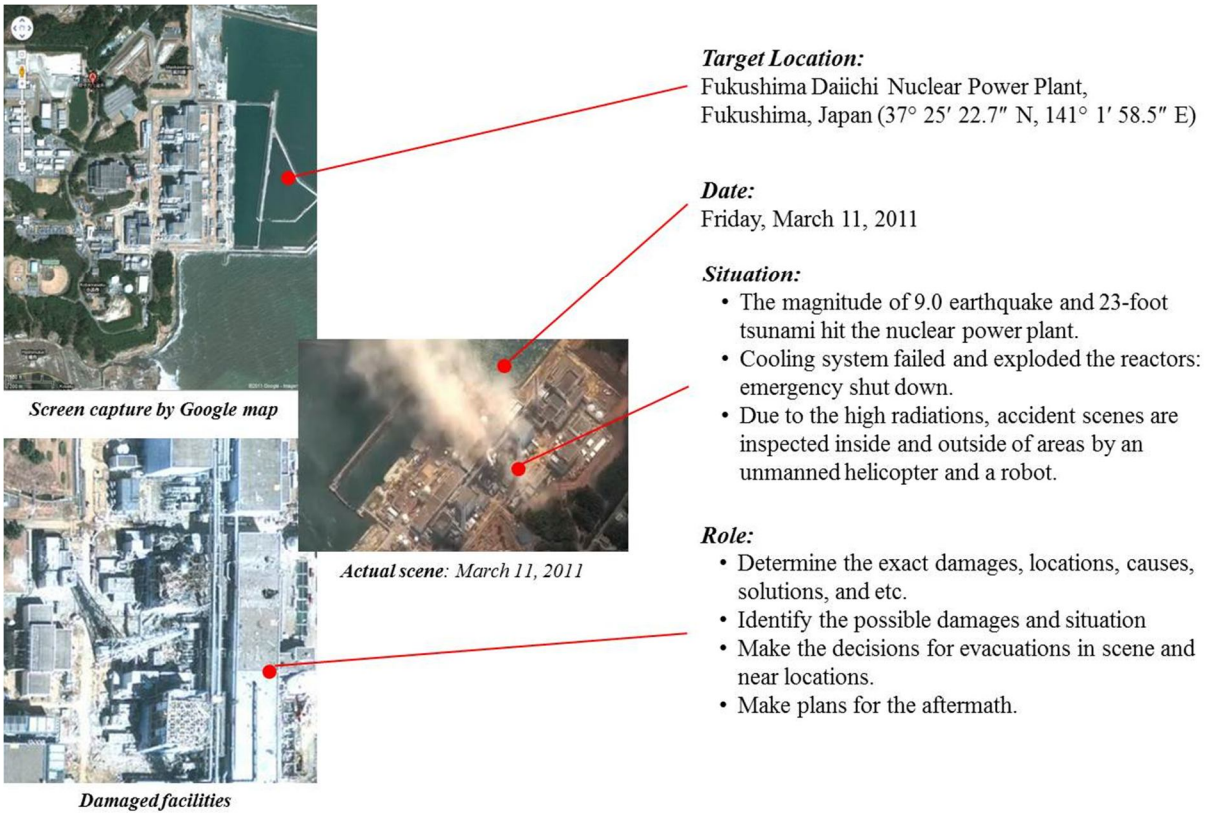

Figure 31. Sample micro-cognitive knowledge seeding: Fukushima's nuclear emergency.

More so, CKS allows knowledge to be internally represented by values of the connected weights and the topology of connections (or relationship between knowledge codes). For application in this dissertation, CKS is intended to allow distributed representations of individual evaluation of knowledge progression along the macro-and micro-coding dimensions.

The primary knowledge node represents the general descriptions of knowledge elements at the eight generic knowledge levels. For example, when we describe a temporal knowledge, we assign a generic characteristic of time dimension with information stamped with respect to time of occurrence: symbolically by (past, present, future), (before, after), and numerically captured by computer clock time. At the secondary knowledge node (sub-node) we look at the relationship of extraneous variables on the primary knowledge nodes. Some examples are the effects of vegetation and climate conditions as a satellite image. At the human cognitive level,

secondary knowledge node may capture such knowledge seeds as contexts, patterns, and lexicons used to describe information tokens.

It is argued that each of the knowledge levels has knowledge codes which are assigned according to the processing requirements and strategies of the analysts. The framework serves as an interpretative device for network information processing and linkages between and among concepts across the analyst's knowledge levels. For example, prime nodes may have sub-nodes, which may be connected to the other parent codes or sub-nodes of other knowledge levels. VACOM is driven by the cognitive network developed from the knowledge levels. The model builds on hierarchical and interacting network of cognitive structures. The cognitive network structure and the knowledge seeding are described in next.

4.2 A Descriptive Model of Knowledge Seeding

In order to properly characterize the knowledge levels for cognitive network modeling and simulation, a description of knowledge "seeding" is described. The descriptive models of knowledge seeding consist of spatial, temporal, contextual, prototype, pragmatic, semantic, inferential, and intentional, respectively. Information abstractions of knowledge are discussed in each of the descriptive models.

4.2.1 A Descriptive Model of Spatial Knowledge. Figure 32 is used to illustrate the hierarchical relations of knowledge seeding for spatial knowledge. Any element of spatial knowledge can trigger the first level perception processing of the analyst. The knowledge seeding can take place at many singular and for collective levels, either concurrently, or in sequence. These may involve the following information: (a) location and space geometry defining where the image was captured, such as city, village, metropolis; (b) developmental features such as population size; (c) geographical features, e.g., forest, desert, coast, river,

mountain (valley, rock, etc.) areas; (d) terrain risk features; and, (e) religious features defined by beliefs and worships, such as mosques, churches, temples, and so on.

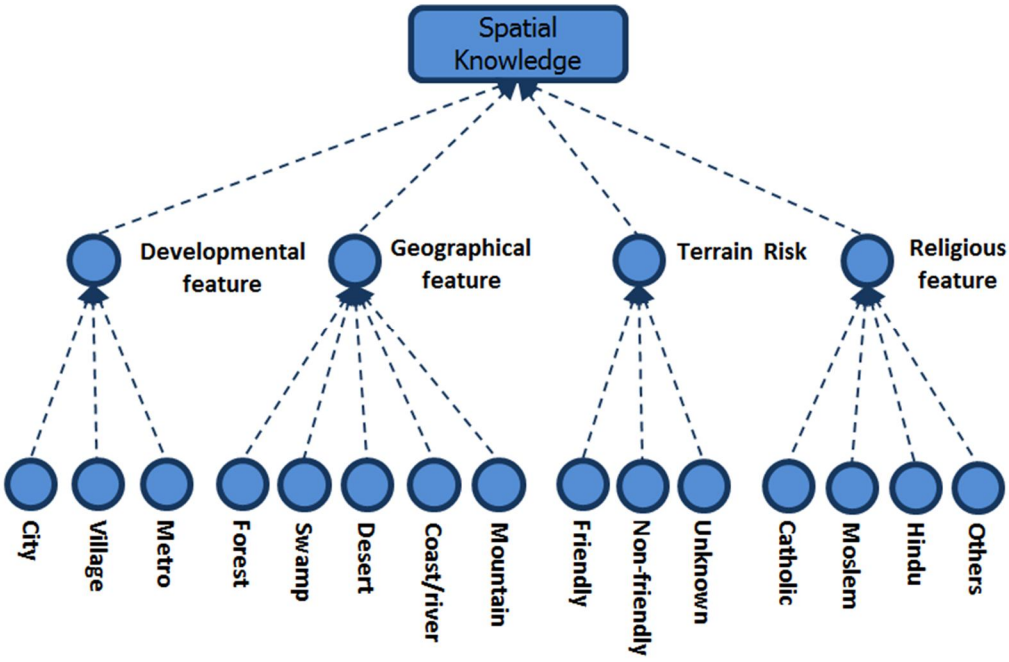

Figure 32. A descriptive model of spatial knowledge.

4.2.2 A Descriptive Model of Temporal Knowledge. Temporality of image attributes can be defined by at least three ways: (a) a continuous shift in image location even though the image is stationary at a specific geographical point; (b) a static image remaining in a static location; and (c) both geographic locations and image are shifting as in Google Earth. Temporality is measured as a function of time which can be defined in various ways, e.g., semantically, as "now", "before", and "after." In general, temporality creates patterns of information with time series features. This periodicity is used to manage episodic information and help the analyst to understand information footprints as snapshots of observable events. An example descriptive model is shown in Figure 33.

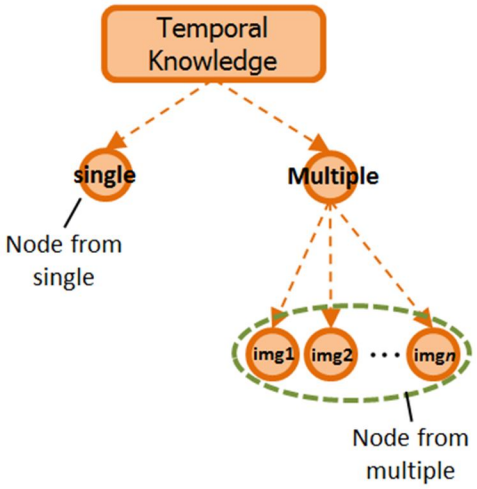

Figure 33. A descriptive model of temporal knowledge.

4.2.3 A Descriptive Model of Contextual Knowledge. Each situation for analysis creates a seeding of contexts for particular cases. Cognitive codes or seeding are enabled by framing of hypotheses or/and by selecting situation of interest for analysis (for attention cueing) and selecting a context based on the situation of interest. An example of a contextual level analysis is shown in Figure 34.

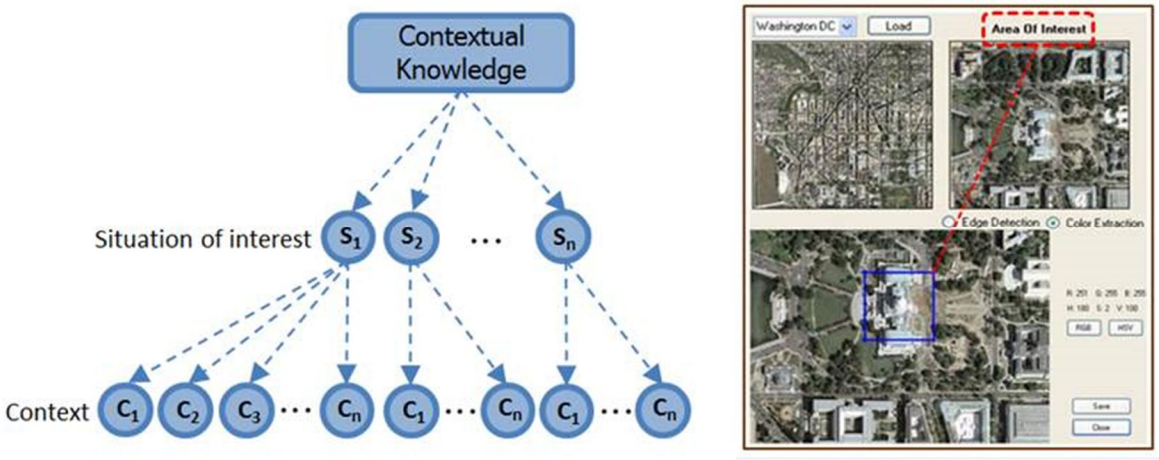

Figure 34. A descriptive model of contextual knowledge.

4.2.4 A Descriptive Model of Prototypical Knowledge. A prototypical knowledge usually has many features that tend to replicate the behavior of real objects. The knowledge

seeding has prototype objects which can take many forms of representation ranging from hierarchical system level representation to database structures. The purpose of the knowledge seeding at this node is primarily to enable learning or encourage nodes to share experiences. Prototype features are useful as exemplars to Bayesian networks that can learn prototype features (target object) from trained sample features. Prototypes are used in this dissertation for color algorithms to recognize known features. Figure 35 is used to illustrate a prototype seeding from an image environment.

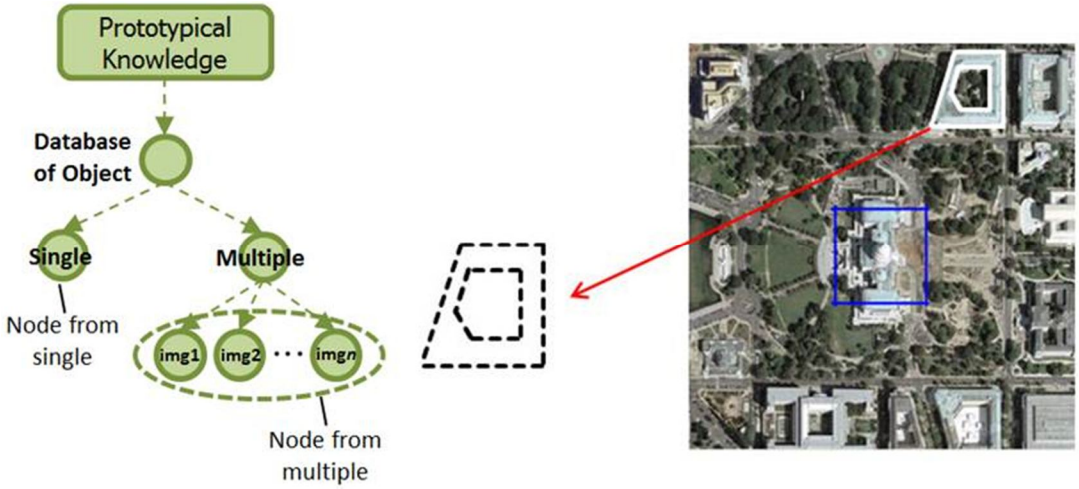

Figure 35. A descriptive model of prototypical knowledge.

4.2.5 A Descriptive Model of Pragmatic Knowledge. The model deals with how expert and novice analysts perform theirs tasks. The coding process is based on information derived from the CTA, which can use an objective- approach, subjective-approach, or a combination of both. The coding process takes a particular cognitive task and expands its function along a single cognitive trajectory or many cognitive dimensions based on the analyst's knowledge level. For example, in the detection of a threat object from an image background, such as those performed by an airport security on a passenger checking in a luggage, the inspector uses many invariants of cognitive mapping techniques for associating target objects to mental model prototypes. The

seeding process can be a procedure-base or a performance-base. Such instances may occur in the following cognitive question-answering systems, “How do you do?”, “When do you start and stop?”, “What do you normally achieve?”, “What attributes allow you to recognize the threat?” and so on. The coding process should then capture the intuitive as well as the analytical aspect of the expert reasoning process. Figure 36 shows an example network.

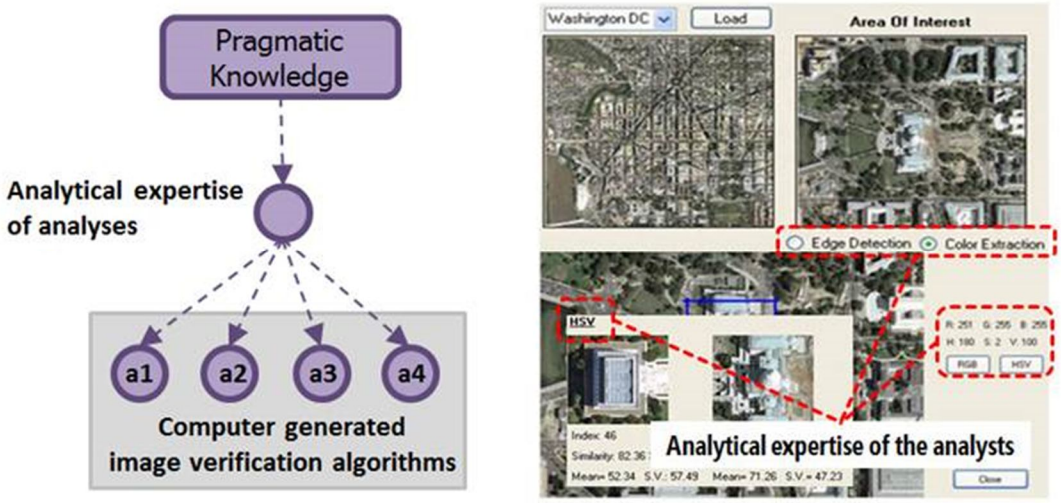

Figure 36. A descriptive model of pragmatic knowledge.

4.2.6 A Descriptive Model of Semantic Knowledge. Each agency in a society has a set of language rules in which meanings are implicitly embedded. It would not be complete if the lexicons and language styles of GEOINT analysts (and any other intelligence analyst for that matter) are not embellished into the cognitive modeling process. Semantic knowledge has a knowledge seeding that allows analysts to look for meaning in information relevant to the task goals. It also allows the analysts to associate situational information to memory information; and to compare and contrast situations of ambiguity and deception in communications. Precisely for modeling purposes, a semantic knowledge represents what an expert analyst knows, such as giving meaning and interpretation to an object of interest. Figure 37 is an illustration of this construct.

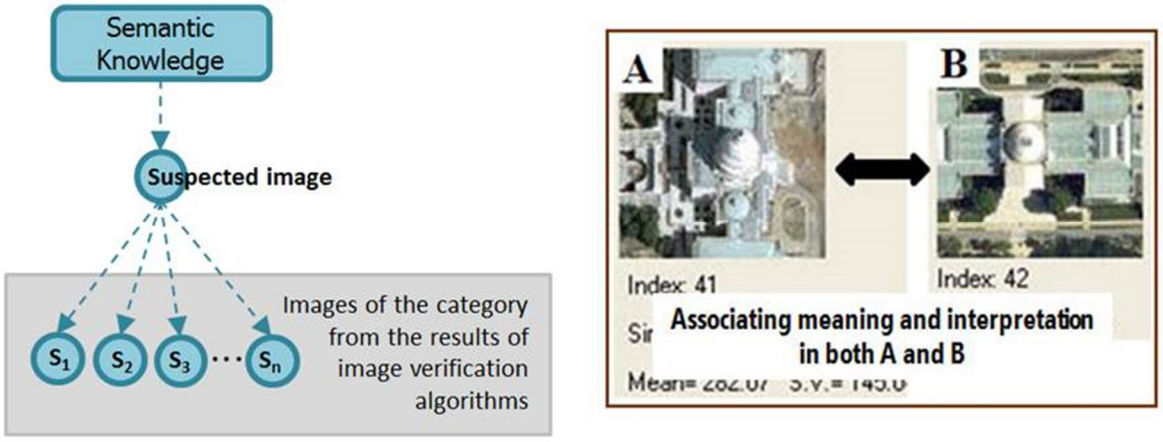

Figure 37. A descriptive model of semantic knowledge.

4.2.7 A Descriptive Model of Inferential Knowledge. The traditional definition of inferential knowledge is attributed to formal logic at three levels: (a) deductive, in which an expert frames a hypothesis, and through some observations, make some conclusions; known as a forward-based reason, a conclusion necessarily follows from a set of truths given the premise statements; (b) inductive, where data is given and the experts analyst tests some hypotheses to validate some claims; known as a data-driven reasoning, it is possible for the conclusion to be false even though the premises are true; and (c) abductive reasoning, where the analyst tries to conjure the most plausible explanation of a situation based on dynamic on-going information. Here, satisficing solutions are sought for in a complex problem situation by looking for the most likely causes through diagnostic cause-effect mapping. Coding inferential seeding requires a dynamic memory (whether by human or by machine constructs). This is because of the many techniques for representing the coding rules. It may be one or a combination of several coding rules. Instances are a production system represented by "If {situation} then {action}", neural networks represented by many constellations of network structures, object-attribute-value triplets, semantic networks, and so on. Figure 38 illustrates a generic coding for inferential knowledge.

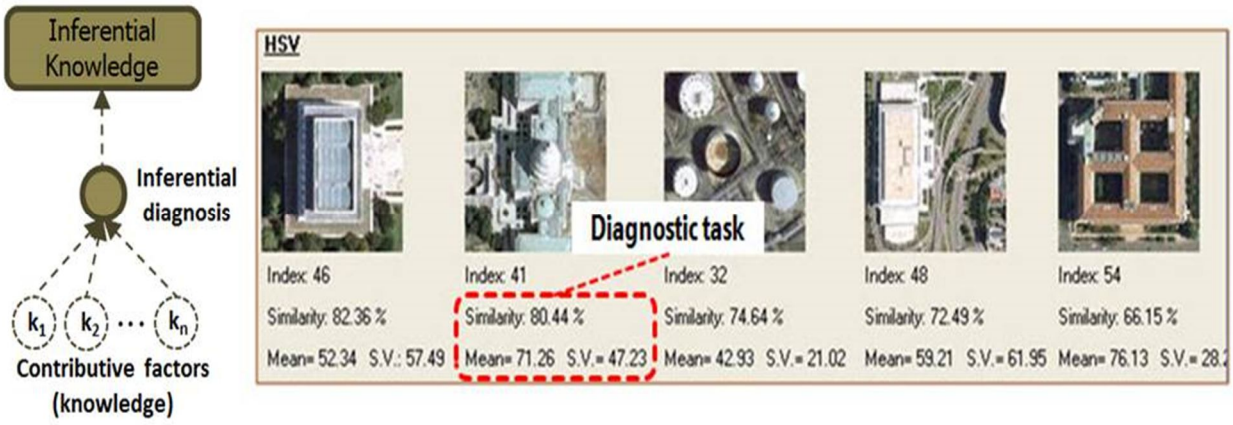

Figure 38. A descriptive model of inferential knowledge.

4.2.8 A Descriptive Model of Intentional Knowledge. One of the premises advanced to construct a cognitive model for the GEOINT analyst is that the interaction between the analyst and satellite information is causal and intentional. Causal systems have components that allow the interacting elements to realize the goal of the system. Such an interaction obviously occurs as a result of attributing individual functionalities to cope with the realization of context-situation goals through laws of nature or functional relationships. The functionality of the system is realized through information processing designed to aid the system.

Intentional systems are goal-directed. In most cases, the goals are fixed or wired into the system behavior. Decision-making in control of intentional systems is based on knowledge about the value structures of the system, the actual input from the system's environment, and its internal limiting properties (Rasmussen, 1985). For example, a GEOINT analyst trying to make sense of a satellite image must initially develop some cognitive constructs (such as framing a hypothesis) to explain and justify the first level processing of information as enabled by perception of the situation.

VACOM uses an intent-inference model to capture, collect, and assemble associated data about a satellite image. The analysts also use the data to certify the degree of beliefs. For

example in Figure 39, the analyst has to decide whether to accept the computer model recommendation that the satellite image represents a government building.

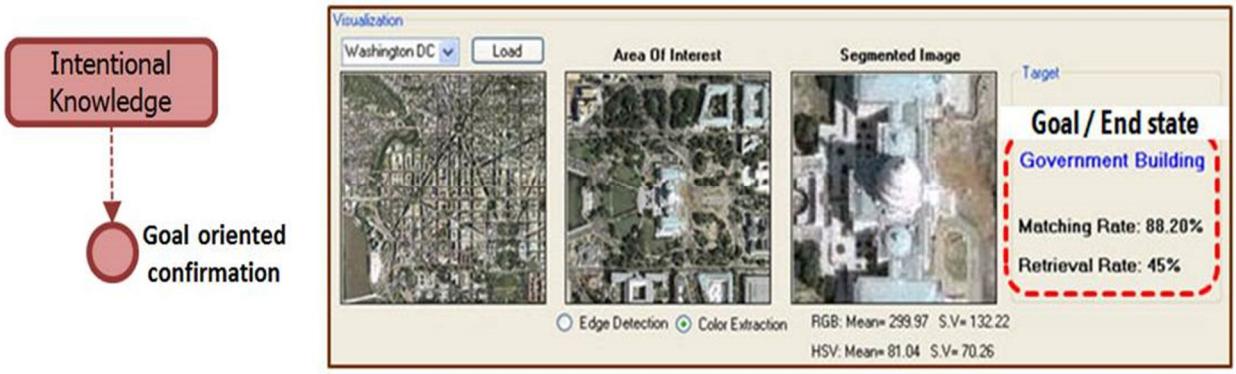

Figure 39. A descriptive model of intentional knowledge

4.3 VACOM Design Process

The descriptive models of knowledge were introduced to capture the relevant information for the VACOM design. The complete cognitive network was developed by the descriptive models and the subjective questionnaires. The specific network implementations are discussed with the analytical models.

4.3.1 Subjective Questionnaires for Knowledge Acquisition. CTA was employed to understand the knowledge required for VACOM design. A question-answering questionnaire was used. These were specific inquiries, such as location-based inquiry (where), object-based inquiries (which, what, and why), time-based inquiry (when), and method-based inquiry (how). The primary tasks and detail of knowledge seeding are derived from these cognitive questions as shown in Figure 40.

The questionnaires allow information to be collected as follows:

- *Contextual knowledge.* State the hypothesis based on the context information.
- *Spatial Knowledge.* Select an area of interest in the map for analysis.
- *Temporal knowledge.* Identify the time stamps on the satellite.

- *Prototypical knowledge.* Use available similar prototypes as exemplars to compare with scenes from the area of interest.
- *Pragmatic knowledge.* Recognize and describe the utility of the 'object of interest' that appears on the map.
- *Semantic knowledge.* Interpret concepts of contextual events in time and space.
- *Inferential knowledge.* Makes inference about objects of interest from the satellite image.
- *Intentional knowledge.* Confirm situational goals and hypotheses.

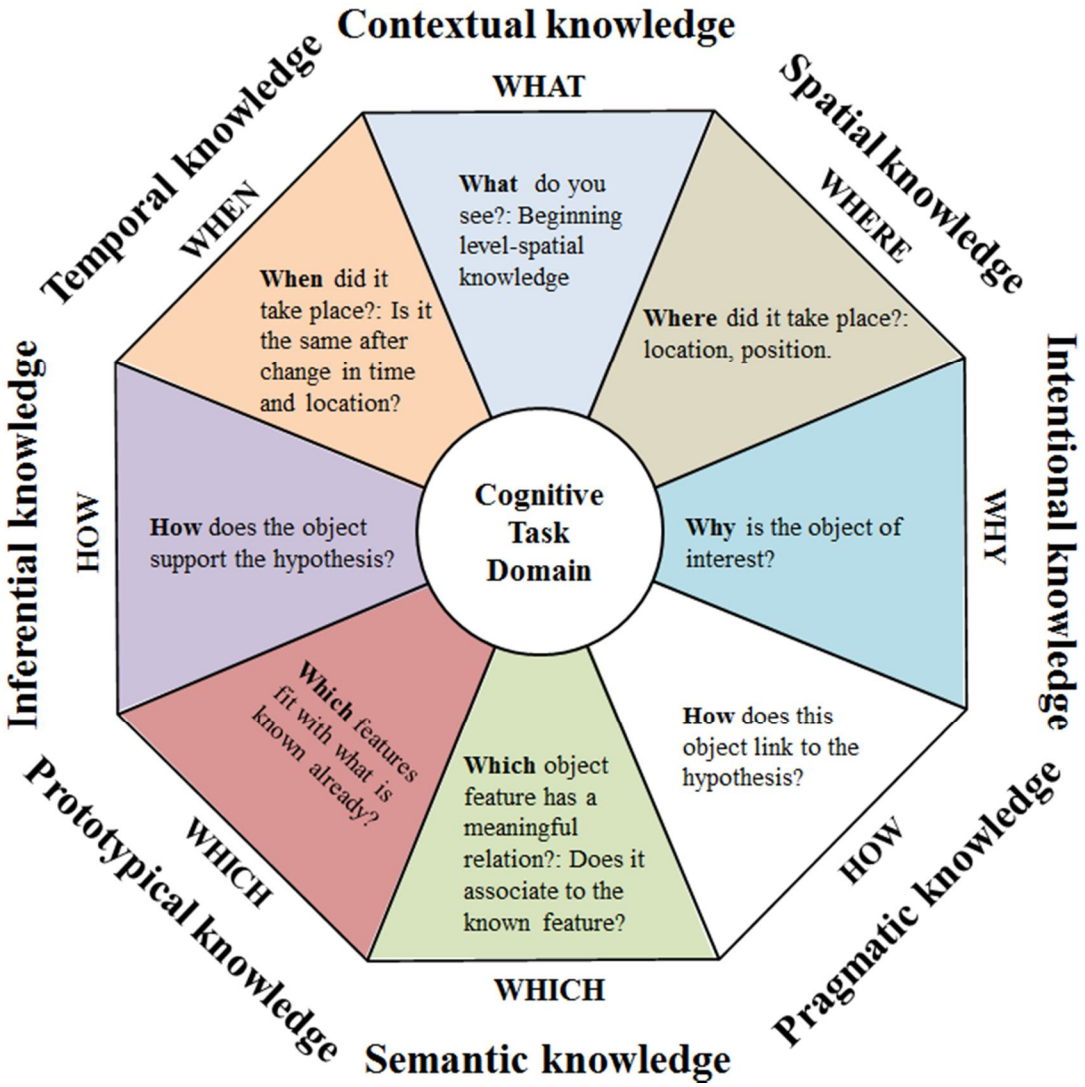

Figure 40. Conceptual relationship of knowledge levels from CTA.

4.3.2 Cognitive Network (CN) Development. Figure 41 illustrates a notional CN of VACOM constructed from the knowledge levels and questionnaires data.

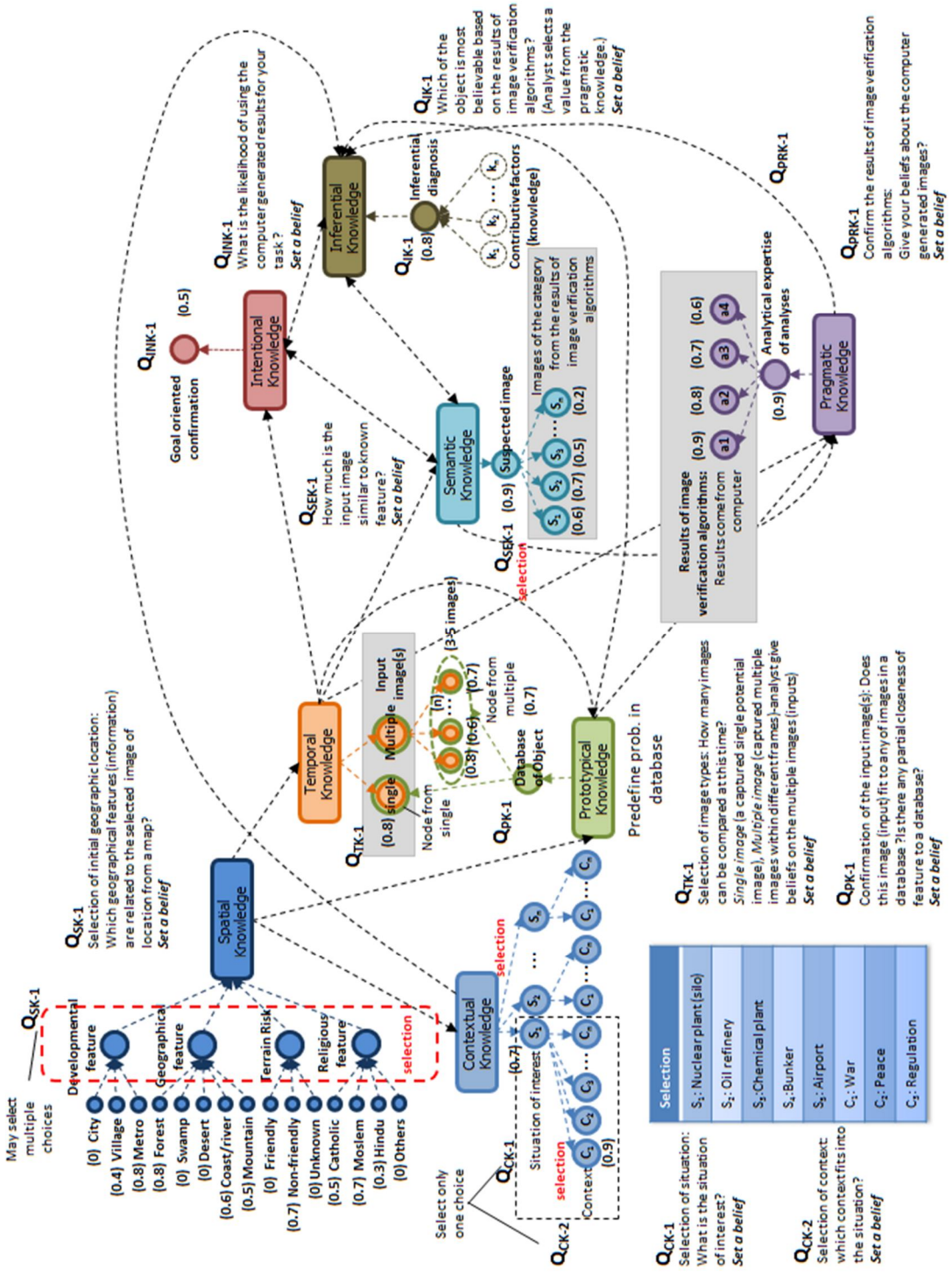

Figure 41. Cognitive network representations generated from analysts concepts.

VACOM network is constructed by the computer generated analytics (based on the image verification algorithms) and the analyst's beliefs of cognitive process for the image analysis tasks. Each knowledge level has a subjective questionnaire that allows the analysts to populate the nodes with information. The value of each analyst's beliefs is 0 to 1 as described in Figure 41. The questionnaires are required to knowledge levels as follows:

- *Spatial Knowledge.* Which geographical features (information) are related to the selected image of location from a map?
- *Contextual knowledge.* What is the situation of interest? Which context fits into the situation?
- *Temporal knowledge.* How many images can be compared at this time? (*Single image*-a captured single potential image, *Multiple image*-captured multiple potential images within different frames)
- *Prototypical knowledge.* Does the image (input) fit to any of images in a database? (Is there any partial closeness of the features to a database? Do you recognize this image?)
- *Pragmatic knowledge.* Give your beliefs about the computer generated images? (Confirm the results of image verification algorithms)
- *Semantic knowledge.* How much is the input image similar to known feature?
- *Inferential knowledge.* Which of the object is most believable based on the results of image verification algorithms? (Analyst selects a value from the pragmatic knowledge.)
- *Intentional knowledge.* What is the likelihood of using the computer generated results for your task?

In the network analysis, the challenge is on defining and quantifying the relationship metrics between the nodes. This is where the Bayesian belief network and conditional residuum

is employed (Ntuen, Chenou, and Kim, 2010). Figure 42 captures the sample data which is based on the schematic representation of the cognitive linkages across the knowledge levels.

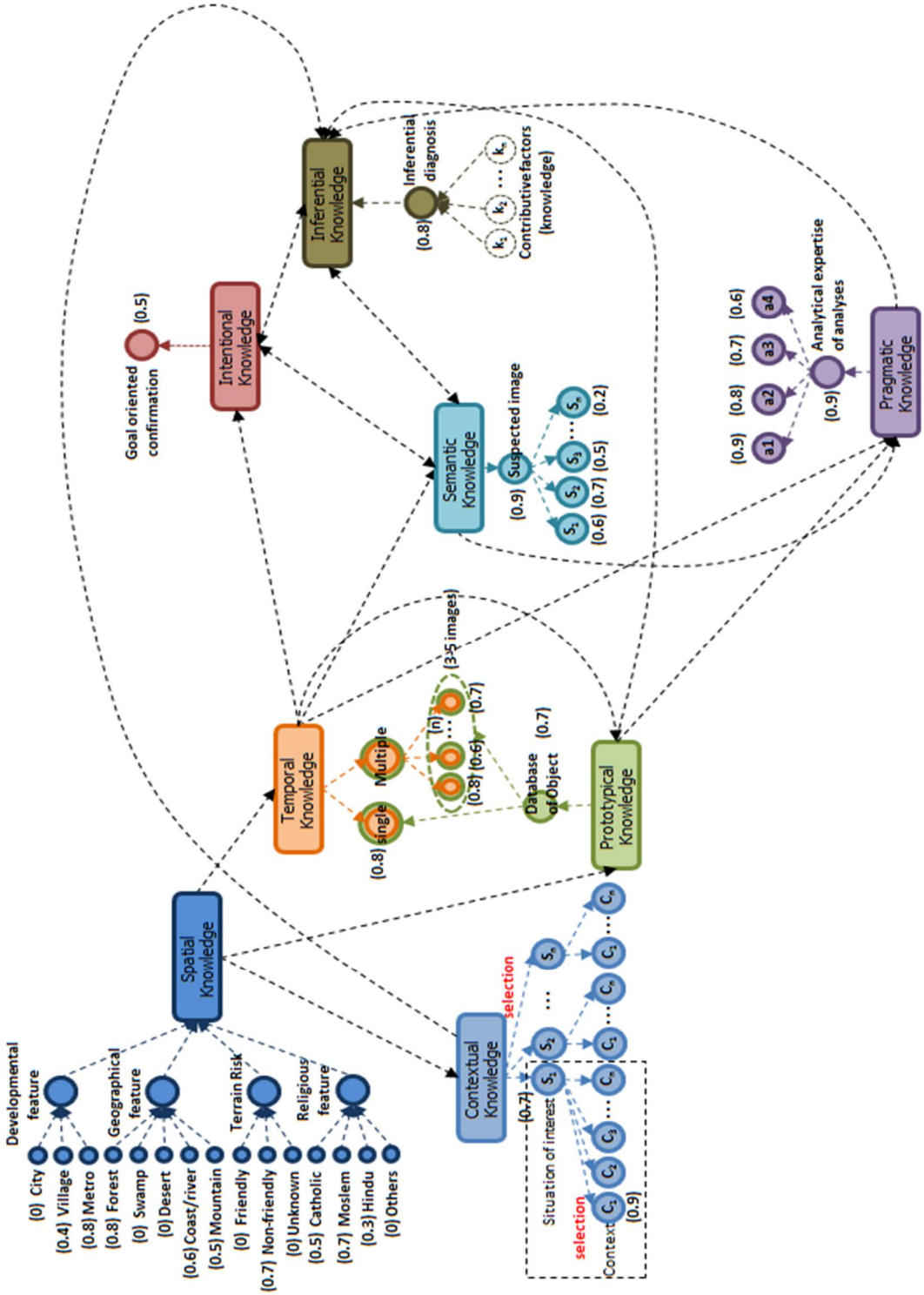

Figure 42. A sample data for the cognitive network.

The detail descriptions of individual cognitive nodes are shown in Figure 43 and 44. These detailed descriptions are used to explain the relationships between and within nodes in terms of data acquisition.

As shown in Figure 43, the analyst selects mutiple geograpical features (e.g., developmental, geographical, terrain risk, and religious feature) with the analyst beliefs. These selections by the analyst are the inputs to the cogntive network. In Figure 43, a fuzzy norm was applied to compute the analyst belief function of spatial knowledge. The norm of form $p(x, n)$ is used as defined by $\left[\sum_{i=1}^{n}(x_i - x_0)^2/_n\right]^{1/2}$.

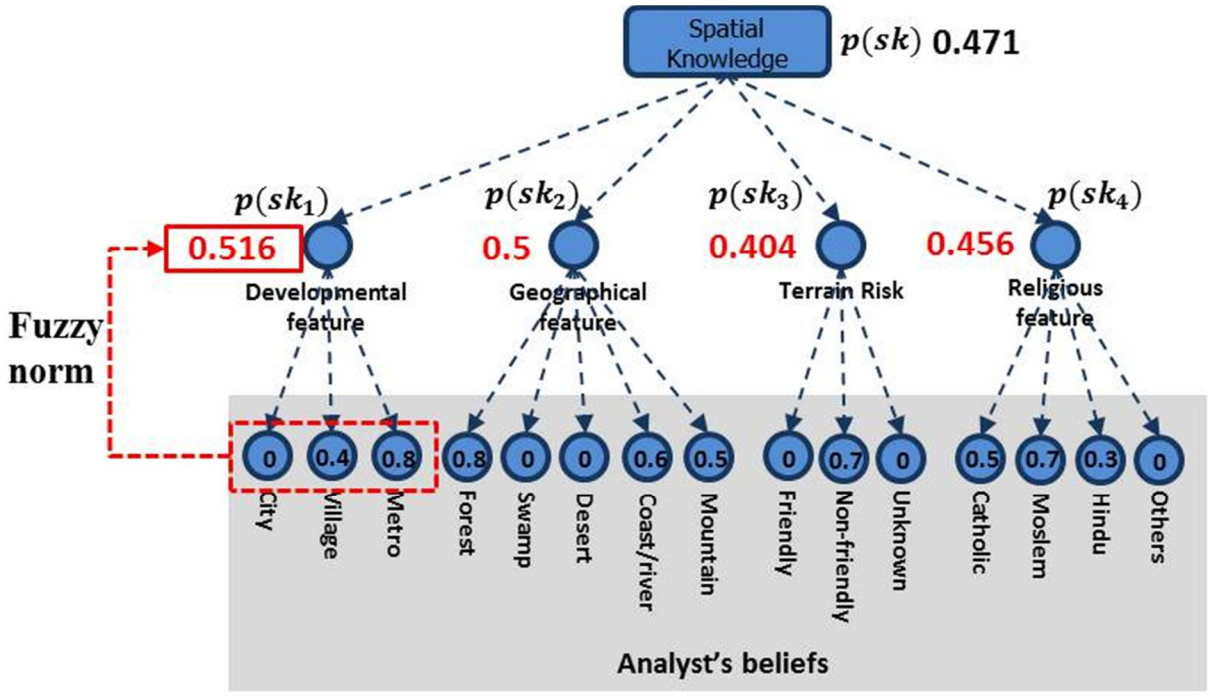

Figure 43. An example of cognitive node for spatial knowledge.

For example, a fuzzy norm applied to get the belief on sk_1, is $p(sk_1)$ calculated with the distance from the user rating of developmental feature to zero vectors is defined by $\left[\sum_{i=1}^{n}(x_i - 0)^2/_n\right]^{1/2}$.

If the developmental feature vector is $[0, 0.4, 0.8]$, $p(sk_1)$ is $\sqrt{\frac{(0.0-0)^2+(0.4-0)^2+(0.8-0)^2}{3}} = 0.516$.

Using same fuzzy norm, the other beliefs ($p(sk_2)$, $p(sk_3)$, and $p(sk_4)$) were also calculated . The weighted belief of the analyst on spatial knowledge, $p(sk)$ was computed by the values of sub-nodes ($p(sk_i)$, $i = 1, 2, 3, 4$) . $p(sk)$ is 0.471 .

On the contextual knowledge in Figure 43, the analyst selects the situation of interest such as, nuclear plant, oil refinery, chemical plant, bunker, or airport and its context (e.g., war, peace, regulation, etc.). As shown in Figure 43, the analyst has a single selection on each question (e.g., Q_{CK-1} and Q_{CK-2}), respectively.

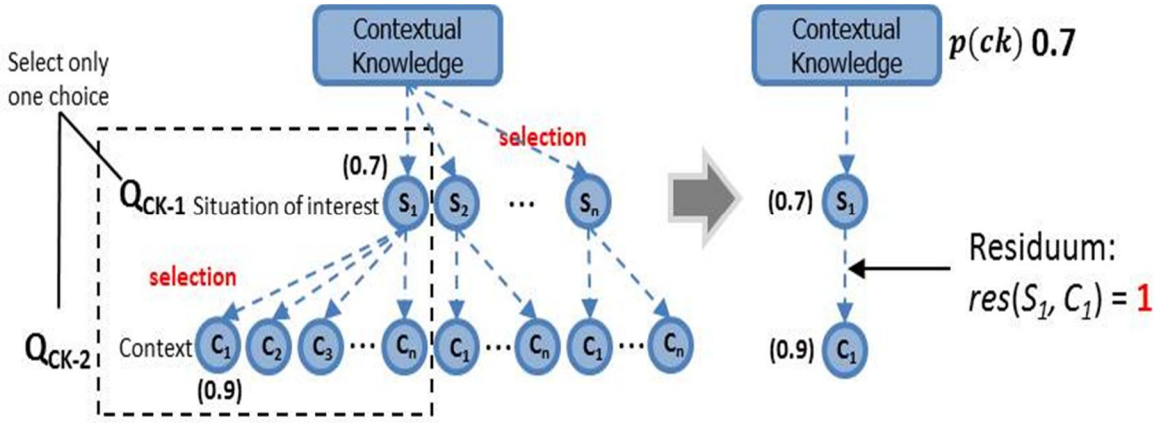

Figure 44. An example of cognitive node for contextual knowledge.

In the contextual knowledge, the continuous T-norm and its residuum were applied to estimate the conditional probabilities. A residuum concept was discussed in Chapter 3. For the contextual knowledge node, the residuum between S_1 and C_1 is $res(S_1, C_1) = min(1 - S_1 + C_1, 1) = min(1- 0.7+0.9, 1) = 1$. To get the $p(ck)$, T-norm of x and y defined by $max(0, x+y-1)$ was used. Therefore, $p(ck)$ is $S_1 \oplus res(S_1, C_1) = max(0, 0.7+1-1) = 0.7$. The methods described above are applied throughout each knowledge levels.

4.3.3 Bayesian Belief Network Implementation. Figure 45 presents the application of cognitive model and Bayesian belief network for the VACOM. The image 'A' in Figure 45

represents the general knowledge network relationships. The image ‘B’ in Figure 45 represents the knowledge network relationship, which was produced by Python 2.7. The process was to obtain a ‘Directed Acyclic Graph’ (DAG) for a topological order in network. The image ‘C’ in Figure 45 was a screen capture of the cognitive network from the eight knowledge levels. The image ‘D’ in Figure 45 represents a linear graph (DAG) of knowledge network from the Python result. Once Python software evaluated the network inputs, it generated the required topological order. This topological order was to confirm the dependency of connections among the knowledge levels and created a linear graph.

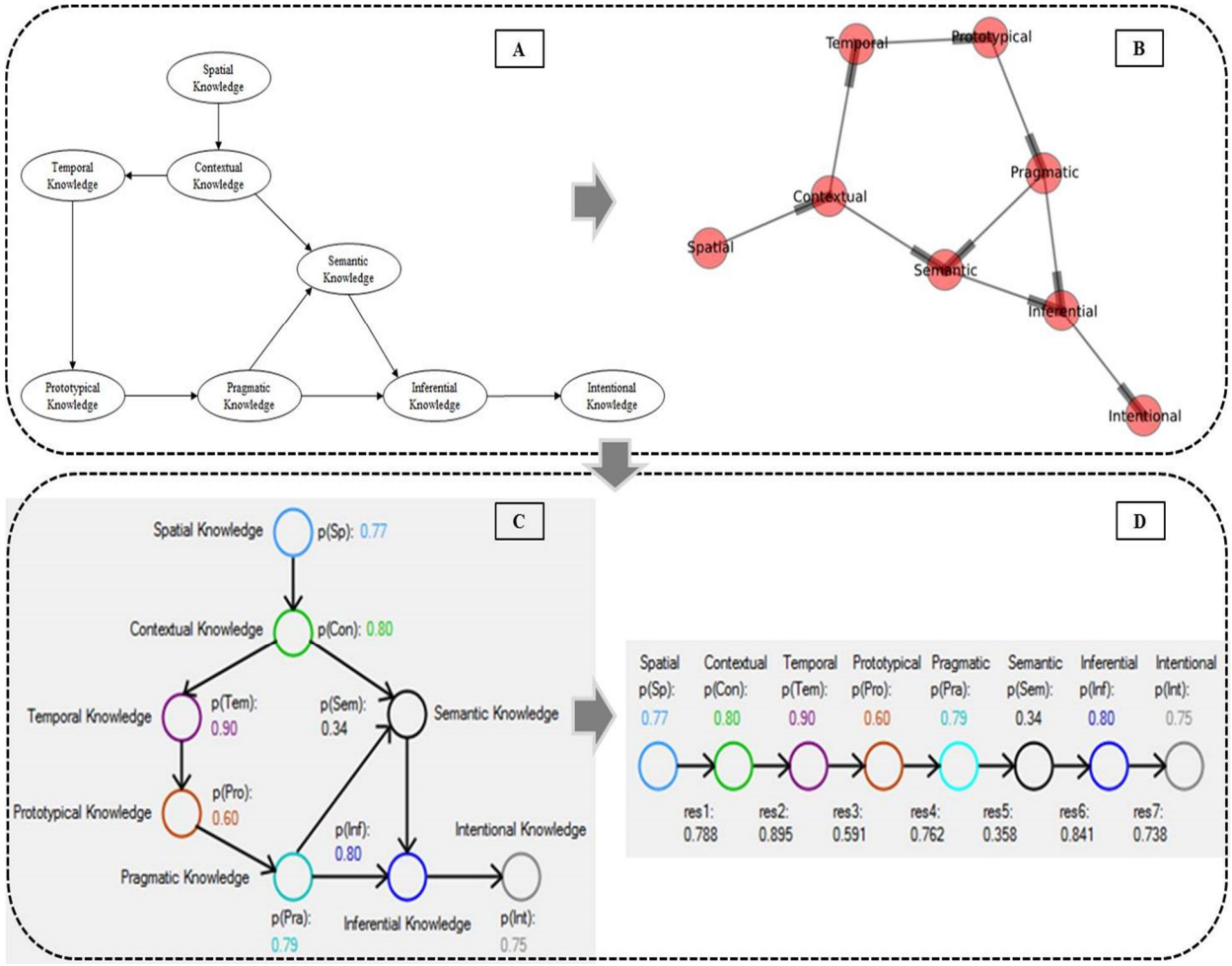

Figure 45. Example of knowledge network representation (Bayesian belief network) and Degree of belief computation.

4.3.3.1 Degree of Belief. The calculations of residuum (see Chapter 3.4.2) between knowledge levels are shown in the image 'D' of Figure 44 (e.g., $res_1 = 0.788$, $res_2 = 0.895$, $res_3 = 0.591$, $res_4 = 0.762$, $res_5 = 0.358$, $res_6 = 0.841$, and $res_7 = 0.738$).For example, res 2 was produced by the contextual (x_2) and temporal (x_3) knowledge. Using the calculated residuum values, a degree of belief is calculated to confirm the user selection of the identified image. The degree of belief is defined by $\sum_{i=1}^{n} p(x_{i+1}|x_i) \,/\, \sum_{i=1}^{n} p(x_i)$, $\sum_{i=1}^{n} p(x_{i+1}|x_i)$ is the conditional probability of between two knowledge levels and $\sum_{i=1}^{n} p(x_i)$ is the sum of individual knowledge beliefs.

For example, given $p(x_1) = 0.77$ for spatial knowledge, $p(x_2) = 0.80$ for contextual knowledge, $p(x_3) = 0.90$ for temporal knowledge, $p(x_4) = 0.60$ for prototypical knowledge, $p(x_5) = 0.79$ for pragmatic knowledge, $p(x_6) = 0.34$ for semantic knowledge, $p(x_7) = 0.80$ for inferential knowledge, and $p(x_8) = 0.75$ for intentional knowledge, $\sum_{i=1}^{8} p(x_i)$ is 5.750. Given $res_1 = 0.788$, $res_2 = 0.895$, $res_3 = 0.591$, $res_4 = 0.762$, $res_5 = 0.358$, $res_6 = 0.841$, and $res_7 = 0.738$, the sum of residuum for all knowledge levels $\sum_{i=1}^{7} p(x_{i+1}|x_i)$ is 4.973. Therefore the degree of belief $\sum_{i=1}^{7} p(x_{i+1}|x_i) \,/\, \sum_{i=1}^{8} p(x_i)$ is 4.973/5.750 = 0.865.

In general, the belief function is defined here as

$$b(x_{i+1}|x_i) = \sum_{i=1}^{n-1} p(x_{i+1}|x_i) \,/\, \sum_{i=1}^{n} p(x_i) \text{ , where } i = 1...n \quad (20)$$

4.3.3.2 Human Belief Confirmation from Computer Model. The purpose of the cognitive analytics is to enhance the analysts' decision through interactive beliefs confirmation of image identified by any of the verification methods. Hence, VACOM can help the human analysts to reduce the cognitive overload associated with the complexity of geographical information processing. The first part is, J_1, the computer-generated recommendation using CCV, eCCV, H-RGB, and H-HSV image verification technique. The second part is human

analysts' judgments, J_2 which are generated by the subject questionnaires on the image identifications. To measure fuzzy distance between the computer-generated judgments J_1 and the human analysts' judgments J_2, the intrinsic values are calibrated on a scale between 0 and 1. An example of confirming belief property is given below:

J_1 = [CCV, eCCV, RGB, HSV],

J_2 = $[Judg.analyst_1,\ Judg.analyst_2,\ Judg.analyst_3,\ Judg.analyst_4,\ Judg.analyst_5\ ]^T$.

The confirming belief is

$$Q_{belief}(J_1,J_2) = 1 - d(J_1,J_2) \tag{21}$$

where, $d(J_1 - J_2) = \left[\sum_{i=1}^{n}(J_1 - J_{2_i})^2/n\right]^{1/2}$ (22)

For example, Given J_1 (CCV) = 0.9661, that is image algorithm CCV identify a nuclear facility with precision of 0.9661; $J_2 = [0.5112, 0.5782, 0.5604, 0.5184, 0.5460\ ]^T$, J_2 represents an example of five analysts confirmations. Therefore $Q_{belief}(J_1,J_2)$ is, $Q_{belief} = 1 - [\{(0.9611 - 0.5112)^2 + (0.9611 - 0.5782)^2 + (0.9611 - 0.5604)^2 + (0.9611 - 0.5184)^2 + (0.9611 - 0.05460)^2\}/5]^{1/2} = 0.5810$.

4.4 Chapter Summary

In this chapter, the sample analytical models in VACOM were demonstrated. VACOM represented the expert knowledge levels that developed the cognitive network using concept of Bayesian belief network. The cognitive network was derived from the subjective questionnaires of analysts. The cognitive network captures analysts' cognitive processes for identifying images. As result, it produced the user beliefs on the identified images. The belief function, fuzz norm, calculated the user ratings of each node in knowledge level to confirm belief of each knowledge level. A residuum was derived from the Bayesian belief network to calculate the conditional probability between knowledge levels. Using the residuum, a degree of belief was calculated to

confirm the user selection on the identified image. The confirming belief was applied to the cognitive analytics, which is the combined belief between computer-generated analyses and human beliefs. This approach helps human analysts to reduce the cognitive overload associated with the complexity of geographical information processing.

CHAPTER 5

Visual Analytic Cognitive Model (VACOM) Interface Design

5.1 Structure of VACOM Interface

This chapter describes the interface design for VACOM. This interface is cognitively-driven in line with the tasks performed by the GEOINT analysts. The interface model controls VACOM's analytics support tools which aids the analysts in such tasks as scene interpretation of a satellite image, visual displays, and information fusion.

Figure 46 represents the representation of the interface modules. The left side shows two major tasks. The first stage is the image input and analysis; here signal processing algorithms are used for the image analyses. The second stage is the image coding with the human knowledge levels for geospatial data representation tools, including visualization models.

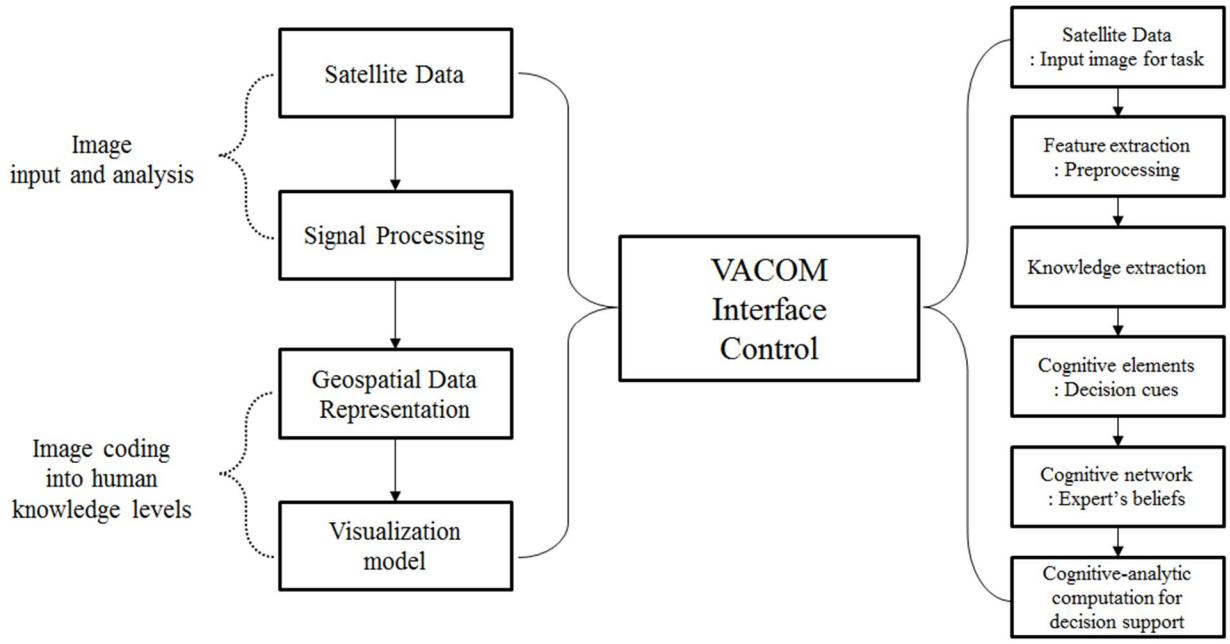

Figure 46. An abstraction of VACOM interface design.

Both processes support the analyst in image perception, comprehension, analysis, and recognition and detection. The analyzed satellite image features are passed into a visualization

module responsible for information rendering, both textually and graphically. At the right side of Figure 46, the interface contains the knowledge facets for satellite data processing. It also has modules for decision support systems (DSS) through analytical algorithms such as Bayesian belief network, color-based segmentation methods, and information fusion algorithms. The right side is the micro-level information processing units embedded in VACOM.

5.2 VACOM Design Process

Figure 47 describes the details of VACOM design process with a road map for developing a useful interface. The left side of Figure 47 represents the primary visual analytics that covers the approaches of image verification algorithms and shows what the interface is supposed to display the results.

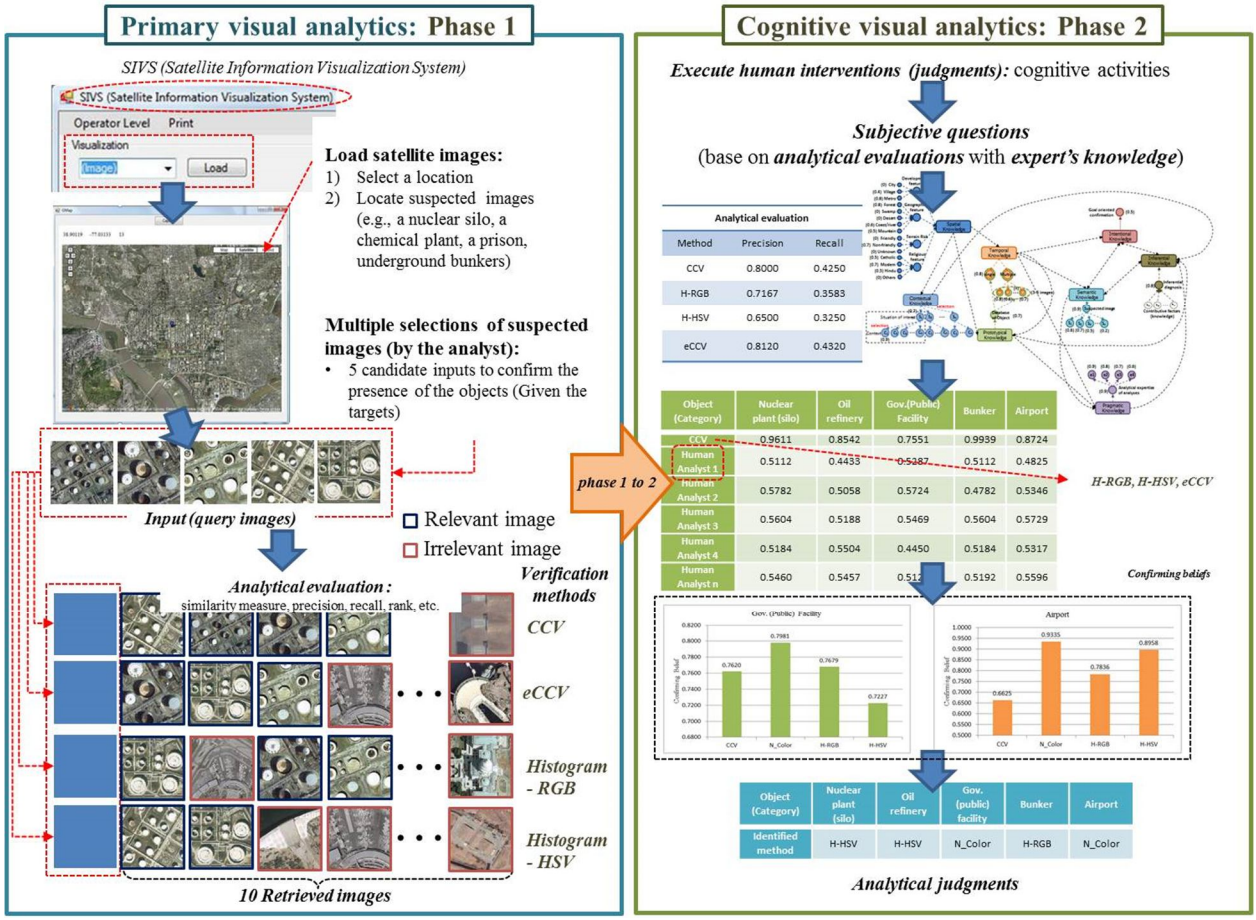

Figure 47. VACOM Design Process.

The right side of Figure 47 has the knowledge representation that includes the analytical evaluations with human analyst's cognitive network.

Figure 48 describes the design of VACOM interface and the entire of interface components at a glance. The first analytic process is 'Primary visual analytics' allows the user to select image analysis methods. These are labeled A1 (non-histogram methods: CCV and eCCV) and A2 (histogram methods: RGB and HSV) at the right side of the screen. The second analytic process is 'Cognitive visual analytics' allows the user to select the knowledge network tools at the left side of the screen. These are labeled B1 (knowledge representations) and B2 (knowledge network implementation and Bayesian belief network computation).

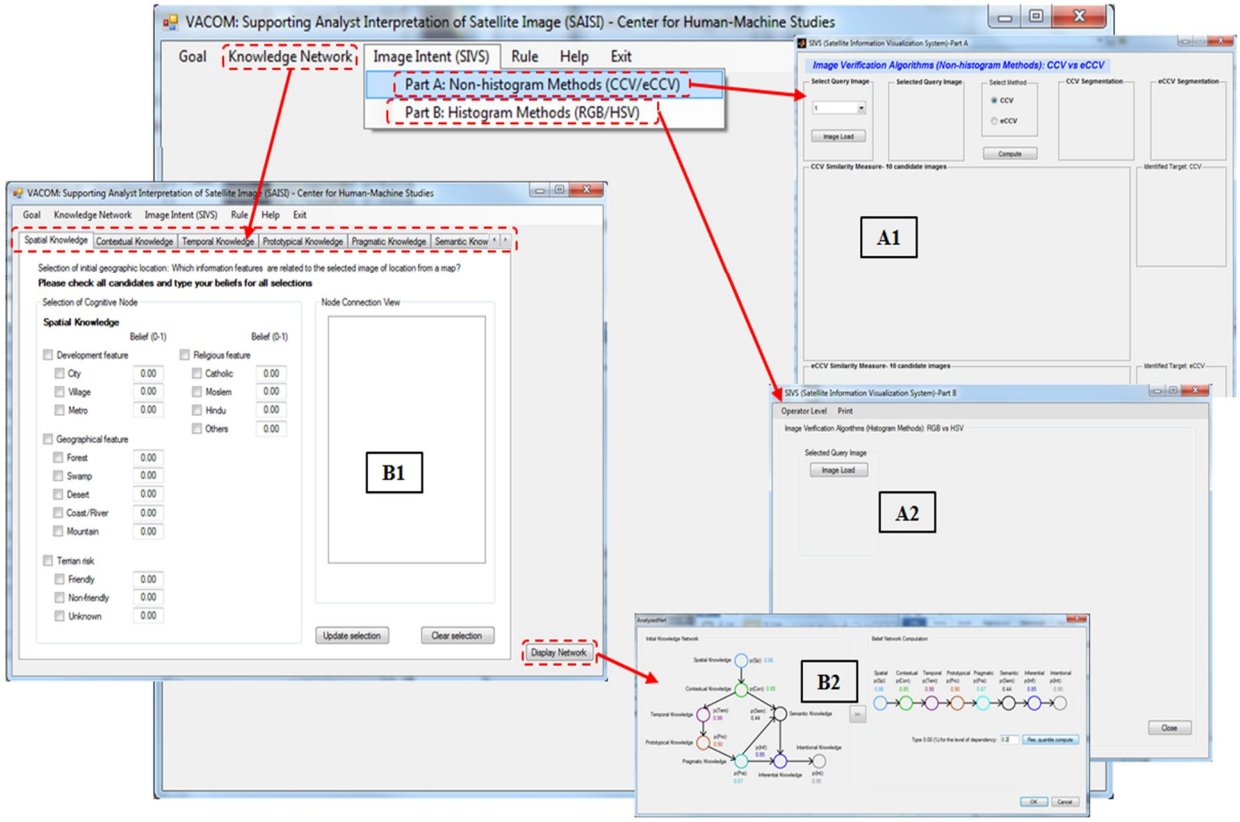

Figure 48. The design of VACOM.

The expanded view of the primary visual analytics is displayed in Figure 49. It represents the non-histogram methods for the image analysis. The user selects the query image (a) and the

selected image is displayed. Then the users selects the image analysis method (either CCV or eCCV) (b). The result of image analysis is displayed in the section labeled c. In part d, the VACOM suggests the likely object in the satellite image representation. For example, "Airport" is identified with accuracy of 86%, precision rate of 80%, and a recall rate of 40%, respectively.

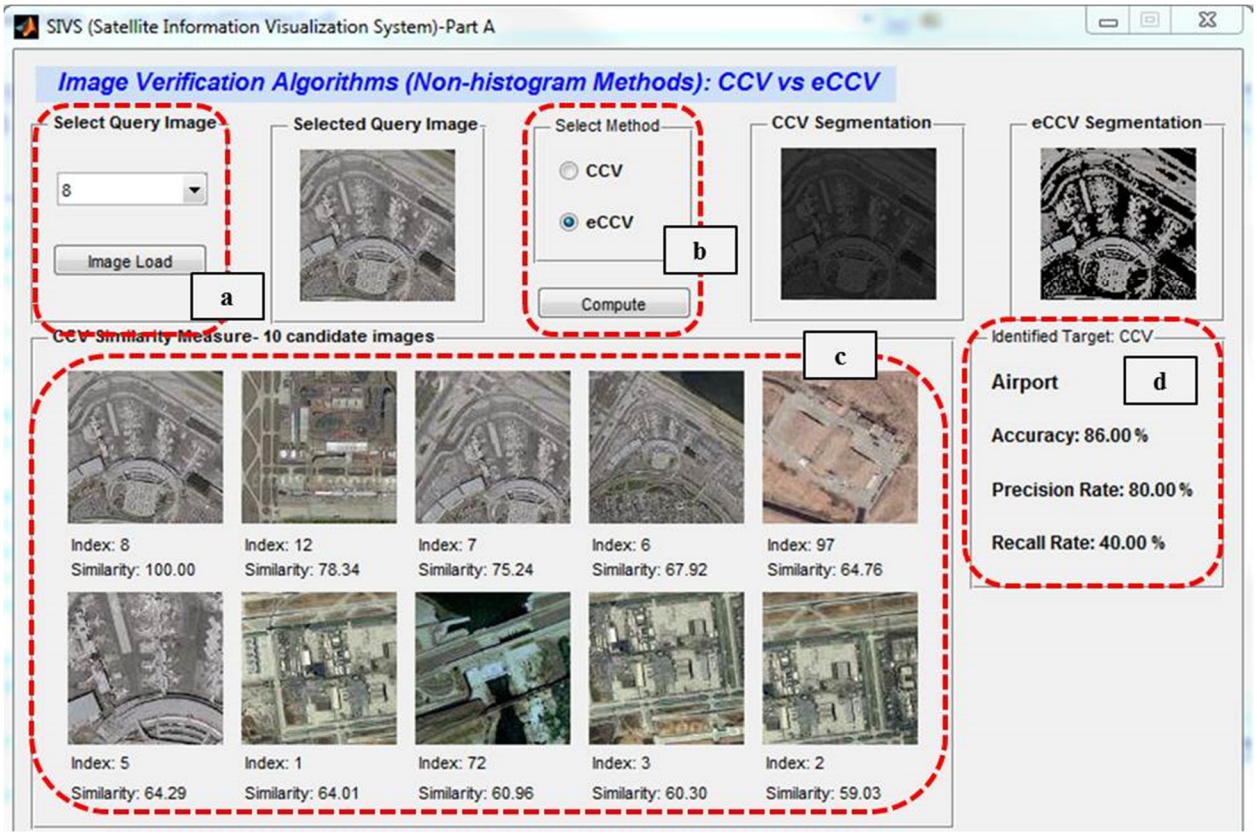

Figure 49. Example of non-histogram methods (CCV/eCCV).

The second visual analytics is displayed in Figure 50. It represents the histogram methods for the image-based analytical evaluations. This interface consists of the three features: (a) image load (a selected image is the same image as the non-histogram methods used), (b) user selection of the image verification algorithms (either RGB or HSV), results of image analyses for the RGB/HSV methods (including candidate images, images index, and similarity measures), and (c) results of analytical evaluations (including identified name of image category, recall and precision rates).

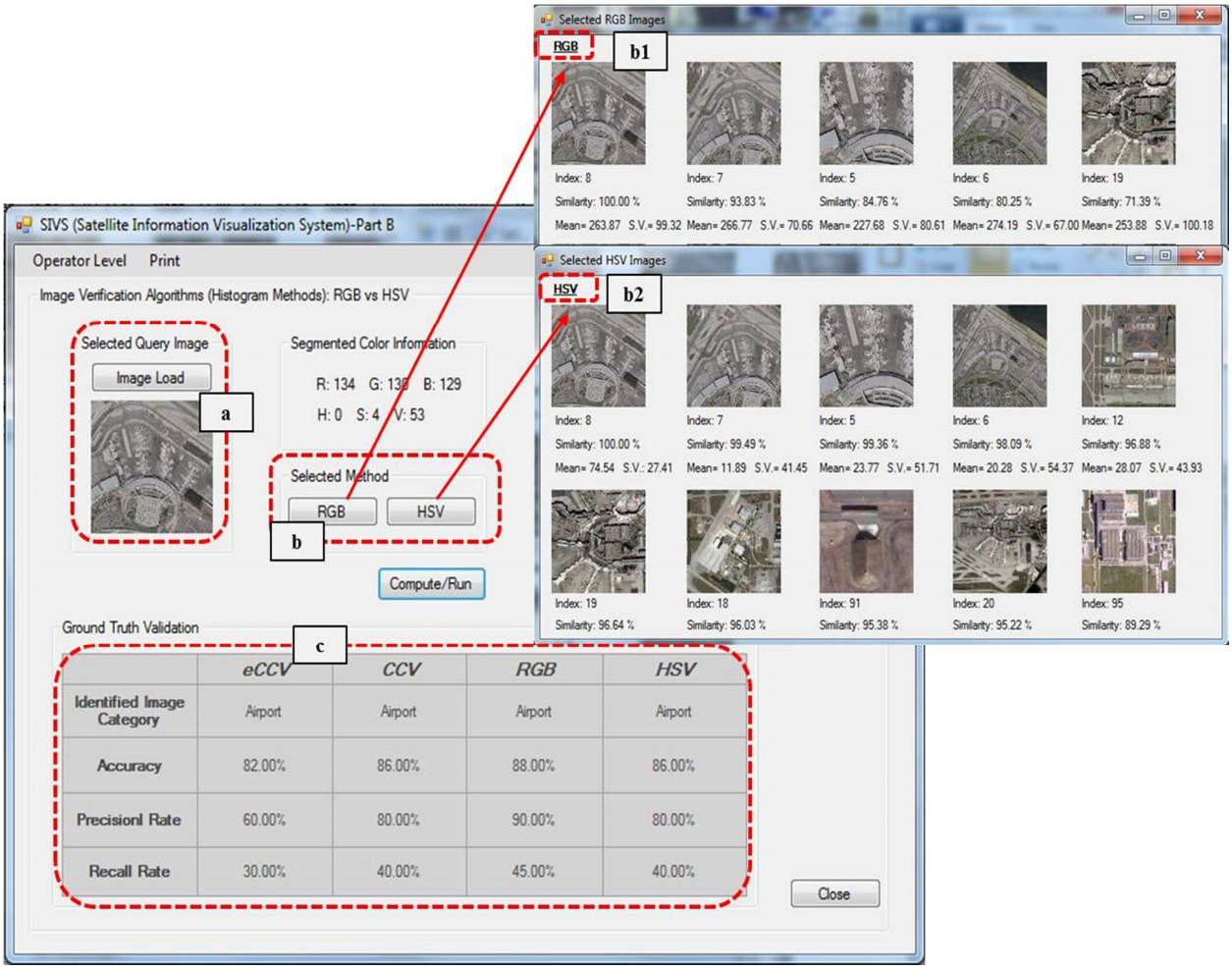

Figure 50. Example of histogram methods (RGB/HSV).

A subjective questionnaire is used to capture the user's cognitive activities at each of the knowledge levels. The cognitive visual analytics consist of the five features (*a-e features*) as shown in Figure 51. These are (a) knowledge selections (the eight knowledge levels as described in previous chapters and the user need to select all knowledge selection on knowledge tabs), (b) the descriptions of user tasks (the tasks are based on the subjective questionnaires), (c1) user selections of suspicious objects, (c2) instruction to the user selections, (d) a display of user hypotheses and belief values (hierarchical node relationships) , (e) computation results using Bayesian data fusion (T-norm, residuum, and fuzzy norm), and (f) the final degree of belief based on the identified image by the user.

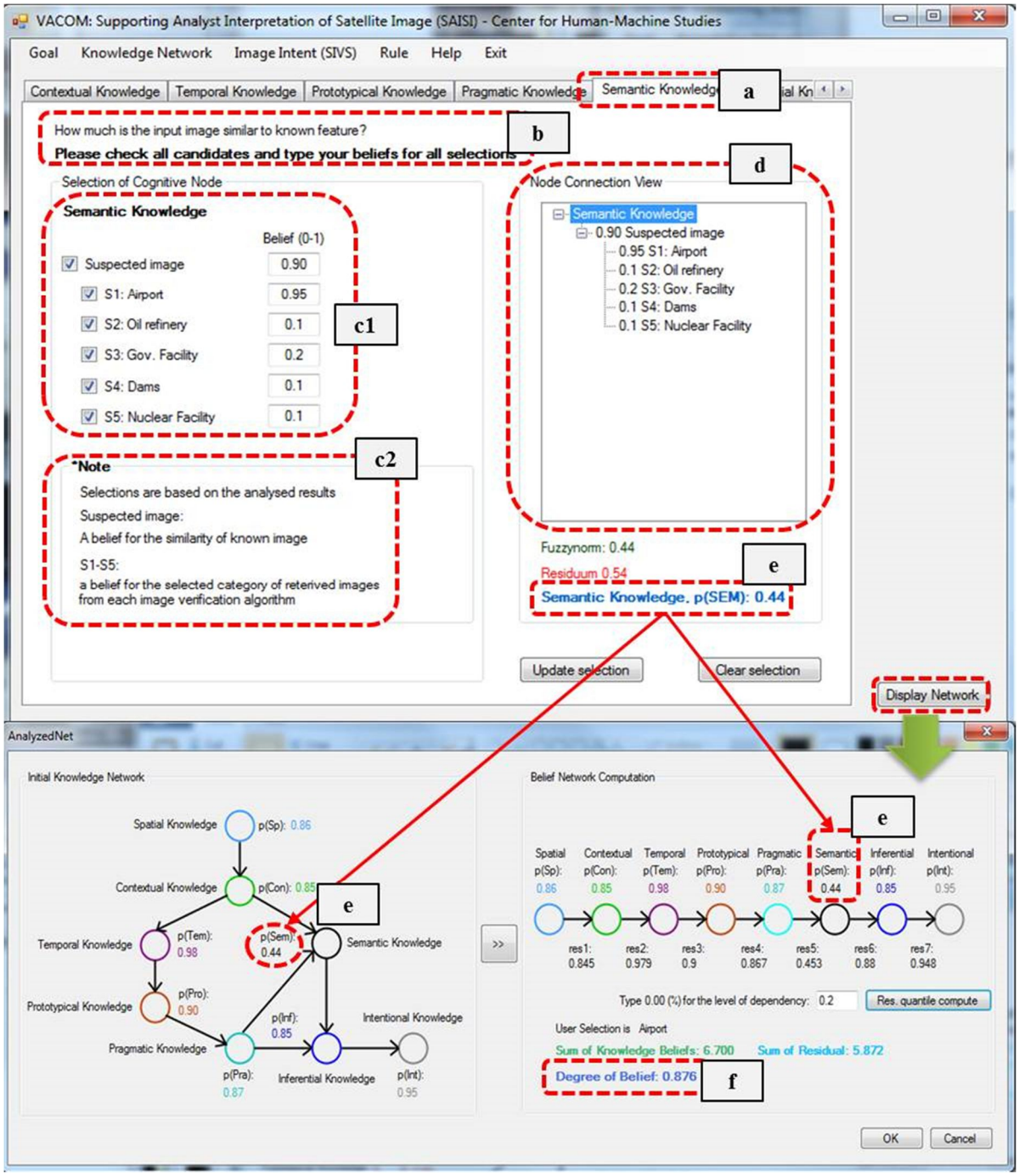

Figure 51. Example of knowledge network: Cognitive visual analytics.

5.3 Image Acquisitions Interface. Figure 52 represents the image acquisition interface. This interface module allows the user to capture and load a particular location of Google map by selecting an area of interest. Figure 52 depicts a process in which the user selects from the 'load

a map' to the 'capture a target image'. The designated 'area of interest' of the sample images is used for analysts.

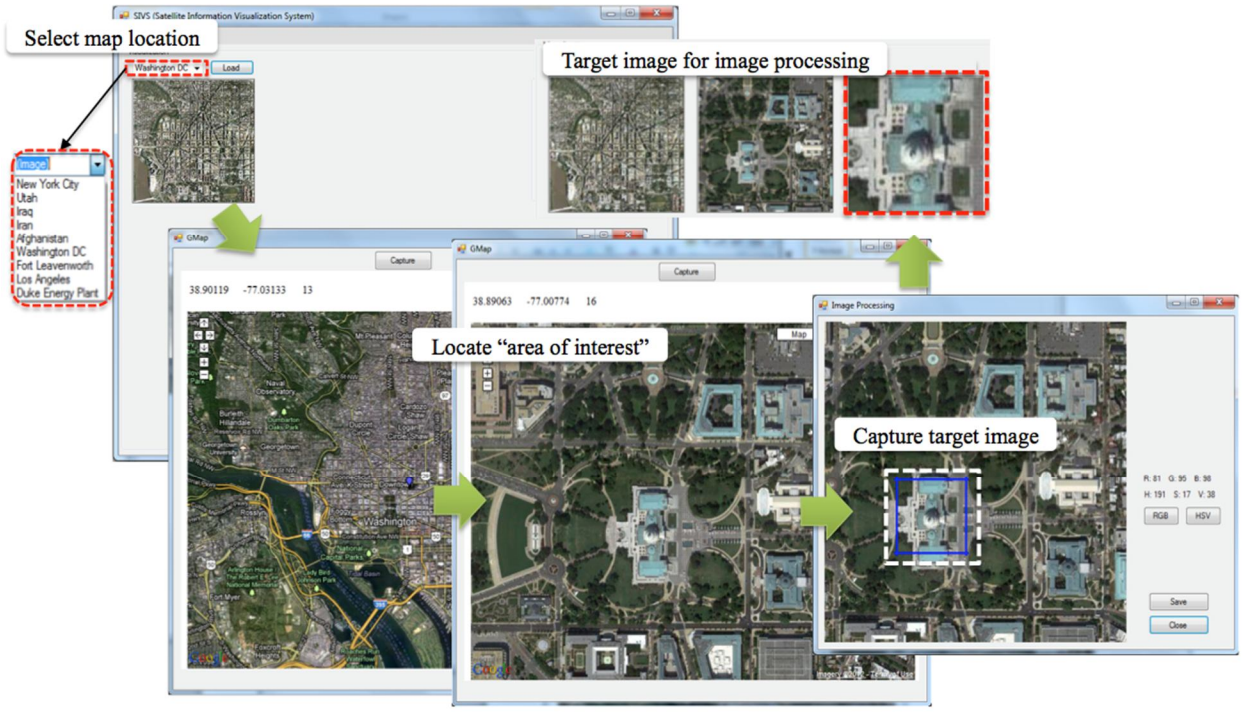

Figure 52. Example of an image acquisition interface for creating sample images.

5.4 Chapter Summary

In this chapter the implementation of VACOM interface was discussed. VACOM interface allows the user to select a satellite image of interest, select each of the image analysis methods for visualization, and compare 'ground-truth' information against the recommendation of VACOM. VACOM interface is designed to capture user intents (mental processes) used for image-based information processing, including identification of suspicious objects of interest. The interface is designed to enhance perception, cognition, and even comprehension to the multi and complex image analyses by the analysts.

CHAPTER 6

VACOM Functionality and Usability

6.1 VACOM Interface Functionality

The purpose of VACOM interface is to create display and visualization capabilities for use in decision making. The current features in VACOM interface allow the user to conduct multiple image verification methods to identify suspicious images with computed degree of beliefs. The construction of interface walkthrough is: 1) steps 1-6 for primary visual analytics of non-histogram methods, 2) steps 7-11 for primary visual analytics of histogram methods, and 3) steps of 12-19 for cognitive visual analytics of knowledge network and Bayesian belief network representation. For a single iteration of image analyses task, the image processing methods and knowledge processes are executed in order as followed by step-by-step instructions.

1. Run 'VACOM: Supporting Analyst Interpretation of Satellite Image (SAISI)' as shown in Figure 53.

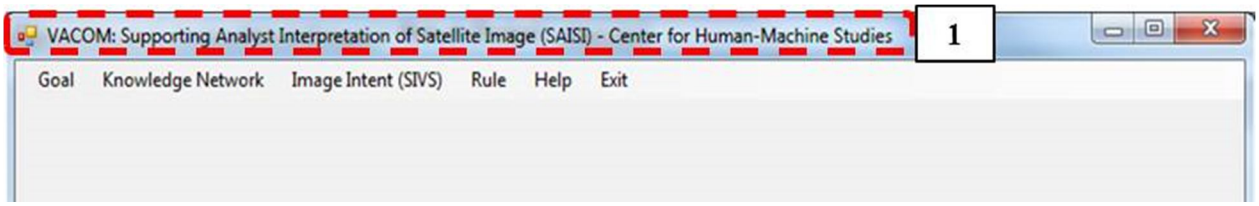

Figure 53. Main view of VACOM: Supporting analyst interpretation of satellite image.

2. Choose (2a) 'Image Intent (SIVS)' from the main menu, and then choose (2b) 'Part A: Non-histogram Method (CCV/eCCV)' from the sub-menu as shown in Figure 54.

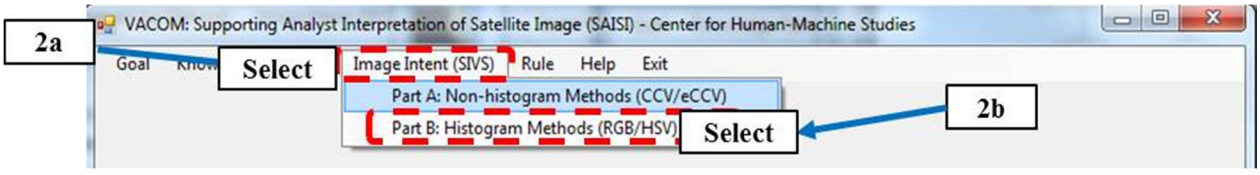

Figure 54. Selection of Part A (Non-histogram) methods.

3. Display main screen of ‘SIVS-Part A: Non-histogram methods (CCV/eCCV)’ as shown in Figure 55.

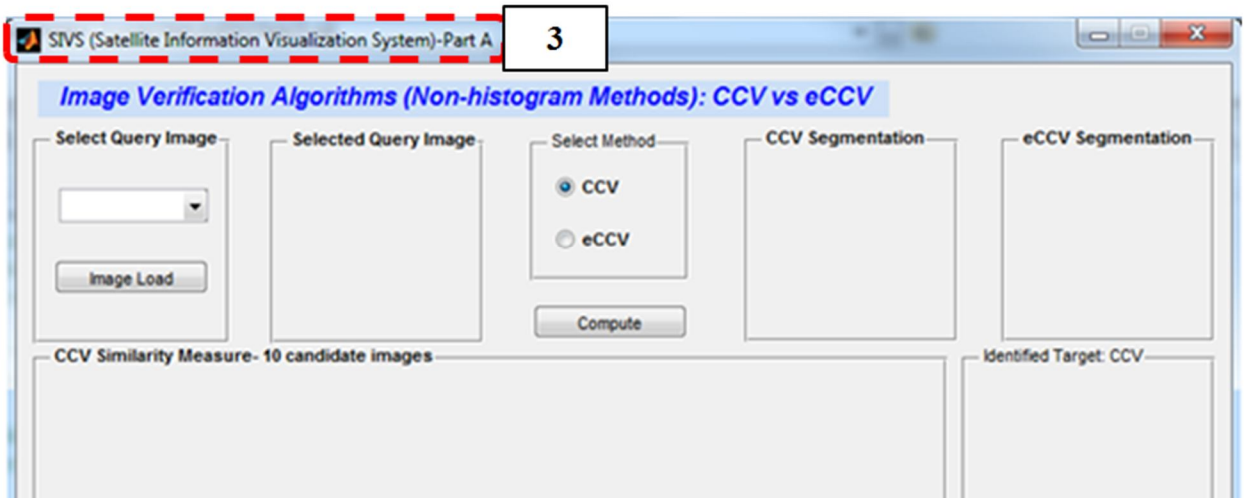

Figure 55. Main view of SIVS-Part A: Non-histogram methods (CCV/eCCV).

4. Click a combo box button (4a) to ‘select a query image’. Scroll up and down a drop-down menu to select an image as shown in Figure 56. Click ‘Image load’ button (4b). A query image will be appeared to ‘Selected Query Image area’.

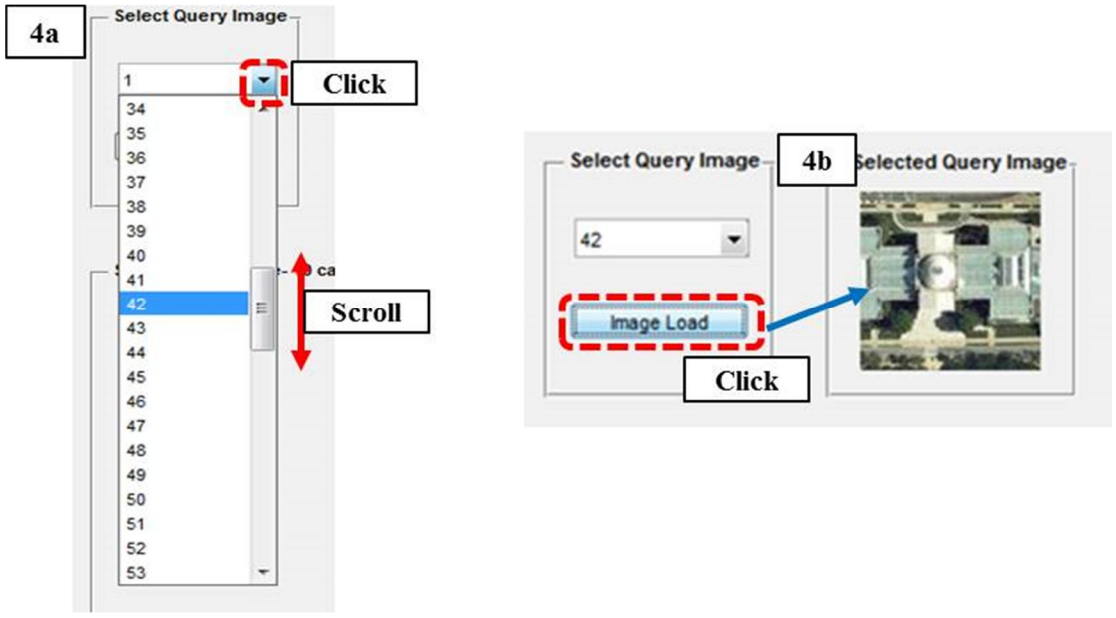

Figure 56. Image selection from the menu and image load from user selection.

5. Choose either CCV or eCCV method (5a). Click ‘Compute’ button (5b). Segmentation results will appear to posture 5c depending on a user selection (either CCV or eCCV segmentation results) as shown in Figure 57.

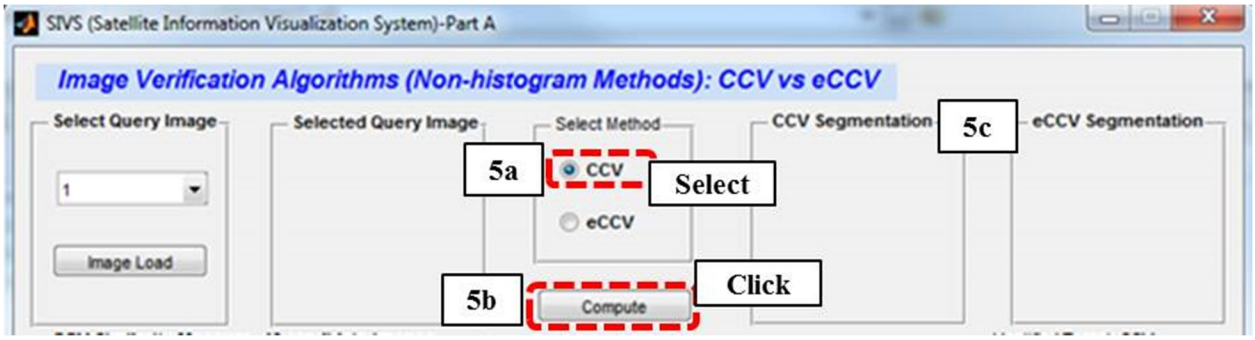

Figure 57. Non-histogram method selection.

6. Display the labeled 6a, 6b, and 6c in Figure 58 for the image-based analytical evaluations after clicking ‘Compute’ button.

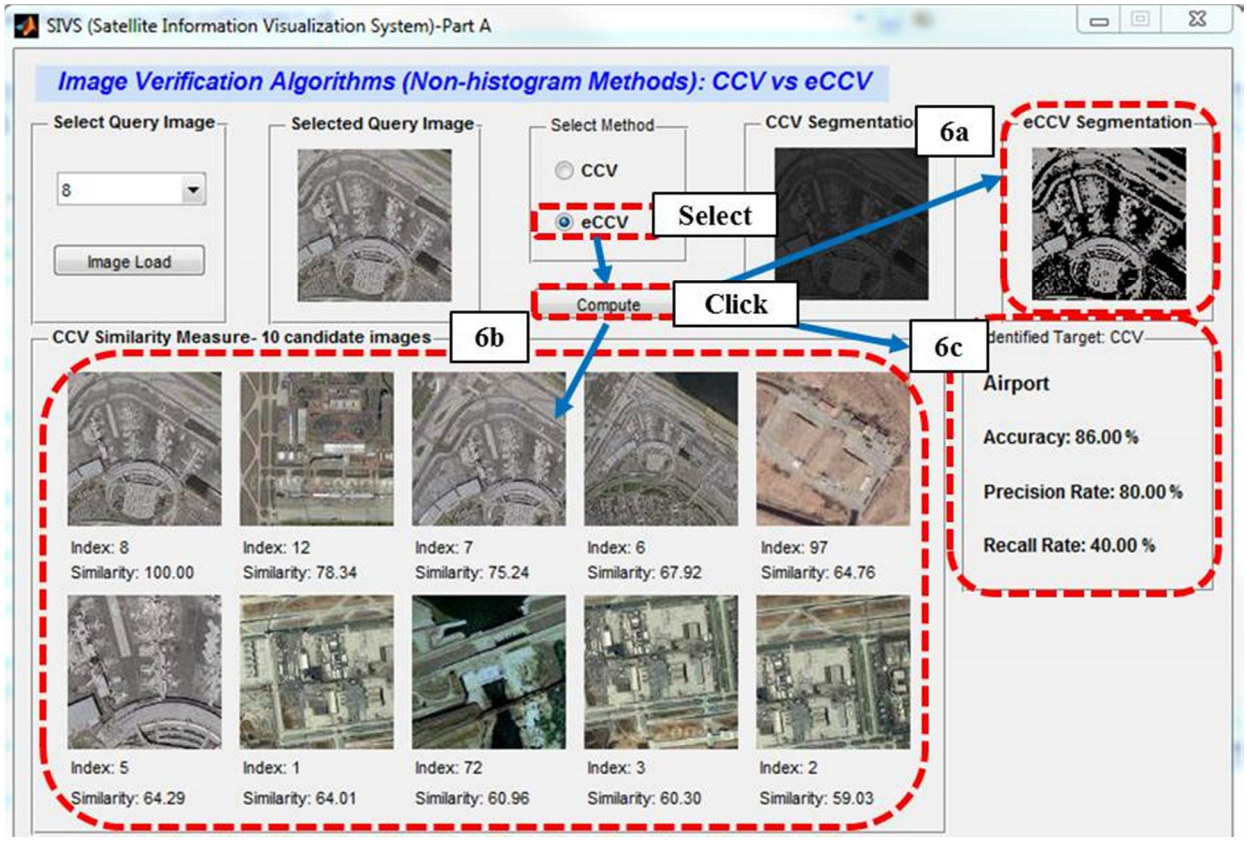

Figure 58. Example screen of image-based analytical evaluations for non-histogram methods.

7. Moves to the histogram methods (RGB/HSV). Choose (7a) ‘Image Intent (SIVS)’ from the main menu, and then choose (7b) ‘Part B: Histogram Method (RGB/HSV)’ from the sub-menu as shown in Figure 59.

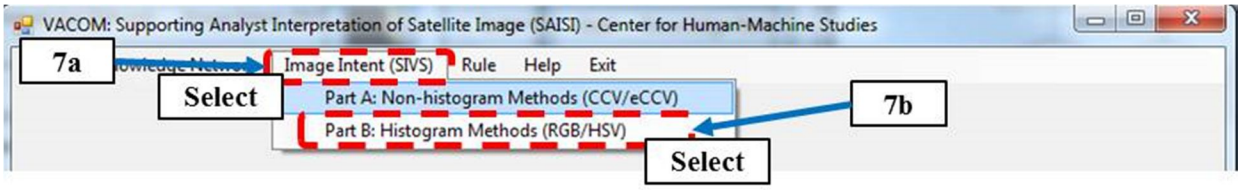

Figure 59. Selection of Part B (Histogram) methods.

8. Displays main screen of ‘SIVS-Part B: Histogram methods (RGB/HSV)’ as shown in Figure 60.

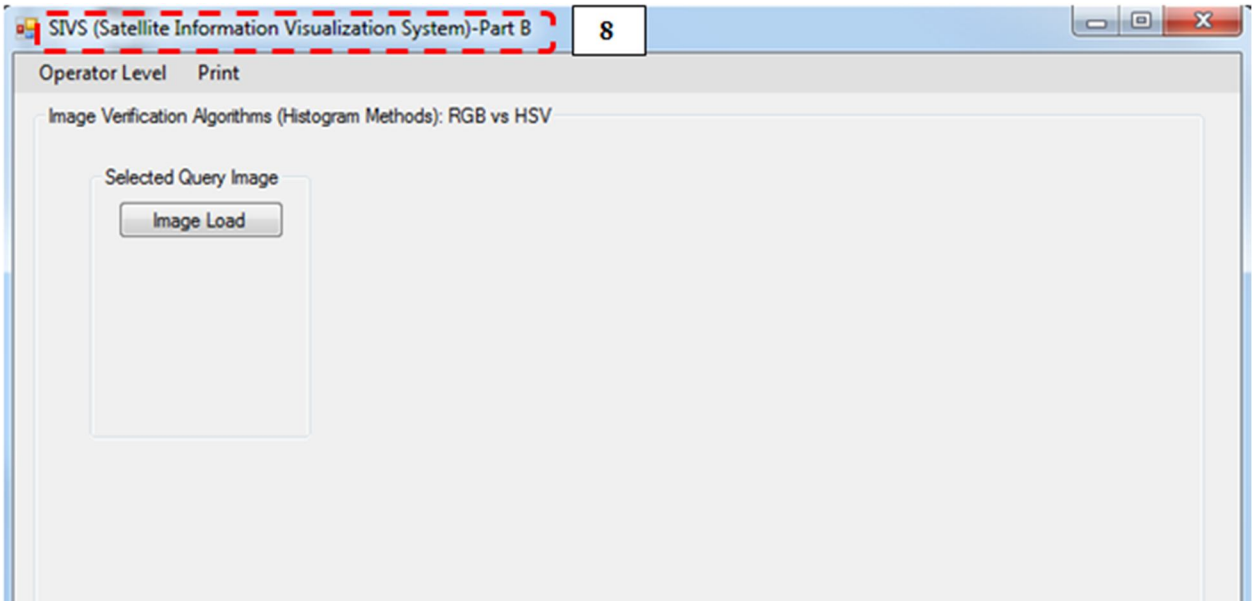

Figure 60. Main view of SIVS-Part B: Histogram methods (RGB/HSV).

9. Click ‘Image load’ button. A query image (9a: a query image is same image where used in the non-histogram methods) and color information (9b) will appear as shown in Figure 61. The image-based analytical evaluations of CCV and eCCV also will be appeared as soon as ‘Image load’ button has clicked.

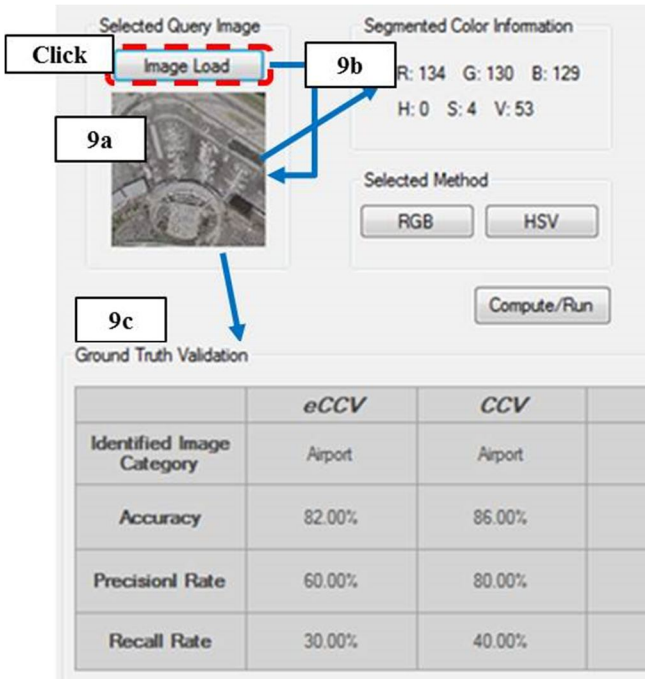

Figure 61. Image load from a selected image.

10. Choose and click either RGB (10a) or HSV (10b) method. The results of image-based analyses will be appeared to the individual widow screens as shown in Figure 62.

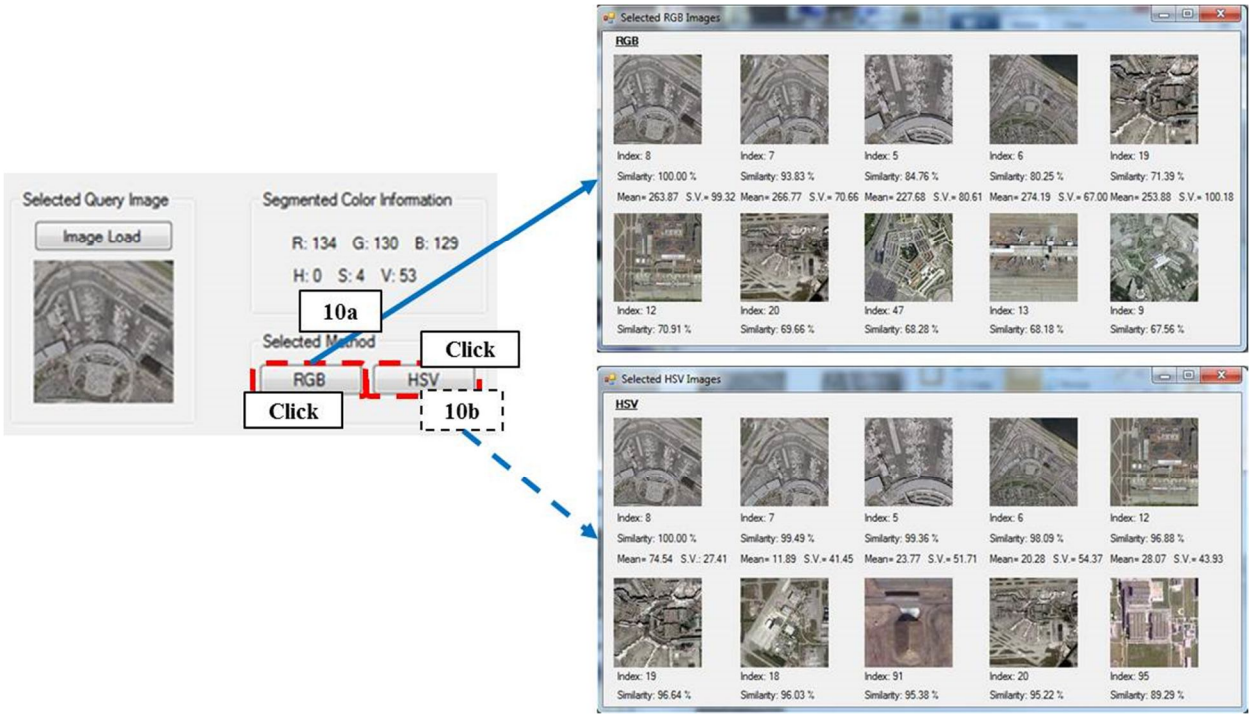

Figure 62. Example screen of the method selection and its results.

11. Click ‘Compute/Run’ button to obtain the image-based analytical evaluations after the step 10 as shown in Figure 63.

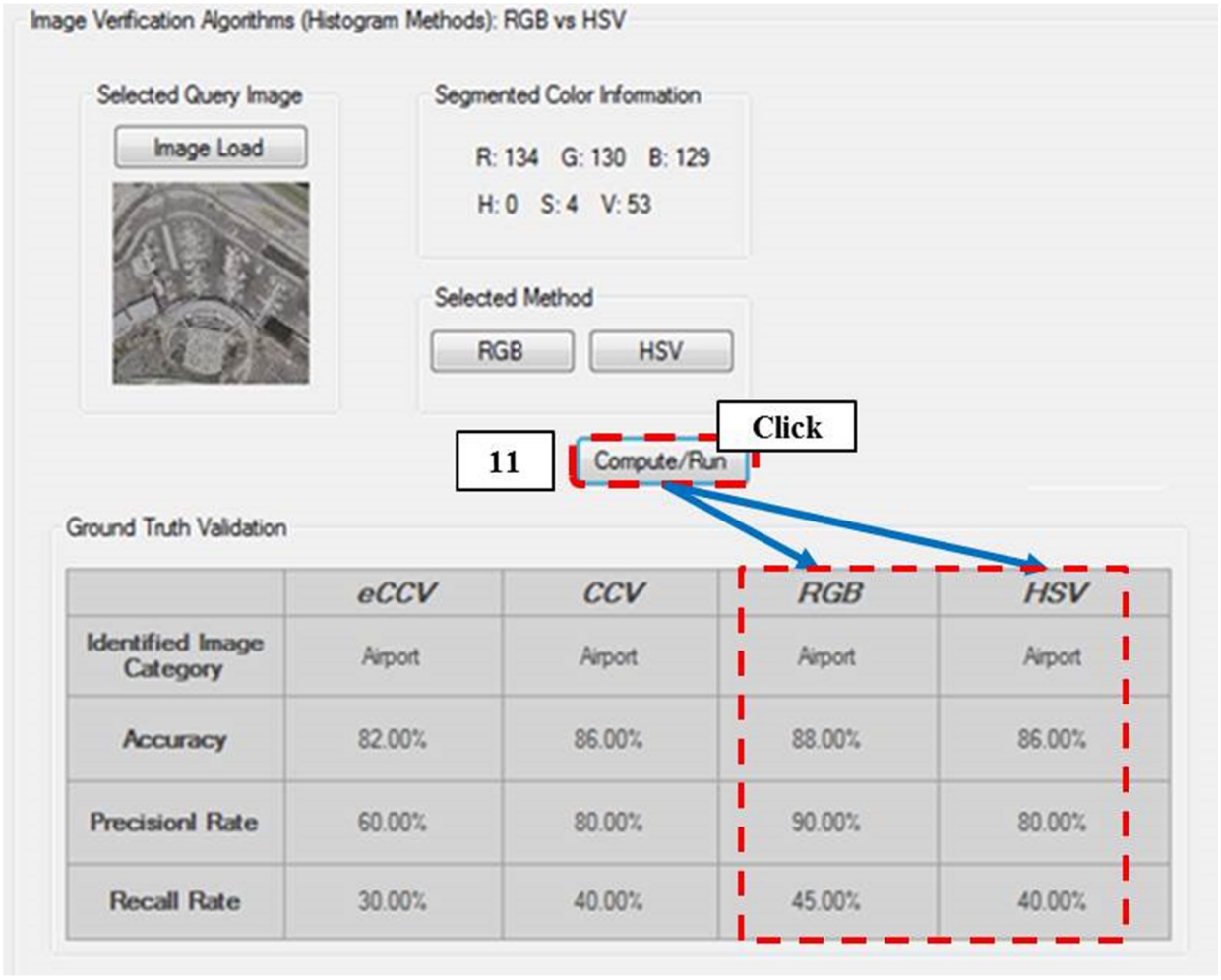

Figure 63. Example screen of image-based analytical evaluations for histogram methods.

12. Go back to the main menu and choose ‘Knowledge Network’ from the main menu as shown in Figure 64. Then knowledge levels tab window will be appeared.

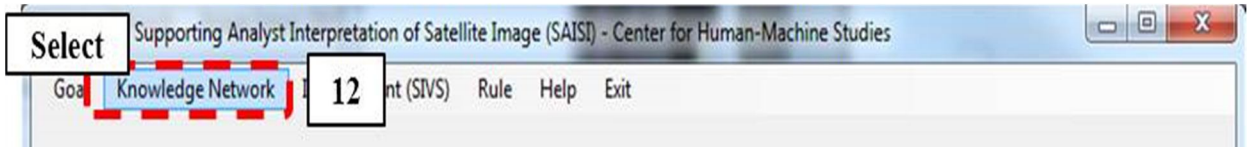

Figure 64. Selection of ‘Knowledge Network’ menu.

13. Choose one of the 'Knowledge Tabs' (13a) to engage in cognitive tasks as shown in Figure 65. User is able to select a 'Knowledge Tab' at a time and use a button (13b) to move the next tabs.

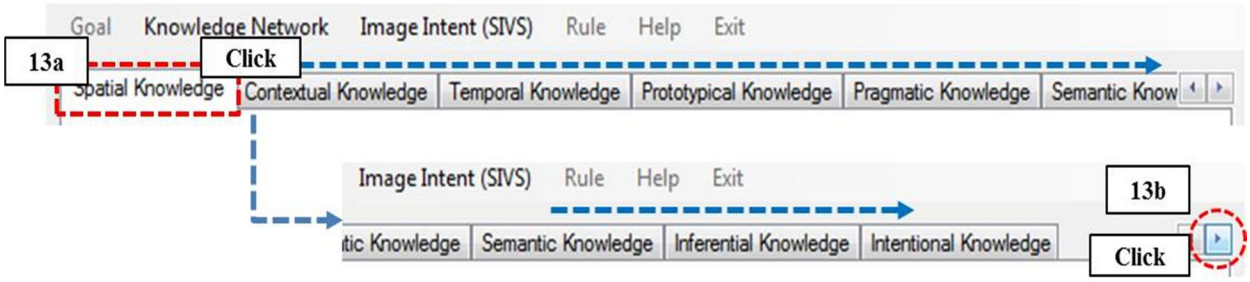

Figure 65. Selection of 'Knowledge Network' menu.

14. Read two types of instructions (14a or/and 14b) to each knowledge tab as shown in Figure 66. The user needs to read the subjective questionnaire(s) (14a) for the all knowledge tabs. Note-14b is a detail instruction to guide more directions to the tasks.

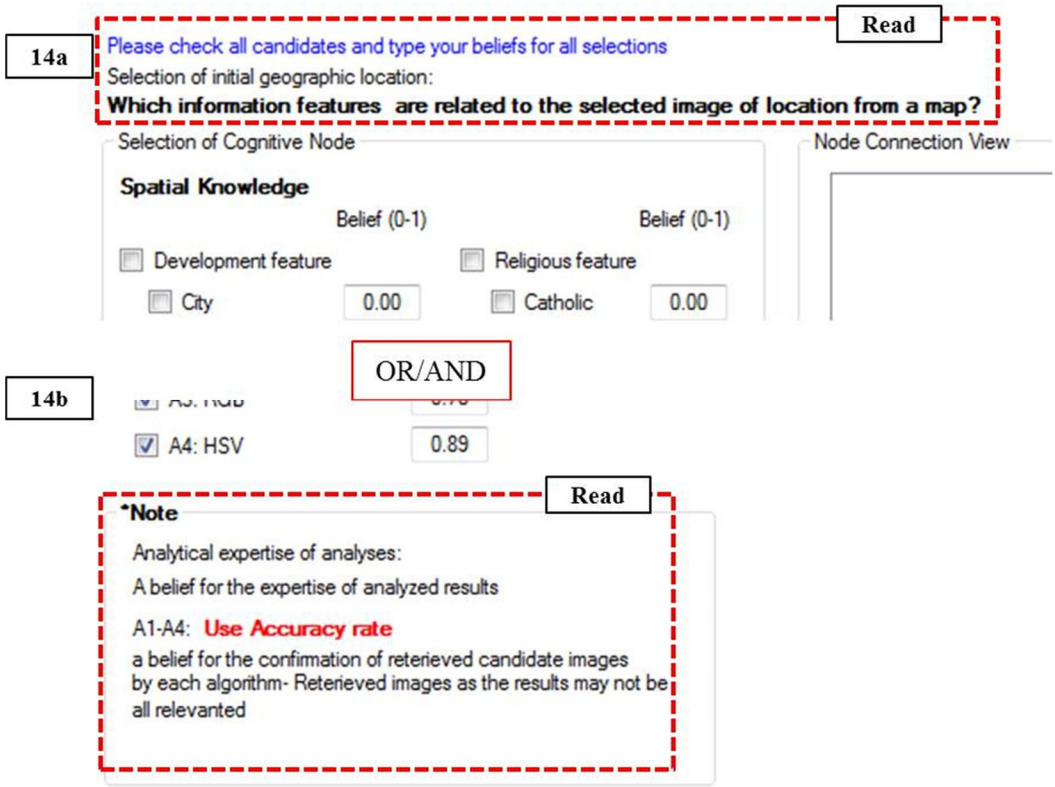

Figure 66. Example screenshots of cognitive tasks' instructions.

15. Select the number of check boxes (15a type) or radio buttons (15b type) on the 'Selection of Cognitive Node' section as shown in Figure 67. Input the user beliefs of the selected choices on the text boxes. Depending on the knowledge levels, user may use 15a or 15b to perform the tasks.

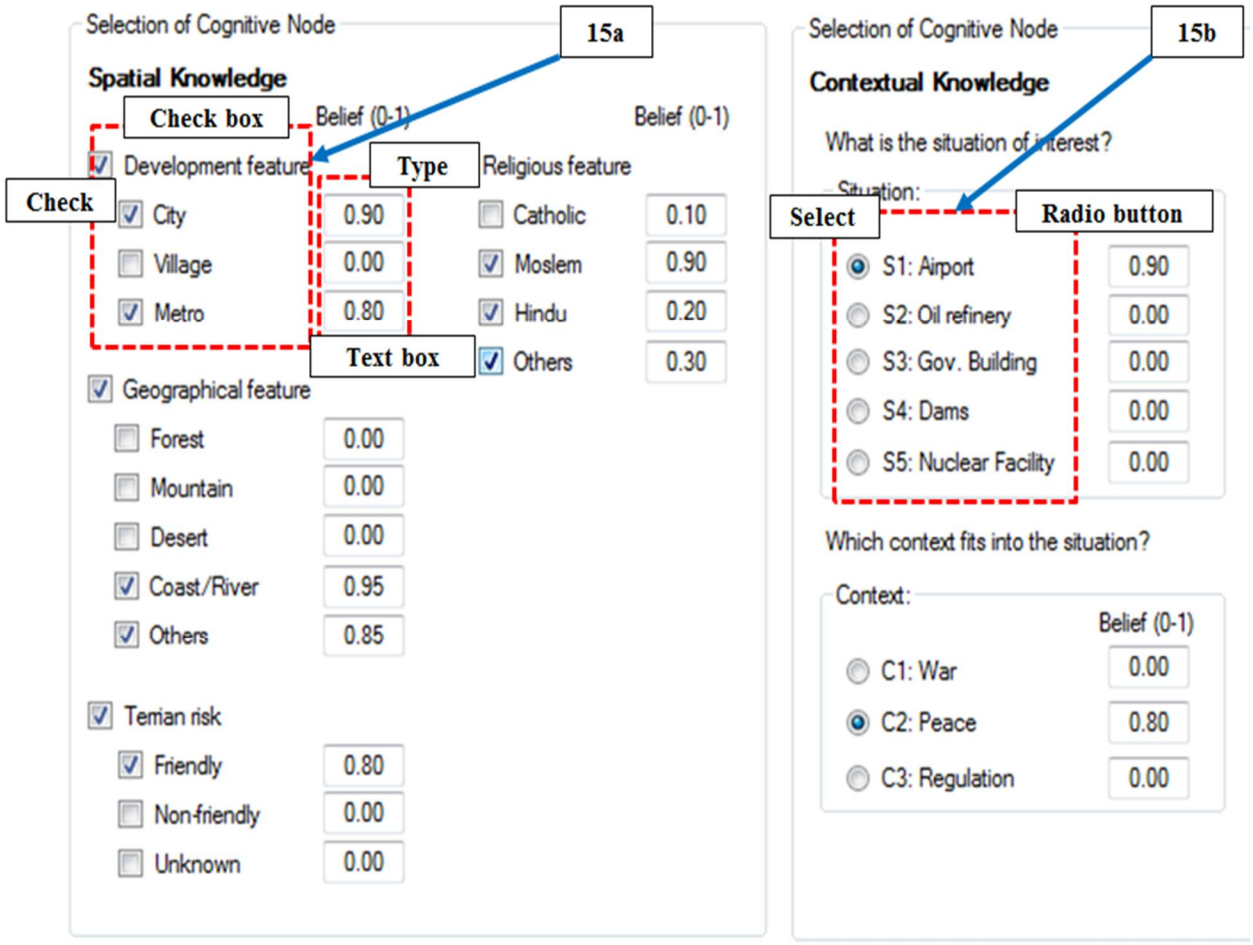

Figure 67. Example screenshots of 'Selection of Cognitive Node'.

16. Click 'Update selection' button when 'Selection of Cognitive Node' is done as shown in Figure 68. 'Update selection' displays (1) a structure of cognitive connections, and then show (b) total belief of each knowledge level. 16a and 16b explain the different types of computation results. User can cancel user selections in anytime when user click 'Clear selection' button.

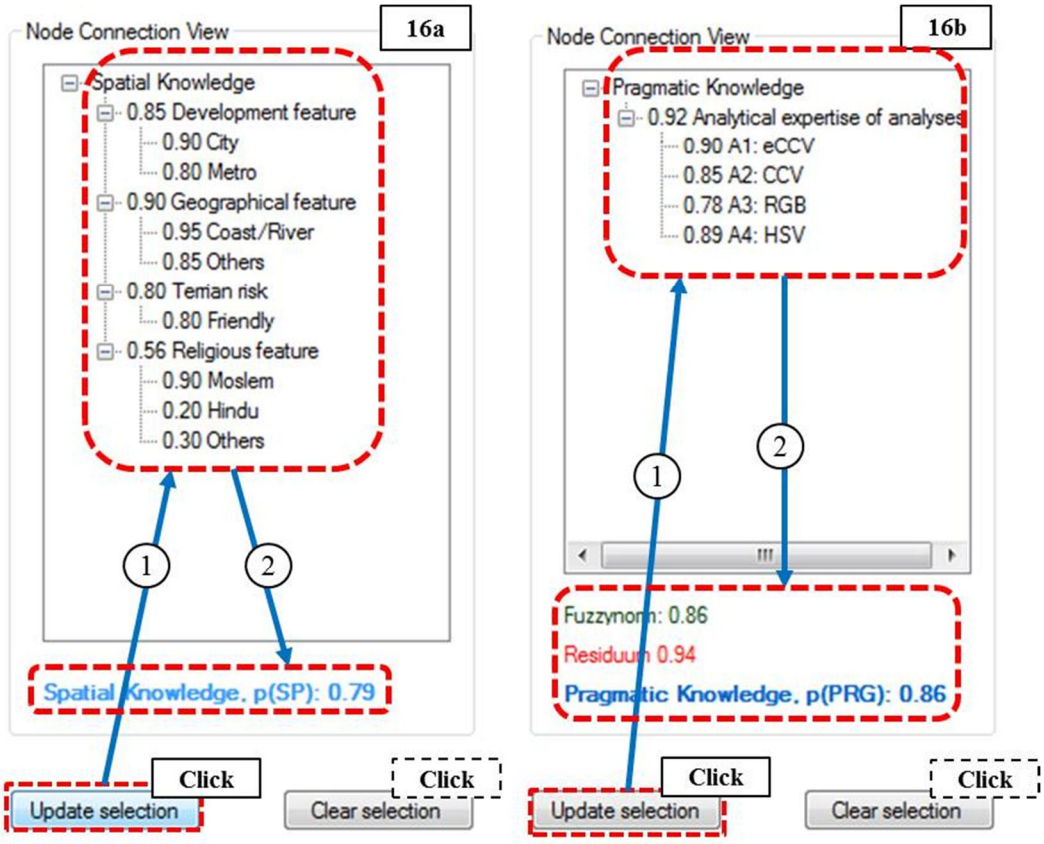

Figure 68. Example screenshots of 'Nod Connection View'.

17. Click 'Display Network' button when user has finished to all tasks of knowledge tabs as shown in Figure 69. New widow will appear to show cognitive visual analytics.

Figure 69. Example screenshots for execution of cognitive visual analytics.

18. Figure 70 will display knowledge network representation (18a) and data fusion with Bayesian belief network representation (18b). Type the level of dependency rate (e.g., $\alpha = 0.2$, $0 < \alpha \leq 1$) to the text box (process of 2), and then click 'Res. quantile compute' button (process of 3) as shown in Figure 70.

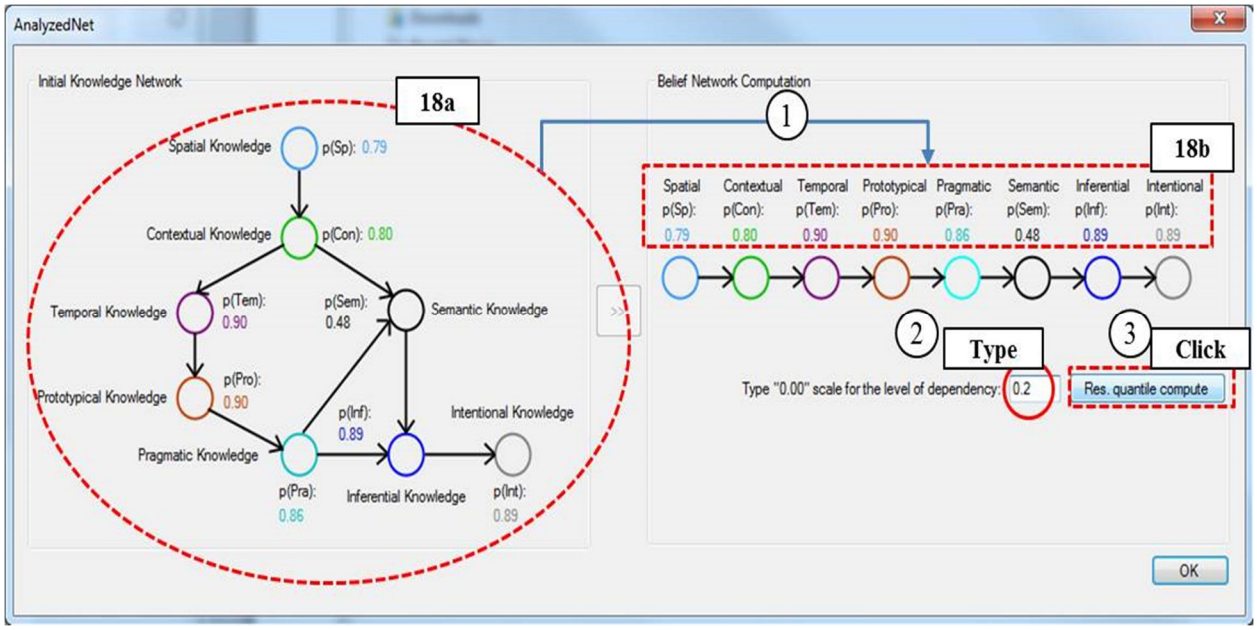

Figure 70. Example screenshots of knowledge network and Bayesian belief network representation.

19. Display the result of 'degree of belief' computation with residuum of each knowledge nodes as shown in Figure 71.

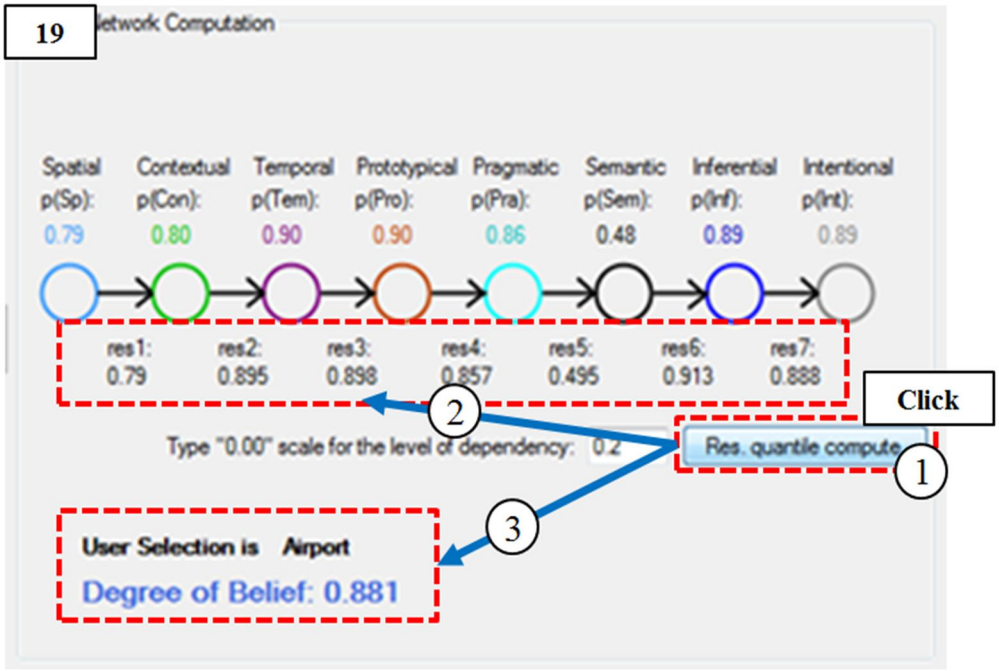

Figure 71. Example screenshot of 'degree of belief'.

6.2 Usability Study

Heuristic evaluation involves having a small set of evaluators examine the interface and judge its compliance with recognized usability principles ("heuristics"). The usability principles refer to Nielsen's 10 usability heuristics and Tognazzini's 16 design principles (Nielsen, 1992; Tognazzini, 2003). A heuristic evaluation includes the identification of usability problem with description, the identification of violated design principles, and "severity rating" (Nielsen, 2003) on each finding. The severity value (0 to 4) prioritizes the usability issues. Highest rating is most severe usability issue which needs to be resolved prior to product release. Three main usability metrics possibly are used in the evaluation of interfaces such as effectiveness, efficiency and satisfaction. Effectiveness and efficiency serve as quantitative measurement scales while satisfaction is a qualitative measurement scale.

As designers of this system, it was possible for us to overlook certain significant aspects of VACOM interface. Despite having done the background research on the task domain, the system must still be developed and revised based on the actual user interaction. To that end, usability study was required. In ideal world, this design would fulfill all the important usability goals: effectiveness, efficiency, satisfaction, speed of performance, learnability, error rate, etc. Usability testing provides benchmarks for designers in the early design phases of a system, preferably before the system has full functionality.

The usability study of VACOM interface did not include all three main usability metrics. Our main goal in this usability study was to evaluate VACOM interface in terms of usefulness, effectiveness, learnability, and attitude. Only qualitative measurement was tested to improve the VACOM interface for supporting better decision. This usability study excluded the quantitative measures (e.g., number of mistakes, errors, etc.) for the testing, because the VACOM interface is to improve the interfaces' functionalities.

6.2.1 Participants. The estimated number of human subjects for the study was derived from the power of test formula. The power is defined as the probability of committing type II error, that is, failure to reject null hypothesis when in fact the alternative is true (Cohen, 1977). Based on the hypothesis, the sample size expression is shown in Equation 23.

$$n = \frac{2v\sigma^2\Phi^2}{\Delta^2} \tag{23}$$

Where, n = number of subjects; v = number of treatment levels; σ = standard deviation; Φ = power of the study, and Δ = effective size of the study. Using a power of 0.80 at the 0.05 significant level, an Φ-value of 1.824 was interpolated from the power of the F-Test table provided by Dean and Voss (1999). A v-value of 4 was obtained based on the levels of different image verification algorithms.

Using three subjects to conduct a pilot usability study for stand-alone identification gave a sample standard deviation of 3.33 and estimated the effective size (Δ) of 15.37. The sample size required was established by

$$n = \frac{2\times4\times3.33^2\times1.824^2}{15.37^2} = 4.99 \approx 5 \text{ subjects.}$$

Hence 5 participants were used for the study.

6.2.2 Post-Study Questionnaire. Users were required to take post-study questionnaires for qualitative measures. The measurements collected the satisfaction of the user interface to improve its design for enhancing the usage of interface functionality. Three types of questionnaires were used as shown in Table 10-12. The question of Table 10 asked for the overall interface of functional flows when users perform tasks through the interface. Table 11 asked questions to analyze the prototype interface. The subject users were asked to mark the degree of satisfaction as described in Table 10 and 11. Subject users were required to answer overall interface evaluations as described in Table 12.

Table 10

Sample post-study questionnaire 1 for the satisfaction of interface

	Very Difficult		Neither Easy Nor Difficult		Very Easy
Learning to operate the system	1	2	3	4	5
Performing task is straightforward	1	2	3	4	5
Exploring system process	1	2	3	4	5
Remembering name and use of commands	1	2	3	4	5

Table 11

Sample post-study questionnaire 2 for the satisfaction of interface

	Very Difficult		Neither Easy Nor Difficult		Very Easy
Visual Appeal	1	2	3	4	5
Organization of information	1	2	3	4	5
Usefulness of menu (e.g., menu, tab)	1	2	3	4	5
Ease of use interface items (e.g., buttons, check boxes, etc.)	1	2	3	4	5

Table 12

Sample post-study questionnaire 3 for the satisfaction of interface

	Poor		Satisfactory		Excellent
Overall reaction to the interface	1	2	3	4	5

Users also were able to give their suggestions, which were not included in the post-study questionnaire for the improvement of interface.

6.2.3 Results of Post-Study Questionnaire. The five users conducted the Post-Study Questionnaire. Users were all graduate students at North Carolina A&T State University who were familiar with use of computing software. The difference of gender and age were not a concern in applying the experiments. No disability of any required computer usage was found by the participants of experiments. Figure 72 below shows the mean response for the post-study questionnaires. These questions sought to explore the satisfaction levels of participants toward the interface. The highest and lowest mean responses were aesthetics (visual appeal) and interface's functionalities (menus and items) respectively.

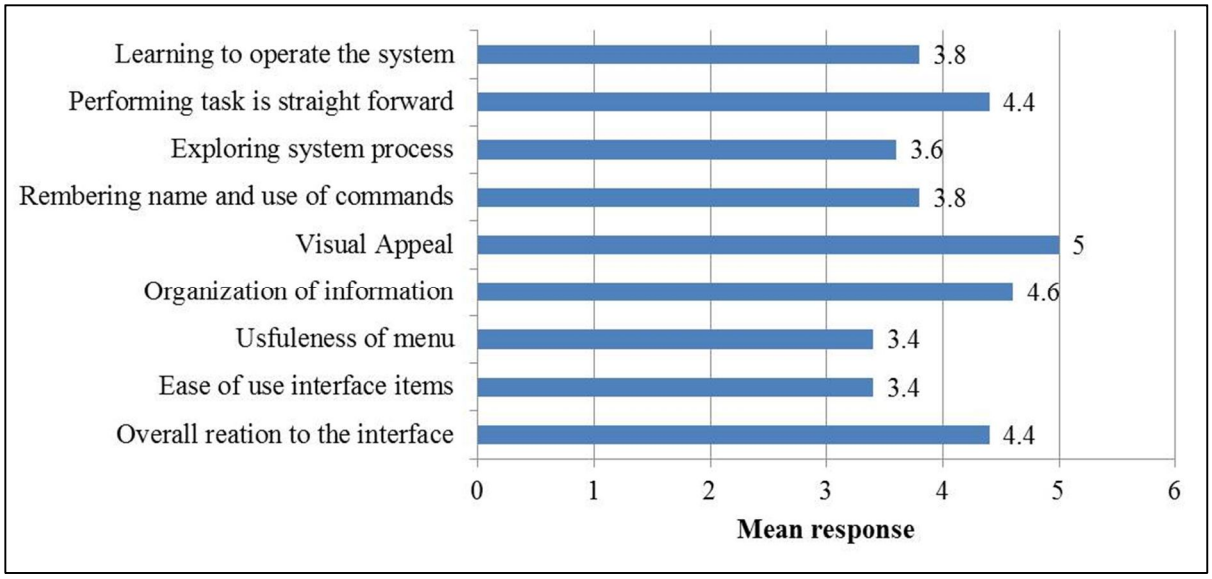

Figure 72. Mean response for post study questionnaire with a sample size of 5.

From the post-study questionnaires, the participants also suggested the valuable comments which were not covered in the questionnaires:

- Multiple interactive windows can decrease users' attentions or increase visual fatigues. (Use minimal windows).
- Unnecessary functions and items can increase confusion of users' tasks (Redesign user-centered functions and items or Delete unnecessary lists).

- Operation steps were not clear, even though users' tasks were straightforward. (Use clear notifications for operation steps to the interface).
- Only single cycle of simulation was executed to run the cognitive network interface (Make multiple cycle of simulation capability for users).

6.3 Sample Database of Satellite Images

In this dissertation, most of the sample databases of satellite images are selected from Google Map©. Through the 'Google Search Maps', selected satellite images are collected as possible candidates. There are few steps to select a sample satellite image for the area of interest as shown in Figure 73.

Figure 73. A simple process of selected image for database and target.

The area of interest target in 'Search Maps' of Google Map© are manipulated with zoom levels to select a candidate sample from the map. The zoom level determines a reduced image scale for a particular location. A reduced scale image is defined as the ratio of a distance on the

map to the corresponding distance on the ground. The particular zoom level of 200ft/100m, which is right before maximum zoom level, was used in the study. The selected zoom level was manageable and comparable size to feature detection and recognition aspect when certain features were cropped for comparison with the others. Figure 74 explains the degree of zoom level and how sample satellite images were captured for the analytic computation. The images in a database were created by the selected zoom level.

Figure 74. Capturing sample satellite image for the analytic computation.

The database consisted of 100 images which were captured from Google Earth for the implementation of the proposed algorithms. Query images in the database were placed into five different categories as shown below in Table 13. Each single image's detail was different within the same category such as

- rotation and translation of objects in the images,
- occlusion and subtraction of objects in the image,
- change angle viewpoint and magnification,

- similar key shape of objects in the image, and
- similar color environment of objects in the image

Table 13

The major categories of images in the database

Category	# of Relevant Images
Airport	20
Building (e.g., Gov., etc.)	20
Oil refinery	20
Plant (e.g., Nuclear, etc.)	20
Dams	20

An individual image was 100 by 100 pixels of color image. The selected images were not the same as the usual satellite imagery. The images were captured in a selected area of interest because of some constraints of building a satellite database, such as, limited access of satellite imagery, cost, computation time, and complexity of image analysis methods. Figure 75 shows sample images from the database that have similar colors schemes within the same categories. Basically a query image compares its color characteristics with all images in the database.

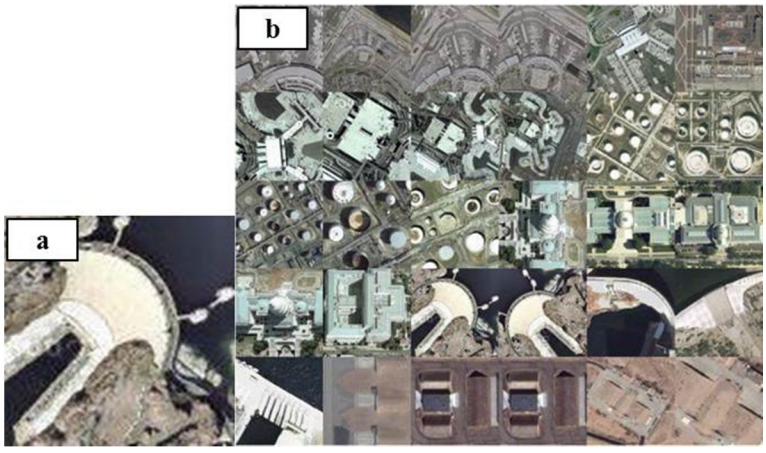

Figure 75. Query image retrieval example: (a) Left: Query image-Input and (b) Right: Example of database-30 images out of 100 images.

6.4 Design of Experiment

The VACOM visualization tool runs on a 2.93 GHz Intel (R) Core (TM) 2 Duo CPU with Microsoft Windows 7 Home Edition and Professional. Two computer monitors (Wide 22 inch size) were used to display the VACOM interface. The VACOM interface was developed by MATLAB 7.11.0 (R2010b) and Visual Studio 2008 (Visual Basic). As data analysis tools, SAS 9.2 and Microsoft Excel 2010 were used to obtain descriptive and inference statistics.

The five human subjects were selected to perform this study. Each user had 5 images which were randomly selected within different image categories from a database. As described in by section 6.1, each user performed the experiments of VACOM to confirm object was identified by computer models based on the selected satellite images. Each subject repeated a single cycle of experiment with the given images for a total 5 iterations. Therefore, total 25 trials were executed (5 tasks × 5 human subjects). Figure 76 presents an information flow of user experiment process from the beginning of image selection to the end of the experiment for obtaining the degree of belief.

Independent variables (IVs) was the image verification method (with 4 levels: CCV, eCCV, RGB, and HSV). As the dependent variable (DV) for the experiments, the accuracy rate was used. Human subjects became another IV to compare human performances against the other methods. One-way ANOVA is used to analyze the produced results for comparing methods (including human judgments (degree of beliefs). Tukey's HSD test was also used to produce post hoc multiple comparison of the image verification methods.

Two statistical data analyses were used for the experiments. Microsoft Excel 2010 was used for the descriptive statistics (mean and standard deviation) with the graphical analyses. For the inference statistics, SAS 9.2 was used to verify the initial hypotheses of this study.

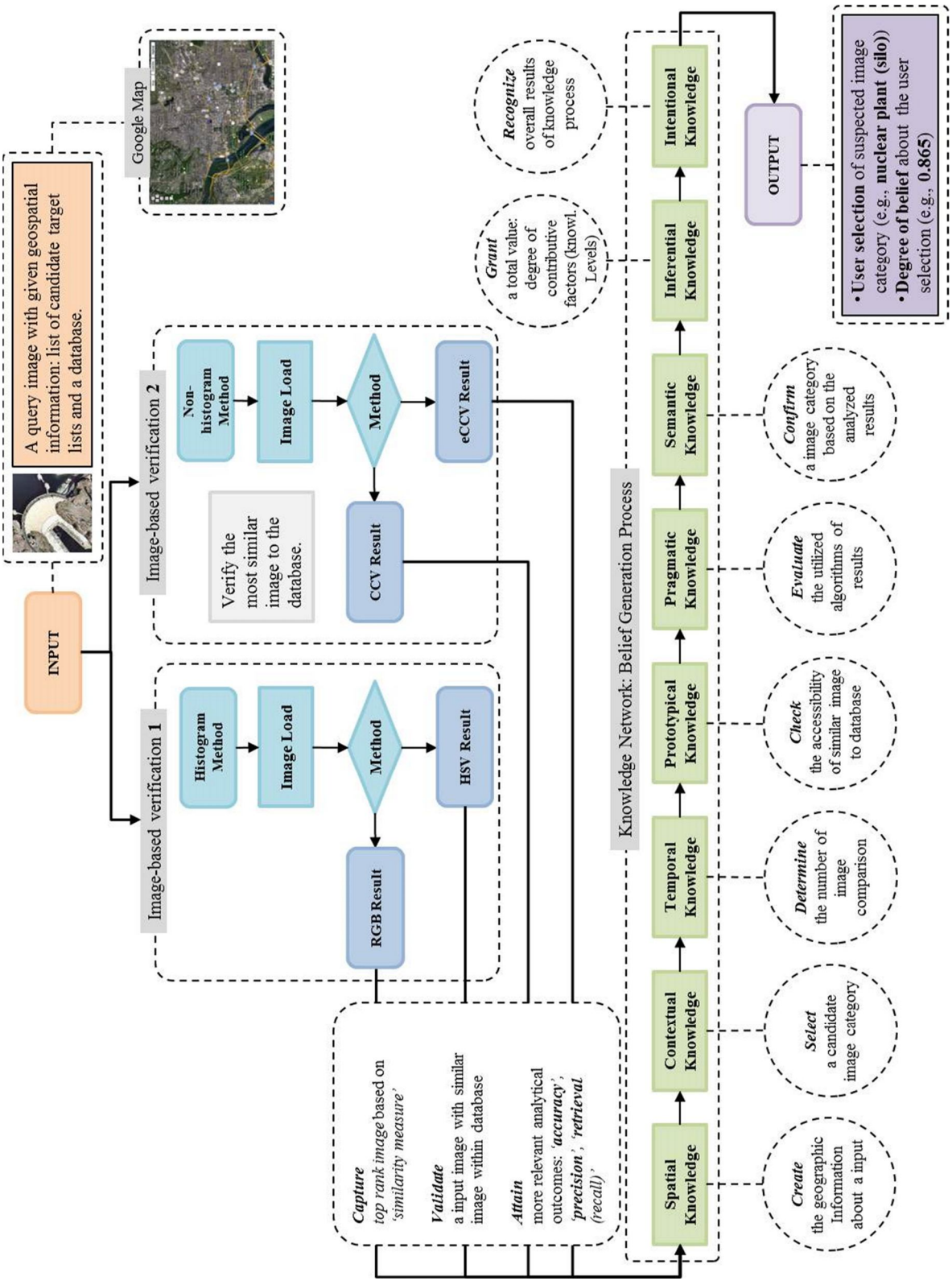

Figure 76. A schematic experimental process.

6.4.1 Human Belief Confirmation (with Degree of Beliefs). The participants generated their beliefs on each knowledge level through the cognitive tasks based on the subjective questionnaires. Degree of belief were then calculated using the beliefs generated by participants (see section 4.3.3.1) consistent with the identified images as shown in Table 14. The table shows the accuracy rates and the degree of beliefs to the identified images by the human analysts. In the Table 14, the accuracy rates of methods were based on the computer-generated methods, and the degrees of beliefs were based on the participants' ratings of the analytical cognitive tasks. The values of human judgments (degree of beliefs) in Table 14 indicate the best accuracy rates within the applied methods. The human judgments had better outcomes compared to the computer-generated methods.

Table 14

A comparison of image verification results between methods and human analysts

Image category	Accuracy				
	CCV	eCCV	RGB	HSV	Human analysts (Degree of belief)
Airport	0.848	0.800	0.788	0.764	0.8708
Oil refinery	0.820	0.788	0.860	0.832	0.8736
Gov. Building	0.844	0.816	0.808	0.844	0.8682
Dams	0.808	0.796	0.772	0.740	0.8636
Nuclear Facility	0.844	0.856	0.772	0.780	0.8684

Table 15 summarizes the comparison of accuracy rates within the applied methods. As described in Table 14, the mean of accuracy for human judgments (degree of beliefs) has the highest value (0.869) with the lowest standard deviation (0.004) in Table 15 and Figure 77. The second most

method was CCV with higher mean (0.833) and lower standard deviation (0.018). The variation of results within the computer-generated methods have also relatively small values comparing to the human analysts, however, these were still larger values against the human judgments.

Table 15

A summary of analytical evaluations: methods vs. human judgment (degree of belief)

		Accuracy	
Method		Mean	SD
Non-histogram	CCV	0.833	0.018
	eCCV	0.811	0.027
Histogram	RGB	0.800	0.037
	HSV	0.792	0.045
Human analysts (Degree of belief)		0.869	0.004

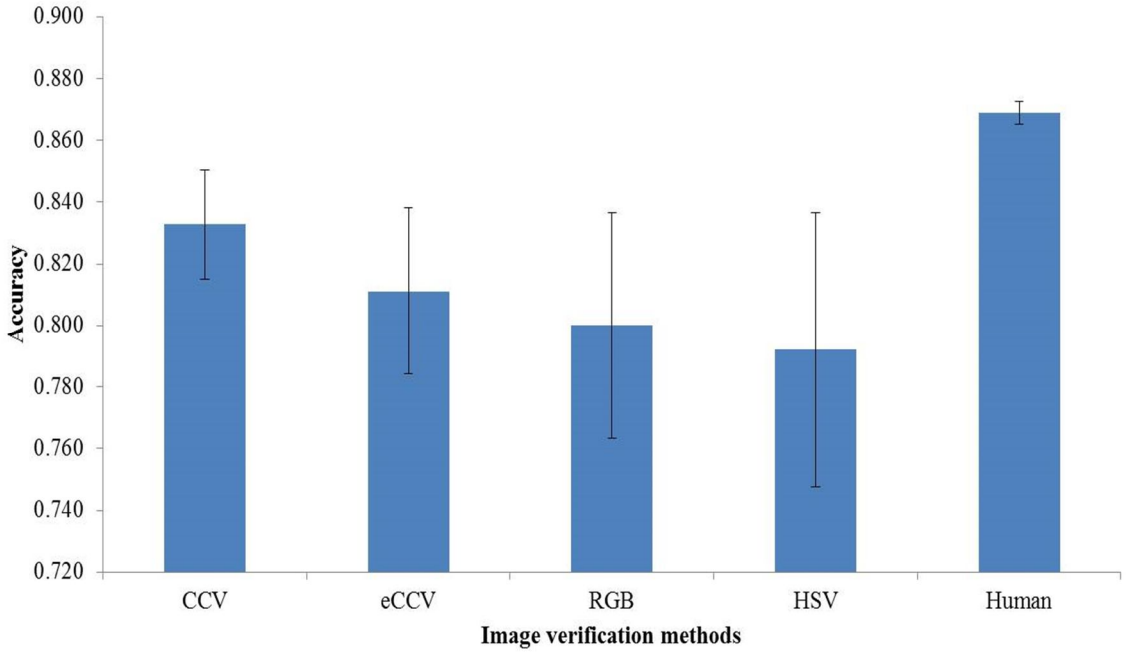

Figure 77. A summary of analytical evaluations: methods vs. human judgment (degree of belief).

As shown in Figure 77, the mean of human analysts was relatively higher, and the standard deviation of human analysts was so narrow within the judgments of human analysts. The one-way ANOVA confirmed that there was significant difference in the analytical evaluation (accuracy rates) between the applied methods including human judgments (degree of belief), $F(4,20) = 5.43$, $p < .0040$ ($\alpha = 0.05$). The one-way ANOVA determined whether a method is differentially expressed in any of the conditions tested. However, it did not indicate which a specific method was the ones where statistical differences occur.

Therefore a Post hoc test was required, so Tukey (multiple comparisons) was used to verify the differences of the applied methods. The Tukey Grouping table displays the difference among the compared methods as shown in Table 16. The Tukey Grouping table displays the difference between the applied methods as it was shown in Table 15. Notice the grouping labels "A" and "B" in this table.

Table 16

Tukey's Studentized Range (HSD) Test for accuracy of the applied methods including human analysts

Accuracy				
Tukey Grouping		Mean	N	Algorithm
	A	0.86892	5	Human
	A			
	A	0.83280	5	CCV
B	B			
B		0.81120	5	eCCV
B				
B		0.80000	5	RGB
B				
B		0.79200	5	HSV

There were two mean associated with the "A" group in accuracy, and that were human judgment and CCV methods. There was no significant difference between "A" group (human judgment and CCV methods). There were three means associated with the "B" group in accuracy, and that were eCCV, RGB, and HSV methods. Since the three means are grouped, they were not found to be significantly different. The results showed that the mean for human judgment was significantly higher (0.86892) than the means of all other groups. The mean for CCV was also significantly higher (0.83280) than the means of eCCV, RGB, and HSV methods (excepting the human judgment). There was enough evidence to conclude that the human judgment with cognitive analytics was statistically superior to the other methods (excepting CCV method). There were non-histogram methods statistically better than histogram methods.

Overall, unlike the computer-generated methods, the human judgments with cognitive analytics reduced the deviation of image identifications, and received much less the constraints of image characteristics or situations so that produced low deviation of the results and the better outcomes.

6.4.2 Application of Results to Visual Analytics. The cognitive analytics with the human subjects' confirming beliefs are described in Table 17-20. Each human subject confirmed a degree of belief to the identified images that were used to calculate the confirming beliefs as described in Chapter 4. Each table shows the results of each method, the beliefs of human analysts, and the confirmation of beliefs to the identified images. The highest belief (close to '1') is the most effective one, which can suggest that analysts made appropriate decisions.

Table 17 shows the confirming beliefs of CCV to the identified images. The CCV method had a better outcome (0.976) with the airport images compared to the other images.

Table 17

Sample judgments of human analysts and CCV method for image identifications

	Object category				
Method/Subject	Airport	Oil refinery	Dams	Gov. Building	Nuclear Facility
CCV	0.848	0.820	0.844	0.808	0.844
Human analyst 1	0.884	0.888	0.877	0.869	0.861
Human analyst 2	0.870	0.867	0.867	0.867	0.863
Human analyst 3	0.863	0.871	0.873	0.858	0.865
Human analyst 4	0.865	0.866	0.872	0.862	0.865
Human analyst 5	0.872	0.876	0.852	0.862	0.888
Confirming belief	0.976	0.946	0.974	0.944	0.974

Table 18 shows the confirming beliefs of eCCV to the identified images. The eCCV method had a better outcome (0.888) on with the oil refinery images compared to the other images.

Table 18

Sample judgments of human analysts and eCCV method for image identifications

	Object category				
Method/Subject	Airport	Oil refinery	Dams	Gov. Building	Nuclear Facility
eCCV	0.884	0.888	0.877	0.869	0.861
Human analyst 1	0.870	0.867	0.867	0.867	0.863
Human analyst 2	0.863	0.871	0.873	0.858	0.865
Human analyst 3	0.865	0.866	0.872	0.862	0.865
Human analyst 4	0.872	0.876	0.852	0.862	0.888
Human analyst 5	0.546	0.546	0.512	0.519	0.560
Confirming belief	0.884	0.888	0.877	0.869	0.861

Table 19 shows the confirming beliefs of RGB to the identified images. The RGB method had a better outcome (0.984) with the images of oil refinery images compared to the other images.

Table 19

Sample judgments of human analysts and RGB method for image identifications

	Object category				
Method/Subject	Airport	Oil refinery	Dams	Gov. Building	Nuclear Facility
RGB	0.788	0.860	0.808	0.772	0.772
Human analyst 1	0.884	0.888	0.877	0.869	0.861
Human analyst 2	0.870	0.867	0.867	0.867	0.863
Human analyst 3	0.863	0.871	0.873	0.858	0.865
Human analyst 4	0.865	0.866	0.872	0.862	0.865
Human analyst 5	0.872	0.876	0.852	0.862	0.888
Confirming belief	0.917	0.984	0.939	0.908	0.903

Table 20 shows the confirming beliefs of HSV to the identified images.

Table 20

Sample judgments of human analysts and HSV method for image identifications

	Object category				
Method/Subject	Airport	Oil refinery	Dams	Gov. Building	Nuclear Facility
HSV	0.764	0.832	0.844	0.740	0.780
Human analyst 1	0.884	0.888	0.877	0.869	0.861
Human analyst 2	0.870	0.867	0.867	0.867	0.863
Human analyst 3	0.863	0.871	0.873	0.858	0.865
Human analyst 4	0.865	0.866	0.872	0.862	0.865
Human analyst 5	0.872	0.876	0.852	0.862	0.888
Confirming belief	0.893	0.958	0.974	0.876	0.911

The HSV method had a better outcome (0.974) with the dam images compared to the other images. The Figure 78 shows a comparison of confirming beliefs for the categorized images by each image verification method. The results show that CCV was the most effective method based on the confirming beliefs to identify airport images (0.976), Gov. Building images (0.974), dam images (0.944), and nuclear facility images (0.974). The human analysts carry on the multiple analytical comparisons to pursuit the effective cognitive tasks based on these analytics.

Figure 78. Confirming beliefs for an image category by each image verification method.

Human analysts obtained the confirmation of best method by the calculated confirming beliefs. Based on the comparison of confirming beliefs to the applied methods, the summarized analytics about the identified images can be reported to human analysts as shown in Table 21. The analytics inform human analysts the best identified method (CCV) based on the above analyses (see Table 21 and Figure 78) for making effective decision supports. Such visual analytics can develop a method for visualizing human mental information processing in spatial

domains. Therefore, it lessens human limitations in information fusion of multi-modal contents to the appropriate decision supports for the human analysts.

Table 21

A confirmation of the best method to support human analysts

Image category	Airport	Oil Refinery	Gov. Building	Dams	Nuclear Facility
Identified method	CCV	RGB	CCV, HSV	CCV	CCV

As a follow-up statistical test, one-way ANOVA confirmed that there was significant difference in accuracy rates between the confirming beliefs of different computer-generated methods, $F(3,16) = 14.16$, $p < .0001$ ($\alpha = 0.05$). Tukey was used to verify the differences of confirming beliefs with the different methods as shown in Table 22. Unlike those described in Figure 78 and Table 21, the CCV is not significantly different to all others. The CCV was only different to the eCCV.

Table 22

Tukey's Studentized Range (HSD) Test for Accuracy of confirming beliefs

Accuracy			
Tukey Grouping	Mean	N	Algorithm
A	0.96280	5	RGB
A			
A	0.93020	5	HSV
A			
A	0.92240	5	CCV
B	0.84760	5	eCCV

For the second research question, it was concluded that there were no statistical differences between human confirming beliefs with the visual analytical tools (methods). However, the human confirming beliefs can reduce the variation of computer dependent results, so human analysts have more number of and stable visual analytics within applied methods. Analysts can reduce time spent to analyze inadequate results.

For the third research question, there was no evidence to conclude that there were statistical differences between GEOINT decision analysts with visual analytics. As shown in Table 23, the beliefs of human subjects for identifying the selected images showed that standard deviation values were quite low and very similar means values among the human analysts. Statistically, one-way ANOVA also confirmed that the decisions made by participants were not significantly different, $F(4,20) = 1.20$, $p = 0.3423$ ($\alpha = 0.05$).

Table 23

A comparison of user's decision with visual analytics: comparison of 'degree of beliefs'

	Degree of belief	
Human Analyst	Mean	SD
Analyst 1	0.876	0.010
Analyst 2	0.867	0.002
Analyst 3	0.866	0.005
Analyst 4	0.866	0.003
Analyst 5	0.870	0.012

Another part of the third research question is the statistical differences between GEOINT decision analysts without visual analytics. Given the instructions of image categories, none of participants made incorrect decisions. The use of small number of tasks (5 different images) was not sufficient to determine the statistical difference in participants' decisions without visual analytics.

Overall, the statistical results did not show the differences between the methods when confirmation of image identifications with human analysts' beliefs were applied to the computer-generated methods. However, the confirming belief was still valuable and a unique approach to assist human analysts to make effective decisions. The applied computer-generated methods brought somewhat the satisfactory results to identified images using comparison metrics as introduced in the previous chapters. The results of computer-generated methods were not always outstanding or far-reaching results in all situations (images), because it was fully depended on the image characteristics and the algorithm capabilities. Otherwise, the confirming belief was depended on the beliefs of human analysts to the identified images. The confirming belief supplements such difficulties of the computer-generated results, and allows human analysts to confirm the analyzed results with more comprehensive interpretations of the identified images.

6.5 Chapter Summary

The chapter presented the details of VACOM functionality with step-by-step instructions of VACOM interface. The usability study is introduced to obtain users satisfactions and suggestions for improving the VACOM interface. The details of experimental design were introduced: configuration of satellite image database, selection of participants, apparatus, experimental procedures, and experimental results of the research questions.

As we hypothesized, the human judgment with cognitive analytics is statistically superior to the computer generated methods (excepting CCV method). The human judgments with cognitive analytics reduced the deviation of image identifications, and received much less the constraints of image characteristics or situations so that it originated less deviation of the results and better outcomes. The statistics showed the merit of 'degree of belief' as a unique analytical approach to support satellite analysts. However, contrary to the hypothesis, there were

no statistical differences between human confirming beliefs with the visual analytical tools (methods). There was also no evidence to conclude that there were statistical differences between GEOINT decision analysts with visual analytics. Nonetheless, the cognitive visual analytics can develop a method for visualizing human mental information processing in spatial domains. Therefore, it lessens human limitations in information fusion of multi-modal contents to the appropriate decision supports for the human analysts.

CHAPTER 7

Conclusion

7.1 Research Summary

A visual analytic cognitive model (VACOM) was developed as a decision support tool for the intelligence analyst. To accomplish the development of cognitive model (CM), the cognitive task analyses (CTAs) was studied. The CM captures individual analyst's knowledge levels, mental models, and spatial conceptual maps to integrate computational implementations for the development of visual-analytic decision supports.

A robust image analysis method with a new color space and segmentation approach was developed in this study that compared with other image analysis methods to establish analytical evaluations for visual-analytic decision supports. VACOM has representations of the expert knowledge. The analytical models in VACOM are implemented such as the belief function based on fuzzy norm, the residuum computation of conditional probability, and the confirming belief. Such approaches help human analysts reduce the cognitive overload associated with the complexity of geographical information processing.

The detailed implementation of VACOM interface was discussed. VACOM interface allows the user to select a satellite image of interest, select each of the image analysis methods for visualization, and compare 'ground-truth' information against the recommendation of VACOM. The interface was designed to enhance perception, cognition, and even comprehension to the multi and complex image analyses by the analysts.

We conducted experiments to evaluate the differences between the visual analytic tools in satellite image processing. There were no significant differences between the applied image verification methods. To validate applied cognitive model (VACOM), the addressed research

questions on the cognitive analytics (degree of belief and confirming belief) were evaluated by human analysts. The human judgment with cognitive analytics is statistically superior to the computer generated methods (excepting CCV method). It could not conclude that there were statistical differences between human confirming beliefs and the visual analytical tools (methods). There was also no evidence to conclude that there were statistical differences between GEOINT decision analysts and visual analytics.

Overall, human judgments supported with cognitive analytics reduced the deviation of image identifications and received much less of the constraints of image characteristics or situations so that it comes with the low deviation of the results and better outcomes. The statistical results do not show the differences between the methods when it was applied the confirmation of image identifications with human analysts' beliefs to the computer-generated methods. However, the confirming belief is still valuable and unique approach to assist human analysts to make effective decisions. The results of computer-generated methods were not always outstanding or radical results in all situations (images), because it was fully depended on the image characteristics and the algorithm capabilities. Otherwise the confirming belief was depended on the beliefs of human analysts to the identified images.

The confirming belief supplements such difficulties of the computer-generated results, and allows human analysts to confirm the analyzed results with more comprehensive interpretations to identified images. The visual analytics can develop a method for visualizing human mental information processing in spatial domains. Therefore it lessens human limitations in information fusion of multi-modal contents to the appropriate decision supports for the human analysts.

7.2 Contributions

This dissertation contributes towards the development of methods to support intelligence analyst in information processing task to the GEOINT domain, and especially the development of a decision support system (DSS) with visual analytics designed to aid the intelligence analyst. The following are key contributions:

1. *Cognitive Scientific Framework:* This dissertation developed a cognitive scientific framework, which was derived by experts' knowledge levels based on the cognitive task analysis (CTA) of the satellite image analysis. The cognitive framework developed knowledge network to capture cognitive characteristics of the expert's tacit knowledge involved with the GEOINT information processing.
2. *Robust Color Space and Segmentation Technique:* This dissertation developed a robust color space and segmentation technique to enhance the current image analysis method (CCV). The enhanced method was compared with other methods to establish analytical evaluations for visual-analytic decision supports. The analytical evaluations were used in comparison metrics such as precision, recall, and accuracy.
3. *Cognitive Analytics in VACOM:* This dissertation developed the cognitive analytics in VACOM which were based on analytical models using the concept of Bayesian belief network. A belief function was developed by fuzzy norm and residuum computations. The fuzzy norm calculated users' beliefs on each knowledge levels. The residuum calculated conditional probabilities between knowledge levels. These analytical models developed the confirming belief to confirm users' beliefs on the image analysis methods for identified satellite images. Such cognitive analytics help human analysts to reduce the

cognitive overload associated with the complexity of geographical information processing.

4. *VACOM Interface:* This dissertation developed the VACOM interface which was designed to capture users' intents (mental processes) used for image-based information processing, including identification of suspicious objects of interest. The interface was designed to enhance perception, cognition, and even comprehension to the multi and complex image analyses by the analysts.

7.3 Research Limitations

There were two assumptions to the non-histogram methods (CCV and eCCV) about setting up threshold (τ) for creation of CCV table and segmentation of eCCV. The selected threshold (τ) is key factor to make robust image verification methods. The threshold (τ) plays the important role to separate coherent and incoherent colors for constructing CCV vector table and to segment heterogeneous colors from an object. However, the selected threshold (τ) was not the best parameter so that it could not generate an elaborated CCV table and segmentation for the non-histogram methods. As a result, eCCV method produced poor comparison metrics (accuracy, precision, recall and similarity) that could not show statistically significant difference to other applied image verification methods.

The following were discovered as limitations to this research:

1. Due to the limited access of satellite imagery, there were some difficulties to build a database for experiments such as image quality, variety of image category, and variety of image characteristics.
2. Due to the limited resource of computing technology, just one single-cycle experiment took a lot of time to simulate image processing tools and VACOM interface.

3. VACOM interface pays more attention to laboratory setting and functional purposes for the image based analyses, so it could not reflect optimum user-centered interface design and could not capture variety of cognitive activity factors.

7.4 Recommended Future Research

Outlined below are possible future researches in this area of visual analytic cognitive model:

1. Use large sample size of image database to get more appropriate validation for the applied image analysis and the cognitive methods. With larger sample size of database, the study might more conclusively prove the differences of applied image verification methods against the constraints of image characteristics.
2. Increase cognitive activities by using multiple images comparisons as inputs to confirm a type of image category. Based on the review of results, a single image did not achieve the best performances in all cases. Multiple images comparisons with analytical evaluation to determine an image category can reduce possibly faulty verifications.
3. Develop a hybrid image verification method (e.g., texture, edge, etc.) to solve more diverse situations.
4. Develop a dynamic and an interactive decision support system that allows user to change any parameters to both image verification algorithms and knowledge network. The current VACOM interface does not allow user to change any important features.
5. Develop more elaborated knowledge network. The current knowledge levels have equal weight to calculate the data fusion of Bayesian belief network and only offer the total belief of each knowledge level (global information). Knowledge network should allow users to select different cognitive weight for generating elaborated knowledge

computations when the data fusion is performed to calculate a degree of belief to the identified image.

6. Develop cognitive visual analytics system to support human analysts with prompt analytics. The current model and interface as implemented only captures the cognitive activities of human analysts and show cognitive analytics. It does not visualize the cognitive analytics automatically throughout the interface.

References

Allen, J. (1983). Maintaining knowledge about temporal intervals. *Communications of the ACM*, 26, 832-843.

Allen, V. L. (1975). Social support for non-conformity. *Advances in Experimental Social Psychology*, 8, 1-43.

Altunbasak, Y., Eren, P. E., & Tekalp, A. M. (1998). Region-based parametric motion segmentation using color information. *Graphical Models and Image Processing,* 60, 13-23.

Asch, S. E. (1952). Social Psychology. New York: Prentice Hall Inc.

Balasubramanian, R., Bouman, C. A., & Allebach, J. P. (1994). Sequential scalar quantization of color images, *Journal of Electronic Imaging 3*, 45-59.

Barr, A., & Feigenbaum E. A. (1981) (Eds.). The Handbook of Artificial Intelligence, 1, Sanford University/ Kaufman.

Berkeley, G. (1710). The Principles of Human Knowledge. The Berkeley Society.

Bodker, S. (1990). Through the Interface: A Human Activity Approach to User Interface Design, Erlbaum, Hillsdale, NJ.

Bodker, S. (1993). Historical analysis and conflicting perspectives-Contextualizing HCI. In L. J. Bass, J. Gornostaev, & C. Unger (Eds.), *Human-Computer Interaction, 3th International Conference*, EWHCI'94, St. Moscow, Russia (pp.1-10). New York.

Boesch, R., & Wang, Z (2008). Segmentation optimization for aerial images with spatial constraints. *Proceeding of The International Archives of the Photogrammetry, Remote Sensing and Spatial Information Sciences*, 37, 285-290.

Burkhard, R. A. (2004). Learning from Architects: The Difference between Knowledge

Visualization and Information Visualization. *Proceedings of the Eighth International Conference on Information Visualization (IV'04)*, 519-524.

Caers, J. (2011). Modeling Uncertainty in the Earth Sciences. Wiley-Blackwell: John Wiley & Sons.

Carson, C., Belongie, S., Greenspan, H., & Malik, J. (2002). Blobworld: Image segmentation using expectation-maximization and its application to image querying. *IEEE Trans. Pattern Analysis and Machine Intelligence*, *24*(8), 1026-1038.

Chang, C. C., & Wang, L. L. (1996). Color texture segmentation for clothing in a computer-aided fashion design system. *Image and Vision Computing*, 14(9), 685-702.

Clancey, W. J. (1997). Situated Cognition. Cambridge University Press, Cambridge.

Clark, R. E., & Estes, F. (1996). Cognitive task analysis. *International Journal of Educational Research, 25*(5). 403-417.

Cohen, J. (1977). Statistical Power Analysis for the Behavioral Sciences. New York: Academic Press.

Crystal, A., & Ellington, B. (2004). Task analysis and human-computer interaction: approaches, techniques, and levels of analysis. *Proceedings of the Tenth Americas Conference on Information Systems*, 391.

Davis, L. H. (1979). *Theory of Action*. Englewood Cliffs, NJ: Prentice-Hall.

Dean, A., & Voss, D. (1999). *Design and Analysis of Experiments*. New York: Springer.

Decortis, F., & Keyser, V. (1988). Time: The Cinderella of man-machine interaction. *Proc. of The 3rd. IFAC/IFIP/IEA/IFORS Conference on Man-Machine Systems*, Oulu, Finland.

Dietrich, E., & Markman, A. B. (2000). *Cognitive Dynamics: Conceptual and representational changes in humans and machines*. Mahwah, N.J.: Lawrence

Erlbaum Associates.

DuBois, D. A. & Shalin, V. L. (2000). Describing Job Expertise Using Cognitively Oriented Task Analysis (COTA). In J. M. Schraagen, S. F. Chipman, & V. L. Shalin, (Eds.), *Cognitive Task Analysis* (pp. 41-56). New Jersey: Lawrence Erlbaum.

Edwards, G. (1997). Geocognostics - A new framework for spatial information theory. In S. Hirtle, & A. Frank (Eds.), *Spatial Information Theory A Theoretical Basis for GIS* (Vols.1329, pp. 455-471). Springer Berlin, Heidelberg.

Edward, J. G., & Thomas, E. M. (1997). *Digital Color Management.* (1st ed.), Addison-Wesley.

Endsley, M. R. (1995): Toward a Theory of Situational Awareness in Dynamic Systems. *Human Factors*, *37*(1), 32-62.

Engelkamp, J., Seiler, K. H., & Zimmer, H. D (2005). Differential relational encoding of categorical information in memory for action events. *Memory & Cognition*, *33*(3), 371-379.

Foley, J. D., Dam, A. V., Feiner, S. K., & Hughes, J. F. (1990). *Computer Graphics: Principles and Practice*. New York: Addison Wesley.

Fonseca, F. T., Egenhofer, M. J., Davis Jr. C. A., & Borges, K. A. V. (2000). Ontologies and knowledge sharing in urban GIS. *Computers, Environment and Urban Systems.* 24, 251-271.

Freksa, C. (2004). Spatial Cognition: An AI Perspective. *ECAI 2004*, 1122-1128.

Freksa, C. & Barkowsky, T. (1996). On the relation between spatial concepts and geographic objects. In P. Burrough, A. Frank A (Eds.), *Geographic objects with indeterminate boundaries* (pp. 109-121). London: Taylor and Francis.

Gentile, R. S., Allebach, J. P., & Walowit, E. (1990). Quantization of color images based on uniform color spaces, *Journal of Imaging Technology,* 16, 11-21.

Gott, S. (1994). Cognitive task analysis. *Panel discussion at the Second Conference on Naturalistic Decision Making*, Dayton, Ohio.

Guo, S., Keeney, J., O'Sullivan, D., & Lewis, D. (2007). Adaptive Semantic Interoperability Strategies for Knowledge Based Networking. In R. Meersman, Z. Tari & P. Herrero (Eds.). *OTM 2007 Workshops* (Vols. 4806, pp. 1187-1199). Berlin: Springer Heidelberg.

Hafner, J., Sawhney, H., Equitz, W., Flickner, M., & Niblack. W. (1995). Efficient color histogram indexing for quadratic form distance functions. *IEEE Transactions on Pattern Analysis and Machine Intelligence*, *17*(7), 729-736.

Hess, R. F., Dakin, S. C., & Field, D. J. (1998). The role of "contrast enhancement" in the detection and appearance of visual contours. *Vision Research*, 38(6), 783-787.

Heuer, R. J., Jr. (1999). *Psychology of Intelligence Analysis*. Washington, DC: Central Intelligence Agency.

Ho, SH., & Liu, K. (2011). A qualitative study of decision making process between expert and novice teaching students with intellectual disability. Retrieved from www.ditplb.or.id/files/acmr/SuHuaHo.doc

Hoffman, R. R., Shadbolt, N. R., Burton, A. M., & Klein, G. (1995). Eliciting Knowledge from Experts: A Methodological Analysis. *Organizational Behavior and Human Decision Processes,* 62(2), 129-158.

Holyoak, K. J., & Thagard, P. (1996). Mental Leaps: Analogy in creative thought. Cambridge, MA: The MIT Press.

Jeong, S. (2001). Histogram-Based Color Image Retrieval. Retrieved from

http://scien.stanford.edu/pages/labsite/2002/psych221/projects/02/sojeong/

Jolly, M. P. D., & Gupta, A. (1996). Color and texture fusion: application to aerial image segmentation and GIS updating. In *Proceedings of Third IEEE Workshop on the Applications of Computer Vision*, 2-7.

Klein, D. E., Klein, H. A., & Klein, G. (2000). Macrocognition: Linking cognitive psychology and cognitive ergonomics, Proceedings of the 5th International Conference on Human Interactions with Complex *Systems,* 173-177.

Klein, G. (1999). Sources of Power: How People Make Decisions. Personnel Psychology. MIT Press.

Klein, G. (2000). Cognitive task analysis of teams. In J. M. Schraagen, S. F. Chipman, & V. L. Shalin, (Eds.), *Cognitive Task Analysis*. (pp. 417-429), New Jersey: Lawrence Erlbaum.

Klein, G. (2008). Naturalistic decision making. *Human Factors,* 50, 456-460.

Kurugollu, F., Sankur, B., & Harmanci, A. E. (2001). Color image segmentation using histogram multithresholding and fusion. *Image and Vision Computing* 19, 915-928.

Laudy, C., & Ganascia, J. G. (2009). Introducing semantic knowledge in high-level fusion. *IEEE 2009 Military Communications Conference*, 1-7.

Macdonald, G. (1995). Introduction: Tacit knowledge. In C. Macdonald & G. Macdonald (Eds.), *Philosophy of Psychology: Debates on Psychological Explanation* (Chapter 17). Oxford, UK: Blackwell.

MacLennan, B. J. (1994). Continuous Computation and the Emergence of the Discrete. *Processing in Biological Neural Networks.*

MacEachren, A. M. (1995). How Maps Work: Representation, Visualization, and Design, New York: The Guilford Press.

MacLeod, I. S., Hone, G., & Smith, S. (2005). Capturing Cognitive Task Activities for Decision Making and Analysis. *10th International Command and Control Research and Technology Symposium: The Future of C2,* 44, 1-22.

Malhotra, Y. (2001). Expert systems for knowledge management: crossing the chasm between information processing and sense making. *Expert Systems with Application*, 20, 7-16.

Mark D. M., Freksa, C., Hirtle, S. C., Lloyd, R., & Tversky, B. (1999). Cognitive models of geographical space. *International Journal of Geographical Information Science*, *13*(8), 747-774.

Mena, J. B., & Malpica, J. A. (2005). Color image segmentation based on three levels of texture statistical evaluation. *Applied Mathematics and Computation*, *161*(1), 1–17.

Militello, L. & Hutton, R. (1998). Applied cognitive task analysis (ACTA): a practitioner's toolkit for understanding cognitive task demands. *Ergonomics*, *41*(11), 1618-1641.

Miller, H. J. (2008). Geographic Data Mining and Knowledge Discovery. *The Handbook of Geographic Information Science,* 352-366, Blackwell Publishing Ltd.

Mukkamala, S., & Sung, A. H. (2003). Identifying Significant Features for Network Forensic Analysis Using Artificial Intelligent Techniques. *International Journal of Digital Evidence*, *1*(4), 1-17.

Newell, A. (1982). The knowledge level. *Artificial Intelligence*, 18, 87-127.

Nielsen, J. (1992). Finding usability problems through heuristic evaluation. *Proceedings ACM CHI'92 Conference*, 373-380, Monterey, CA.

Nielsen, J. (2003). *Severity Ratings for Usability Problems.* Retrieved from: www.useit.com/papers/heuristic/severityrating.html

Nonaka, I. (1991). The knowledge creating company. *Harvard Business Review,* 69, 96-104.

Ntuen, C. A. (2006). Cognitive Constructs and Sensemaking Process. *Proceedings for11th International Command & Control Research and Technology Symposium*. San Diego, CA.

Ntuen, C. A. (2008). Cognition and visualization in situation understanding. Invited Presentation, OMNI Fusion 2008: Situation Understanding Workshop. Fort Leavenworth: Battle Command Battle Lab. June 23-24.

Ntuen, C. A., & Kim, G. (2008). A sensemaking visualization tool with military doctrinal elements. *Proceeding for international Command & Control Research and Technology Symposium.* Seattle, WA, 67-71.

Ntuen, C. A., Chenou, J., & Kim, G. (2010). Believability of sensemaking support systems using Bayesian belief network. *Industrial Engineering Research Conference*, June 7; Cancun, Mexico (CDROM).

Ntuen, C. A., Park, E. H., & Kim, G. (2010). Designing an information visualization tool for sensemaking. *International Journal for Human-Computer Interaction*, *26*(2), 189-205.

Ogiela, L. (2009).UBIAS systems for cognitive interpretation and analysis of medical images. *OPTO-Electronics Review*, *17*(2), 166-179.

Ogiela, L., & Ogiela, M. R. (2009). *Cognitive Techniques in Visual Data Interpretation*. Berlin, Heidelberg: Springer-Verlag.

O'Gorman, L. (1994). Binarization and multithresholding of document images using connectivity. *Graphical Models and Image Processing*, 56, 494-506.

Omran, Engelbrecht, &Salman, (2005). A color image quantization algorithm based on particle swarm optimization, *Informatica*, 29, 261-269.

Ooi, W.S., & Lim, C.P. (2006). Fuzzy clustering of color and texture features for image

segmentation: A study on satellite image retrieval. *Journal of Intelligent & Fuzzy Systems*, 17, 297–311.

Ooi, W. S., & Lim, C. P. (2006). Hybrid Image Segmentation based on Fuzzy Clustering Algorithm for Satellite Imagery Searching and Retrieval. In A. Abraham, B. de Baets, M. Köppen, & B. Nickolay (Eds.). *Applied Soft Computing Technologies: The Challenge of Complexity* (Vols. 34, 355-372). Springer Berlin/Heidelberg.

Prasanna, R., Yang, L., & King, M. (2009). GDIA: a Cognitive Task Analysis Protocol to Capture the Information Requirements of Emergency First Responders. *Proceedings of the 6th International ISCRAM Conference*, Gothenburg, Sweden.

Pass, G., & Zabih, Z. (1999). Comparing image using joint histogram. *Multimedia Systems*, *7*(3), 234-240.

Pass, G., Zabih, R., & Miller, J. (1996). Comparing images using color coherence vectors. *Proceedings of the fourth ACM international conference on Multimedia MULTIMEDIA 96*, 65-73.

Park, G., Ntuen, C. A., & Kim, G. (2009). The knowledge levels of the intelligence analysts in satellite image processing. *Proc. of 9th Symposium of Human Interaction with Complex Systems*, August 19-22, Greenbelt Marriott, Maryland.

Park, G., & Ntuen, C. A. (2011). A Cognitive Model for Human Terrain Information Processing. *Proc. of 61st Annual IIE Conference and Expo*. May 21-25, Reno, Nevada.

Pearl, J. (1988). Probabilistic reasoning in intelligent systems: Networks of plausible inference. Morgan Kaufmann Publishers, Inc.

Pedrycz, W (1993). *Fuzzy control and fuzzy systems*. Research Studies Press Ltd.

Peirce, C. S. (1931).The Collected Papers (CP, Vols. 8). In Hartshorne, C. & Weiss, P. (Eds.). Cambridge, MA: Harvard University Press.

Peterson, C. R., & Beach, L. R. (1967). Man as an intuitive statistician. *Psychological Bulletin*, *68*(1), 29-46.

Pew, R. W., & Mavor, A. S. (Eds.). (1998). *Modeling Human and Organizational Behavior: Application to Military Simulations.* Washington, DC: National Academy Press.

Polanyi, M. (1966). *The Tacit Dimension*. New York: Anchor Books.

Poppler, K. (1969). *Knowledge and the Body-Mind Problem. Published Lecture in* Emory University.

Poynton, C. A. (1996). *A Technical Introduction to Digital Video*, John Wiley & Sons Inc., p. 175.

Randel, J. M., & Pugh, H. L. (1996). Differences in expert and novice situation awareness in naturalistic decision making, *International Journal of Human-Computer Studies*, 45, 579-597.

Randel, J. M., Pugh, H. L., & Wyman, B. G. (1996). Methods for conducting cognitive task analysis for a decision making task. San Diego, CA: Navy Personnel Research and Development Center.

Rasmussen, J. (1985). The role of hierarchical knowledge representation decision making and system management. *IEEE Transactions on Systems, Man, and Cybernetics*, *15*(2), 234-243.

Rasmussen, J. (1986). Information processing and human-machine interaction-an approach to cognitive engineering. North-Holland Series in System Science and Engineering, 12.

Rigau, J., Feixas, M., & Sbert, M. (2004). An information theoretic framework for image segmentation. *2004 International Conference on Image Processing 2004 ICIP 04*, 1193-1196.

Shafer, G. (1987). Belief functions and possibility measures. In James C. Bezdek (Eds.). *Analysis of Fuzzy Information*. (Chapter 3). Florida: CRC Press.

Shastri, L. (1988). A Connectionist Approach to Knowledge Representation and Limited Inference. *Cognitive Science,* 12, 331-392.

Sapkal, A. T., Bokhare, C., & Tarapore, N. Z. (2012). Satellite image classification using the back propagation algorithm of artificial neural network. Retrieved from www.csre.iitb.ac.in/~csre/conf/wp-content/uploads/.../PS1_6.pdf

Scheunder, P. (1997). A genetic C-Means clustering algorithm applied to color image quantization. *Pattern Recognition*, 30(6), 859-866.

Schraagen, J. M., Chipman, S. F., & Shalin, V. L. (2000). *Cognitive Task Analysis*. Mahwah, NJ: Lawrence Erlbaum.

Searle, J. R. (1983). *Intentionality*. Cambridge: Cambridge University Press.

Sezgin, M., KurugoÈlluÈ, F., & Birecik, S. (1997). An application of multilevel thresholding methods to visual cloth quality inspection. *International Conference on Quality Control by Artificial Vision*, Le Creusot, France, 28-30 May, 281-286.

Shan, Yu, Berthod, M., & Giraudon, G. (1999). Toward Robust Analysis of Satellite Images Using Map Information-Application to Urban Area Detection. *IEEE Transactions on Geoscience and Remote Sensing*, *37*(4), 1925-1939.

Shapiro, L. G, & Stockman, G. C. (2003). *Computer Vision.* Upper Saddle River, New Jersey: Prentice Hall Inc., 199-201.

Simon, H. A. (1960). *The New Science of Management Decisions*. New York: Harper & Row.

Singha, M., & Hemachandran, K. (2011). Color image segmentation for satellite images. International Journal on Computer Science and Engineering (IJCSE), *3*(12), 3756-3762.

Smith, K., & Hancock, P. A. (1995). Situation awareness is adaptive, externally directed consciousness. *Human Factors*, *37*(1), 137-148.

Sowa, J. F. (1984). *Conceptual Structures*. Reading, MA: Addison-Wesley.

Stanton, N. A., Salmon, P. M., Walker, G.H., Baber, C., & Jenkins, D.P. (2005). HFs Methods-A practical Guide for Engineering and Design. Ashgate Publishing Ltd.

Stefania, A., Ilaria, B., & Marco, P. (1999). Windsurf: Region-Based Image Retrieval Using Wavelets. DEXA Workshop, 167–173.

Steyversa, M., & Tenenbaumb, J. B. (2005). The Large-Scale Structure of Semantic Networks: Statistical Analyses and a Model of Semantic Growth. *Cognitive Science,* 29, 41-78.

Stricker, M., & Swain, M. (1994). The capacity of color histogram indexing. In *Proceedings of IEEE Conference on Computer Vision and Pattern Recognition*, 704-708.

Suchman, L. (1987). *Plans and Situated Actions*. Cambridge, UK: Cambridge University Press.

Swain, M., & Ballard, D. (1991). Color indexing. *International Journal of Computer Vision*, *7*(1), 11-32.

Thomas, R. W., DaSilva, L. A., & MacKenzie, A. B. (2005). Cognitive Networks. *First IEEE International Symposium on New Frontiers in Dynamic Spectrum Access Networks 2005, DySPAN 2005*, 8-11.

Tognazzini, B. (2003) First principles of interaction design. In: Ask, T.O.G., Retrieved from: http://www.asktog.com/basics/firstPrinciples.html

Tsai, C., Manjunath, B. S., & Jagadeesan, R. (1995). Automated segmentation of brain MR images. *Pattern Recognition* 28, 1825-1837.

Van der Weken, D., De Witte, V., Nachtegael, M., Schulte, S., & Kerre, E. (2005). Colour Image Comparison Using Vector Operators. *Proceedings of the 2005 International Conference on Computational Intelligence for Modeling*, *Control and Automation, and International Conference on Intelligent Agents, Web Technologies and Internet Commerce (CIMCA-IAWTIC'05)*.

Vicente, K. J., & Rasmussen, J. (1992). Ecological Interface Design: Theoretical foundations. *IEEE Transactions on Systems, Man and Cybernetics*, 22, 589-606.

Wan, S. J., Prusinkiewicz, P., & Wong, S. K. M. (1990). Variance-based color image quantization for frame buffer display. *Color Research and Application,* 15, 52-58.

Weick, K. E. (1995). *Sensemaking in organizations*. Thousand Oaks, CA: Sage Publications.

Wen, L., & Tan, G. (2008). Image Retrieval using Spatial Multi-Color Coherence Vectors Mixing Location Information. *2008 ISECS International Colloquium on Computing, Communication, Control, and Management*, 299-302.

Wickens, C. D.(1999). *Frames of reference for navigation*. In D. Gopher and A. Koriat (Eds.), *Attention and Performance*, 16, 113-144. Orlando, FL: Academic Press.

Wickens, C. D., Lee, J. D., Liu, Y., & Gordon-Becker, S. (2003). *Introduction to Human Factors Engineering* (2nd ed.). Upper Saddle River, NJ: Prentice-Hall Inc.

Wynne, H., Chua, T. S., & Pung, H. K., (1995). An Integrated Color-Spatial Approach to Content-based Image Retrieval. *Proceedings of the third ACM international conference on Multimedia*.